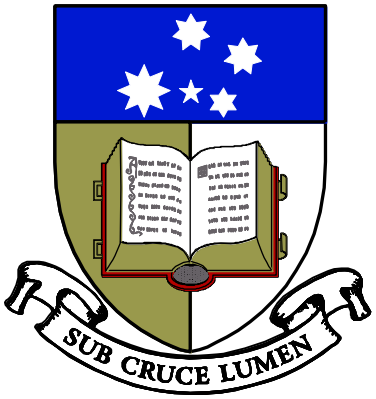

THE UNIVERSITY OF ADELAIDE

Remote sensing to monitor interactions between aquaculture and the environment of Spencer Gulf, South Australia

---

Thesis submitted for the degree of

Doctor of Philosophy

Paul Erich Bierman
B.Sc. (Hons)

The University of Adelaide
School of Earth and Environmental Sciences

May 2010

Chapter 4: Validation of MODIS Chlorophyll-*a* and Sea Surface Temperature imagery in South Australian Coastal Waters

4.1 Introduction

The MODIS instruments routinely obtain images of chlorophyll-*a* concentrations and sea surface temperature that enable us to investigate oceanic processes. However, there are a number of factors that can influence the accuracy of satellite-based estimates of chlorophyll-*a* and SST. Thus it is important to assess the accuracy, applicability and limitations of the MODIS chlorophyll-*a* and SST estimates in an area before applying the products. The areas of interest in this study are the waters of the SBT aquaculture region near Port Lincoln, Spencer Gulf, and nearby coastal waters of South Australia. Since the study area is adjacent to the coastline it is likely that the influence of factors that have the potential to negatively affect the accuracy of satellite-based estimates will be greater than in open ocean regions. No previous study has investigated the accuracy of satellite-based chlorophyll-*a* or SST imagery in southern Australian waters, therefore this study is crucial to understand the accuracy of the imagery for later application.

The purpose of this chapter is to compare satellite-based measurements of chlorophyll-*a* and SST to field-based measurements in Spencer Gulf and coastal South Australian waters to determine whether the imagery is a suitable and reliable data source for understanding these properties in the region. It is acknowledged that for a full validation of MODIS imagery, the accuracies of radiances measured by the sensors and the atmospheric correction procedure should be considered separately from the accuracy of the algorithms that convert observed radiance measures to the physical and biogeochemical parameters. However, for the purposes of this study we are considering the overall accuracy of the derived MODIS products against the values observed in the field. Since errors in remote sensing imagery such as this are cumulative, we do not need to separate the different error sources for the purposes of this study.

4.2 Methods

4.2.1 Field Data

Chlorophyll-a

Five separate datasets of field-based chlorophyll-*a* have been collected within South Australian coastal waters, for comparison with MODIS Aqua derived chlorophyll-*a* estimates. The first dataset consists of chlorophyll-*a* measurements obtained in the waters offshore from Port Lincoln in southwest Spencer Gulf as part of the Aquafin CRC‟s Risk and Response project (Tanner and Volkman 2009). Water quality samples were taken on a transect through the aquaculture region and at a few nearby mooring locations (Figure 4.1(a)) each month between August 2005 and September 2006. One litre water samples were collected from the surface and tested for chlorophyll-*a*, as well as other pigments, via high pressure liquid chromatography (HPLC) (van Ruth et al. 2009). At each station, data were also obtained for nutrients and phytoplankton. In total 128 measurements were made, but only 35 had suitable cloud-free MODIS images available within three hours of sample collection.

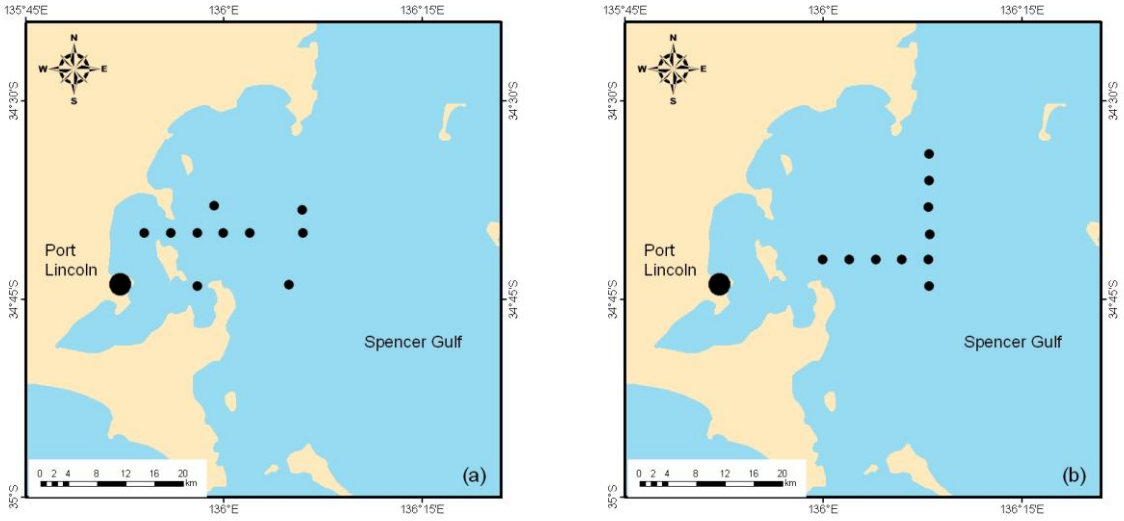

Figure 4.1: (a) The location of field-based chlorophyll-*a* measurements from the Aquafin CRC Risk & Response project and (b) the location of field-based chlorophyll-*a* measurements in May 2008.

Additional field-based chlorophyll-*a* data were also collected within and around the SBT aquaculture region on the 13th May 2008 (Figure 4.1(b)). On this occasion ten 2 L water samples were collected from the sea surface and stored in bottles. Upon returning to shore the water samples were filtered through 0.45 µm Whatman GF/F filters. Filter papers were then frozen at -80 ºC until they could be analysed. Filters were placed in centrifuge tubes with 5 ml methanol and stored in a freezer at -20 ºC for 24 hours to extract the pigments. Filters were then removed from the methanol sample and the tubes centrifuged for 10 minutes to remove particulates from suspension. The resulting sample was transferred to a cuvette and placed into the Thermo Electron Corporation Heλios γ UV Visible Spectrophotometer, which recorded the absorbance at 750 nm and 665 nm. The concentration of chlorophyll-*a* in µg L^{-1} (equivalent to mg m^{-3}) was then calculated via Equation 4.1:

$$Chl = A(\lambda_2 - \lambda_1)(V_m / V_w) \tag{4.1}$$

where V_m is the volume of methanol used to extract the pigments in millilitres, V_w is the volume of sea water filtered in litres, λ_1 is the background absorbance at 750 nm, λ_2 is the absorbance due to chlorophyll-*a* at 665 nm, and A is a coefficient equal to 13.9. The calculation of chlorophyll-*a* is based on Golterman (1978).

Further chlorophyll-*a* measurements were made onboard the SARDI research vessel MRV Ngerin on two cruises for the Integrated Marine Observing System (IMOS) (www.imos.org.au) within and outside of Spencer Gulf during October 2008 and January 2009 (Figure 4.2). On these occasions 4 L surface water samples were collected and filtered through 0.45 µm GF/F filters onboard the MRV Ngerin. The filters were frozen until return to shore. Chlorophyll-*a* concentrations were then calculated as above. For the October 2008 dataset, 34 samples were collected over 5 days, but only 13 had a corresponding cloud-free MODIS image within 3 hours of collection. For the January 2009 dataset, 35 samples were collected over 5 days, but only 18 had a MODIS image for comparison.

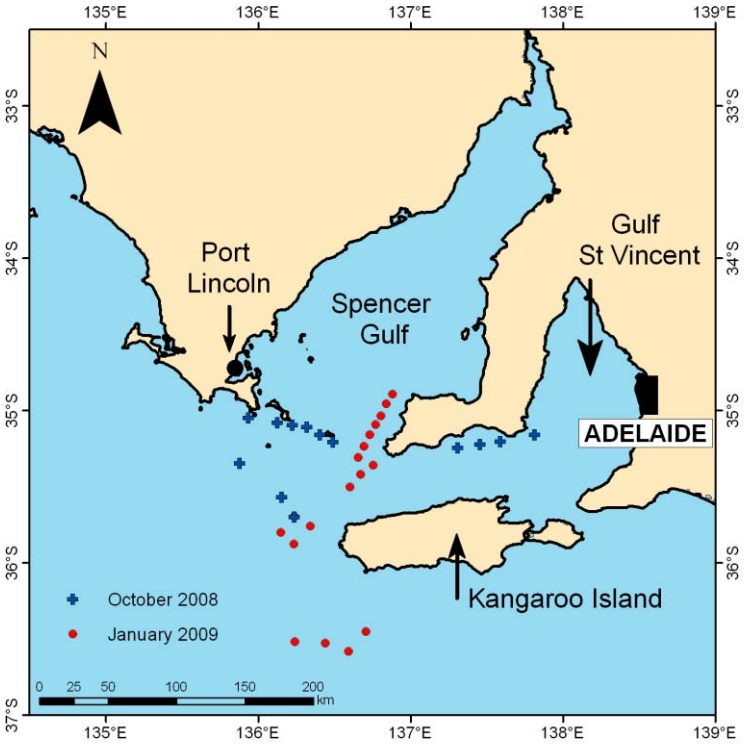

Figure 4.2: The location of field-based chlorophyll-*a* measurements from the IMOS cruises in October 2008 and January 2009. Only locations with a valid MODIS match up are shown.

Finally, chlorophyll-*a* data collected in the eastern Great Australian Bight (GAB), Spencer Gulf and nearby offshore waters has also been made available from a previous study on the productivity of the eastern Great Australian Bight (van Ruth 2009). Chlorophyll-*a* measurements were made at a large number of stations in February and March of 2004, 2005 and 2006 (Figure 4.3). One litre water samples were collected from a depth of 3 metres and chlorophyll-*a* concentrations determined following the spectrophotometer method described earlier. A total of 835 samples were collected over the three cruises, but of these only 127 had a cloud-free MODIS image within 3 hours for comparison of chlorophyll-*a*.

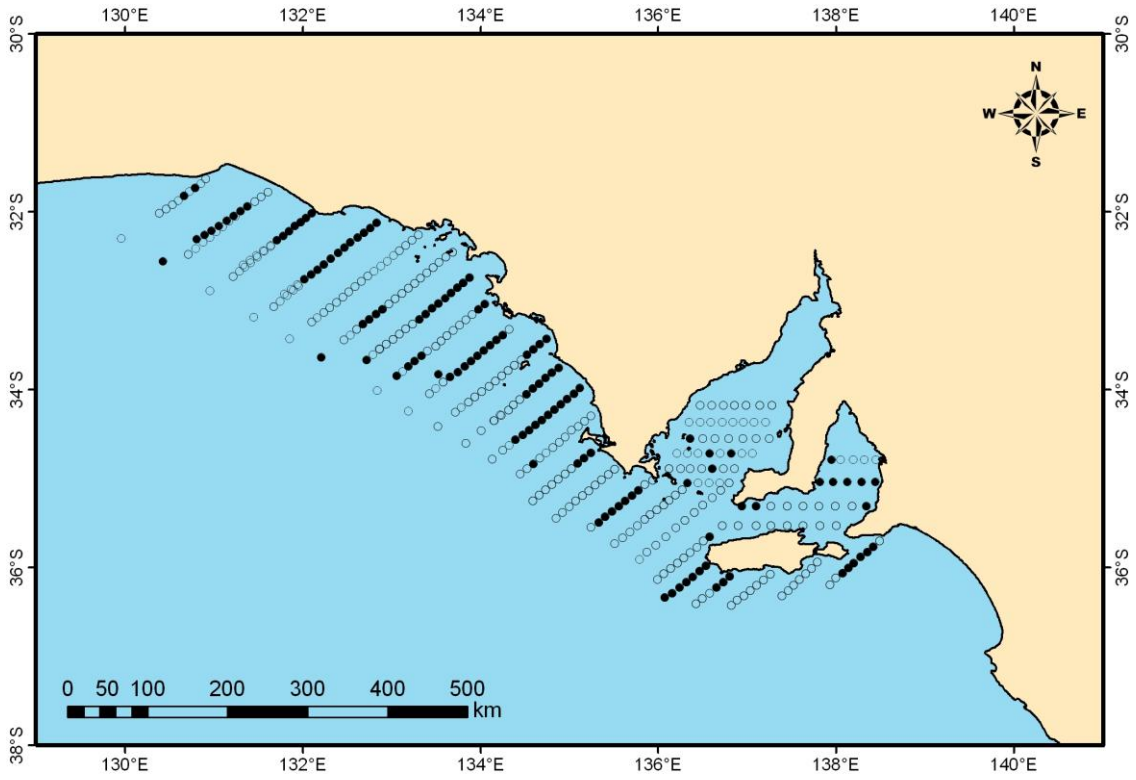

Figure 4.3: The location of stations visited during the cruises to the eastern GAB in 2004, 2005 and 2006 (van Ruth 2009), solid circles show the samples with a valid MODIS match up for validation.

Sea Surface Temperature

Field-based sea surface temperature data have been collected from a number of sites within the study area to be used for validation of MODIS SST imagery. The first SST dataset was collected as part of the Aquafin CRC‟s Risk and Response project (Tanner and Volkman 2009), in conjunction with chlorophyll-*a* measurements (Figure 4.1(a)). SST measurements were obtained from conductivity-temperature-depth (CTD) profiles of the water column and the temperature at a depth of approximately 1 metre taken to represent the SST. Initially 128 measurements were available, but after excluding data where there was no corresponding MODIS Aqua SST value, due to cloud cover or image availability within 3 hours, there were just 20 pairs of measurements.

Sea surface temperature data were also collected as part of the IMOS cruises onboard the MRV Ngerin, in February, March, August, and October 2008 and January and February 2009. Temperature profiles using a CTD were conducted between the surface and just above the seafloor at a large number of stations along the South Australian continental shelf (Figure 4.4). The uppermost temperature value of the profile, at a depth of between 1

and 3 metres, was taken to represent the sea surface temperature. Across the six IMOS cruises from which CTD temperature data was made available, 300 temperature measurements were made; from these 61 day-time and 36 night-time measurements were available with a corresponding cloud-free MODIS image within 3 hours.

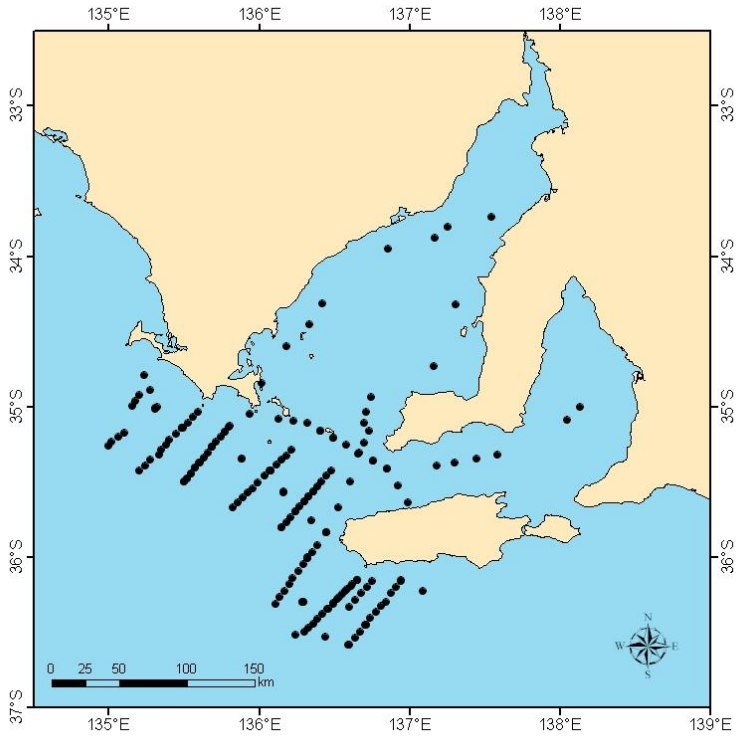

Figure 4.4: The location of CTD profiles conducted on the IMOS cruises of February, March, August and October 2008 and January and February 2009 with valid temperature measurements for MODIS SST validation.

4.2.2 MODIS Imagery

MODIS Aqua level 1A daily imagery in Hierarchical Data Format (HDF) was obtained from the Goddard Space Flight Centre (GSFC) for each date corresponding to chlorophyll-*a* field-data collection. Only MODIS/Aqua imagery was selected for chlorophyll-*a* products and not MODIS/Terra since the chlorophyll-*a* products produced from Terra imagery are known to be affected by calibration issues (Franz et al. 2007). Images were subset to the area between 30 and 40 ºS, and 132 and 142 ºE. The SeaWiFS Data Analysis System (SeaDAS) version 5.0.2 was used to process the MODIS imagery. Geolocation files were created from the level 1A (un-registered) imagery and used to process it up to registered level 1B. The msl12 processing function in SeaDAS was then used to convert the level 1B imagery into level 2 imagery containing the derived variables. The level 2 products selected as outputs were the standard OC3M chlorophyll-*a* (O'Reilly et al. 2000),

Clark chlorophyll-*a* (Clark 1997), GSM01 chlorophyll-*a* (Maritorena et al. 2002), Carder chlorophyll-*a* (Carder et al. 2003), and the Level 2 flags which identify where the output products may be affected by cloud, sunglint and other factors. Not all of the chlorophyll-*a* algorithms could be produced for each date required. The GSM01 and Carder semi-analytical algorithms failed to generate useful outputs on several occasions due to difficulties arising in the SeaDAS processing. This is likely due to aerosols that were not correctly accounted for in the atmospheric correction procedure resulting in negative observations of water-leaving radiance (Gordon and Voss 1999). This issue did not appear to influence the outputs for the empirical OC3M and Clark algorithms. Both Aqua and Terra Level 2 day-time 11 µm SST and the night-time 11 µm and 4 µm SST (Brown and Minnett 1999; Franz 2006) were obtained as level 2 imagery direct from the GSFC and did not require processing in SeaDAS. The level 2 chlorophyll-*a* and SST imagery was then imported into ENVI (Environment for Visualizing Images version 4.3 (RSI 2006)) using the ENVI plug-in for ocean colour obtained from www.ittvis.com (White undated), which converted the HDF files into ENVI image files and reprojected the imagery. ENVI was then used to extract the values from a 3 by 3 array of pixels centred on each of the field-data locations. Nine pixels were used to account for possible positional error in the satellite imagery (Bailey and Werdell 2006).

4.2.3 Comparison between field-based and MODIS data

Chlorophyll-*a* and SST measurements obtained via the field-based methods were compared with those derived via MODIS. For each of the four MODIS Aqua chlorophyll-*a* products (OC3M, Clark, GSM01 and Carder), and the three SST products (11 µm day, 11 µm night, and 4 µm night), the average of the 3 by 3 MODIS pixels centred upon the field station coordinate were calculated to be compared to the field-based values. When MODIS pixels were affected by cloud or other factors, chlorophyll-*a* and SST could not be calculated. Where 1 or more of the 9 pixels were affected, the data point was removed from the dataset. The dataset was further refined by excluding all data where a time difference of greater than 3 hours existed between when the field-sample was collected and the MODIS satellite overpass to limit the influence of temporal variability as suggested by Bailey and Werdell (2006). For each of the datasets, the relationship between the field-based value (x) and the MODIS value (y) was calculated via linear regression in Microsoft Excel. The root mean square error (RMSE) was expressed as a percentage of the average

value of the MODIS data to enable relative differences in the error to be compared between datasets.

4.2.4 Spatial and Temporal Variability in Chlorophyll-*a*

The comparison between field-based chlorophyll-*a* data and MODIS imagery involved comparing chlorophyll-*a* concentrations averaged over an area of approximately 9 km^2 for the MODIS imagery with single point measurements taken within this area for the field-based data. Thus, where considerable spatial variability in chlorophyll-*a* concentrations occurs within the area averaged for the MODIS chlorophyll-*a* value, large differences are likely to be observed when comparing the measurements obtained via the two methods. To determine the variability of chlorophyll-*a* within the MODIS average area, fine-scale transects were conducted on two occasions, 8th May 2007 and 13th May 2008, in the waters offshore from Port Lincoln around the SBT aquaculture region. Two litre water samples were collected from the surface at intervals of approximately 50 m along a transect. Chlorophyll-*a* concentrations from the water samples were determined following the spectrophotometer method described earlier. The range and variability of concentrations within the relatively small area of a few MODIS pixels were investigated to understand the degree of variability one can expect within the area averaged by MODIS imagery.

Temporal variability in the surface chlorophyll-*a* concentrations also needs to be considered when comparing measurements taken via the two different non-simultaneous methods. Large temporal variations in surface chlorophyll-*a* are likely to result in differences between data collected in the field and MODIS estimates when the two measurements are not taken at the same time. Bailey and Werdell (2006) suggest a window of ± 3 hours between the satellite overpass and the collection of field-based data to limit the effect of temporal variability upon the validation. To investigate the temporal variability in chlorophyll-*a* concentrations in the study region, field-based chlorophyll-*a* measurements were obtained from 4 L water samples collected at the same location in northern Spencer Gulf hourly over a 7-hour period. Samples were again analysed for chlorophyll-*a* using the methods previously described. The chlorophyll-*a* concentration was graphed over the 7-hour period to show the degree of temporal variability over the course of a day.

4.3 Results

4.3.1 MODIS v Field-based Chlorophyll-*a* Concentrations

The relationship between field-based chlorophyll-*a* and MODIS Aqua chlorophyll-*a* around the SBT aquaculture region was assessed using the data acquired from the Aquafin CRC Risk and Response project. Results for this relatively shallow coastal region show a poor relationship for OC3M chlorophyll-*a* (R^2 = 0.55, RMSE = 41%), with MODIS frequently overestimating the field-based value (Figure 4.5). The relationship was also assessed for the Clark, GSM01 and Carder alternate MODIS chlorophyll-*a* algorithms and the resultant regression statistics can be seen in Table 4.1 and Figure 4.5. The best performing of the algorithms, in terms of the R^2 value was the GSM01 algorithm, which gave an R^2 of 0.69, while the algorithm with the smallest RMSE was Clark with just 32%. Both the empirical methods, the OC3M and the Clark algorithms, show consistent overestimates by MODIS compared to the field-based measurements, while the semi-analytical algorithms, GSM01 and Carder, both under- and over- estimate components of the field data. While the GSM01 method gave the best fit, this may be because it actually failed for 13 of the 35 data points, and thus the regression analysis was based on a much smaller data set.

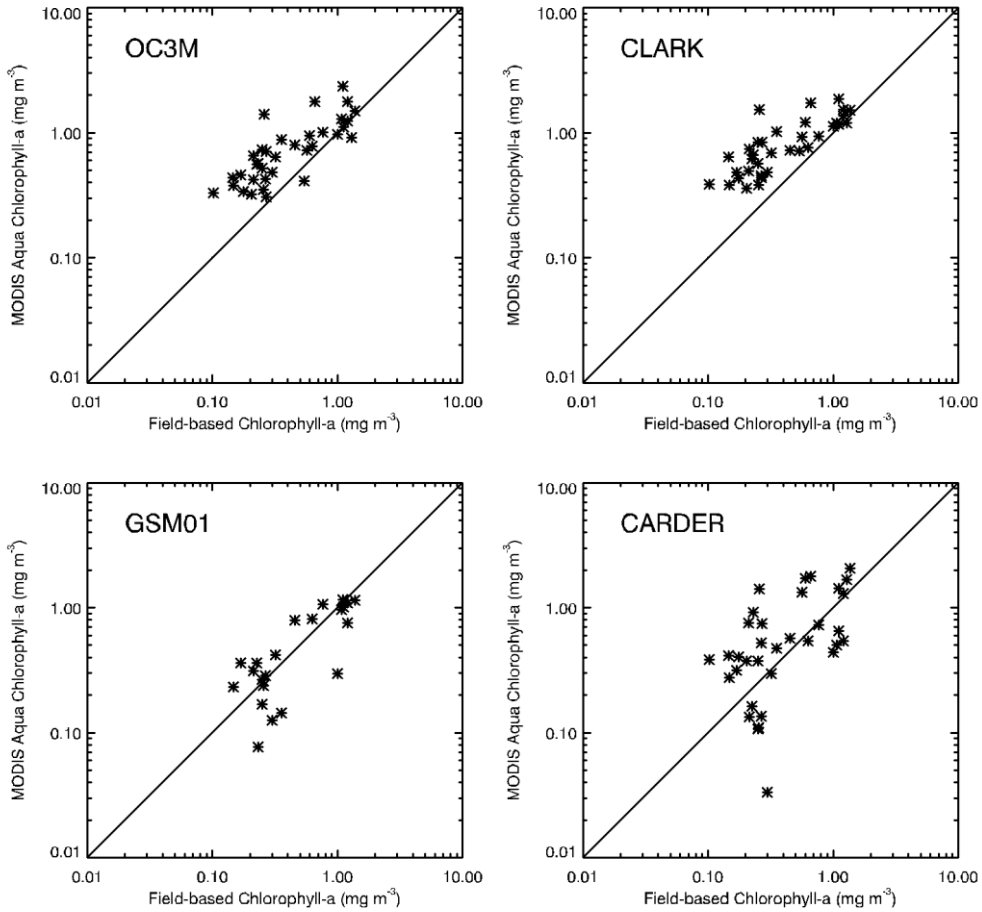

Figure 4.5: Relationship between MODIS OC3M, Clark, GSM01 and Carder chlorophyll-*a* algorithms and the Risk & Response field-based chlorophyll-*a* data.

Table 4.1: Regression statistics for MODIS OC3M, Clark, GSM01 and Carder chlorophyll-*a* algorithms and the Risk & Response field-based chlorophyll-*a* data.

Algorithm	N	R^2	p value	Slope	Intercept	RMSE (mg m^{-3})	RMSE (%)
OC3M	35	0.55	3.2×10^{-7}	0.91	0.34	0.33	41 %
CLARK	35	0.59	6.5×10^{-8}	0.82	0.44	0.27	32 %
GSM01	22	0.69	1.5×10^{-6}	0.75	0.11	0.22	40 %
CARDER	34	0.34	3.0×10^{-4}	0.80	0.28	0.46	66 %

It is possible that in shallow waters seafloor reflectance may occur, which can alter the signal received by the satellite sensor (Spitzer and Dirks 1987; Maritorena et al. 1994). This has the potential to influence the derived chlorophyll-*a* concentrations and possibly result in overestimated chlorophyll-*a* (Estep 1994). To assess whether seafloor reflection was likely to be an issue the dataset was split into two, with water depth of ≤ 20 m or > 20 m. This criterion resulted in a clear improvement in the relationships between MODIS and field-based chlorophyll-*a* measurements. The R^2 of the OC3M algorithm improved from 0.55 to 0.78, after excluding data from the shallower locations. Likewise the RMSE was

reduced from 41% to 26%. There were also great improvements for the Clark and GSM01 algorithms, which give R^2 values of 0.85 and 0.84 respectively, and RMSE errors of 18% and 25%. The Carder algorithm, however, still gave a poor R^2 value and large RMS errors, although the slope and intercept are improved and better than the other algorithms. Figure 4.6 and Table 4.2 show the regression statistics for all four algorithms after the data from the shallowest locations were removed.

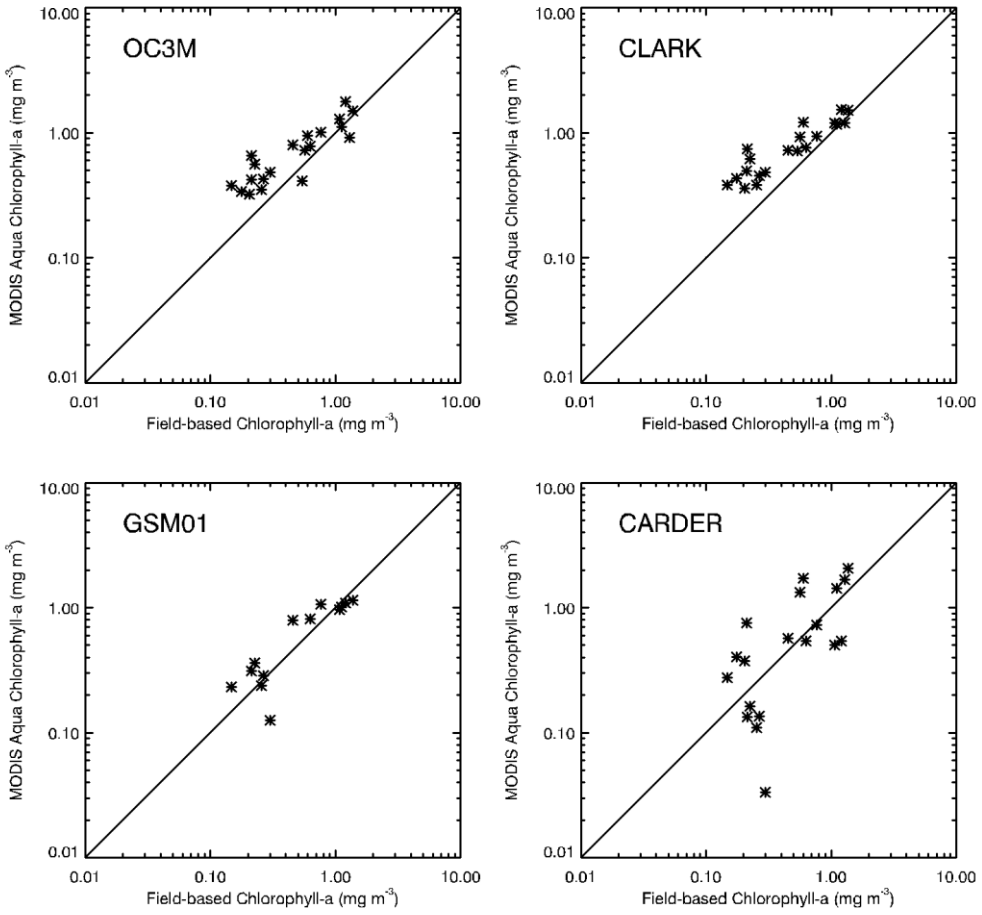

Figure 4.6: Relationship between MODIS OC3M, Clark, GSM01 and Carder chlorophyll-*a* algorithms and the Risk & Response field-based chlorophyll-*a* data, after excluding data from where the water depth was 20m or less.

Table 4.2: Regression statistics for MODIS OC3M, Clark, GSM01 and Carder chlorophyll-*a* algorithms and the Risk & Response field-based chlorophyll-*a* data, after excluding data from where the water depth was 20m or less.

Algorithm	N	R^2	p value	Slope	Intercept	RMSE (mg m^{-3})	RMSE (%)
OC3M	20	0.78	2.3×10^{-7}	0.88	0.25	0.20	26 %
CLARK	20	0.85	6.3×10^{-9}	0.84	0.32	0.15	18 %
GSM01	13	0.84	1.2×10^{-5}	0.81	0.15	0.16	25 %
CARDER	19	0.49	8.2×10^{-4}	1.0	0.11	0.46	64 %

The comparison between MODIS and field-based chlorophyll-*a* measurements around the Port Lincoln aquaculture region on 13th May 2008 shows only a moderate relationship. The R^2 between the OC3M and field-based chlorophyll-*a* was only 0.68, but the RMSE was reasonable at 21% indicating only a small spread in the data. The Clark chlorophyll-*a* algorithm performed slightly worse, with an R^2 of 0.56 and RMSE of 27%. There was a consistent overestimation by MODIS, possibly as a result of the water depth again influencing the MODIS chlorophyll-*a*, but removing shallower samples left insufficient data to analyse. Figure 4.7 shows the graphs of the May 2008 chlorophyll-*a* data against the OC3M and Clark chlorophyll-*a* data and Table 4.3 shows the regression statistics; no GSM01 or Carder chlorophyll-*a* values could be calculated for this date.

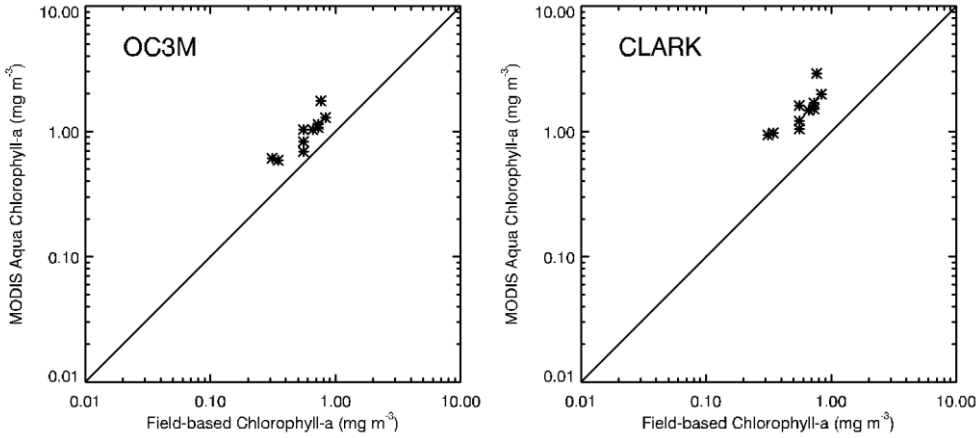

Figure 4.7: Relationship between MODIS OC3M and Clark chlorophyll-*a* algorithms and field-based chlorophyll-*a* data from May 2008 near Port Lincoln.

Table 4.3: Regression statistics for MODIS OC3M and Clark chlorophyll-*a* algorithms and field-based chlorophyll-*a* data from May 2008 near Port Lincoln.

Algorithm	N	R^2	p value	Slope	Intercept	RMSE (mg m^{-3})	RMSE (%)
OC3M	10	0.69	3.0×10^{-3}	1.7	-0.013	0.21	21 %
CLARK	10	0.56	1.3×10^{-2}	2.6	-0.0079	0.42	27 %

The data from the October 2008 IMOS cruise were collected both in coastal areas of Spencer Gulf and Investigator Strait, and also further offshore in deeper shelf waters. Including all data in the regression of MODIS OC3M and Clark chlorophyll-*a* against field-based chlorophyll-*a* showed no significant relationship (Figure 4.8). Both the GSM01 and Carder algorithms failed for the dates required. Although all of the stations were from locations where the water depth was greater than 20 m, there were a number of stations at depths of 20 – 26 m. When these stations were excluded, a much improved relationship

was found for the OC3M algorithm with an R^2 value of 0.89 and an RMSE of only 18% (Figure 4.9; Table 4.4). For the Clark algorithm, however, there remained a number of samples where MODIS overestimated chlorophyll-*a*, although the R^2 and RMSE values for the Clark algorithm were reasonable, 0.85 and 28% respectively (Table 4.4).

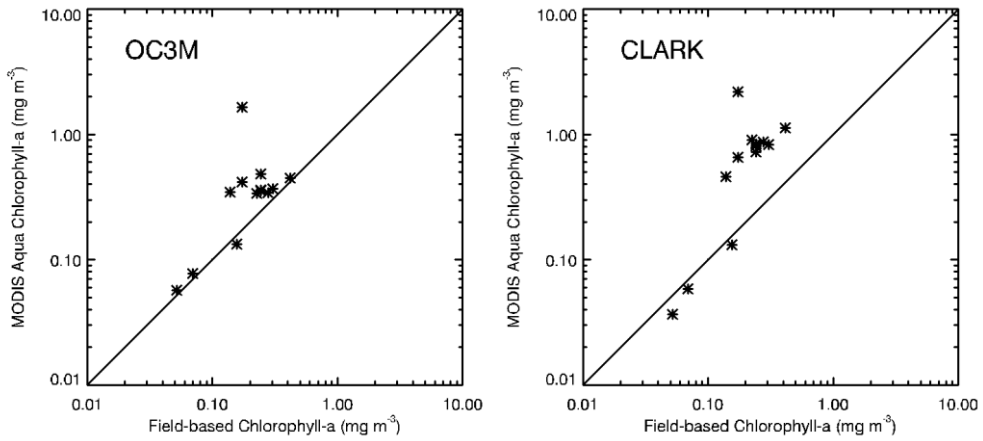

Figure 4.8: Relationship between MODIS OC3M and Clark chlorophyll-*a* and field-based chlorophyll-*a* data for the October 2008 IMOS cruise data, before removing data from the shallowest locations.

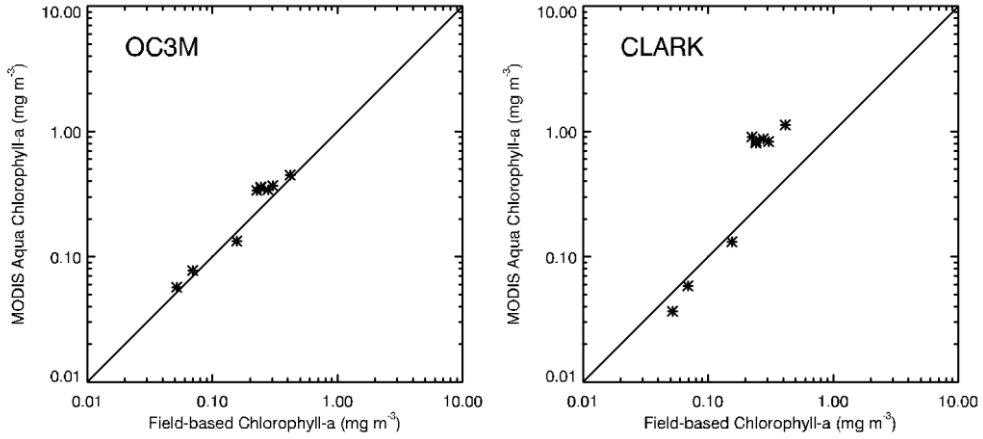

Figure 4.9: Relationship between MODIS OC3M and Clark chlorophyll-*a* and field-based chlorophyll-*a* data for the October 2008 IMOS cruise, after removing data from the shallowest locations.

Table 4.4: Regression statistics for MODIS OC3M and Clark chlorophyll-*a* and field-based chlorophyll-*a* data for the October 2008 IMOS cruise, before and after removing data from the shallowest locations.

Algorithm	N	R^2	p value	Slope	Intercept	RMSE (mg m^{-3})	RMSE (%)
OC3M (All)	13	0.025	0.61	0.64	0.28	0.41	99 %
OC3M (> 26m)	9	0.89	1.2×10^{-4}	1.2	0.011	0.050	18 %
CLARK (All)	13	0.23	0.095	2.7	0.17	0.51	69 %
CLARK (> 26m)	9	0.85	3.7×10^{-4}	3.4	-0.13	0.17	28 %

Chlorophyll-*a* data collected from the January 2009 IMOS cruise agree well with MODIS chlorophyll-*a* concentrations for the OC3M, Clark and Carder algorithms. The GSM01 algorithm again failed for the dates required. The relationship between the field-based and MODIS datasets is stronger than for any of the other datasets analysed, with R^2 values of 0.93, 0.84 and 0.96 for the three algorithms respectively (Figure 4.10; Table 4.5). The good agreement between the datasets on this occasion may be due to the fact that all samples were taken from deeper waters (~43m or deeper) and thus the affects of shallow water observed with previous datasets were not seen on this occasion.

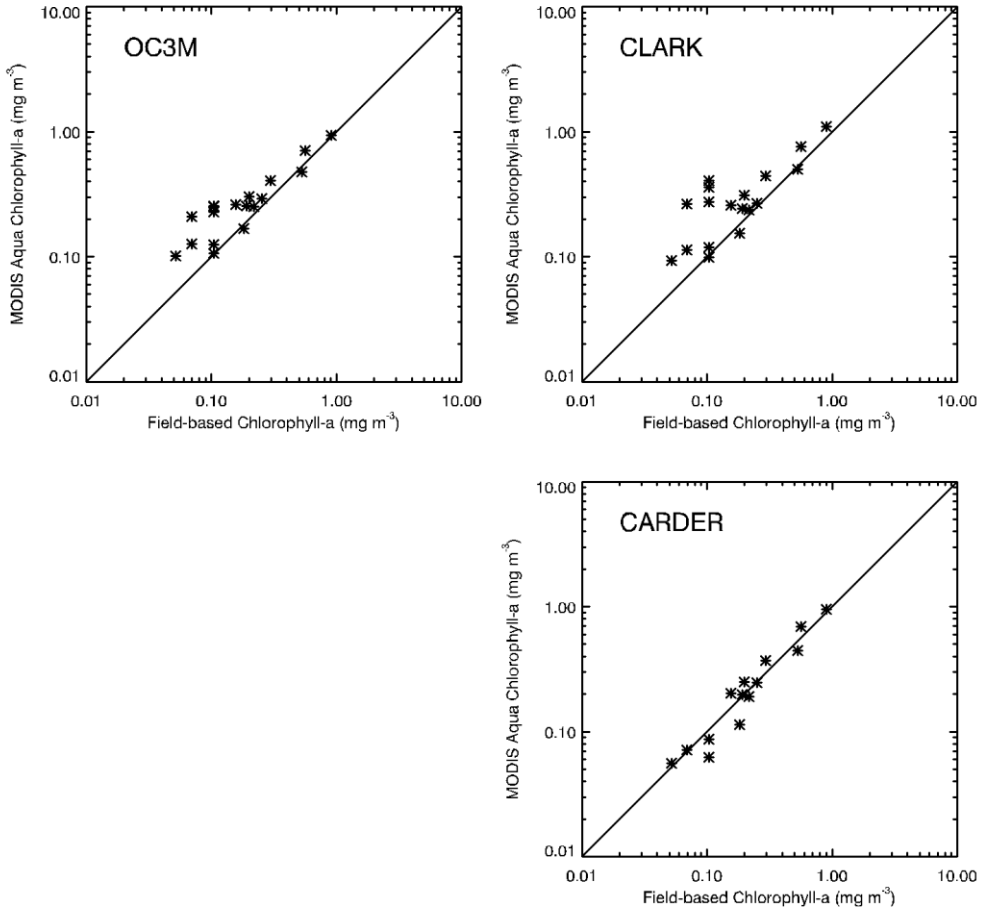

Figure 4.10: Relationship between MODIS OC3M, Clark and Carder chlorophyll-*a* and field-based chlorophyll-*a* data for the January 2009 IMOS cruise.

Table 4.5: Regression statistics for MODIS OC3M, Clark and Carder chlorophyll-*a* and field-based chlorophyll-*a* data for the January 2009 IMOS cruise.

Algorithm	N	R^2	p value	Slope	Intercept	RMSE (mg m^{-3})	RMSE (%)
OC3M	18	0.93	2.0×10^{-10}	0.93	0.084	0.061	20 %
CLARK	18	0.84	8.6×10^{-8}	1.0	0.089	0.10	31 %
CARDER	14	0.96	1.3×10^{-9}	1.1	-0.013	0.056	20 %

The final dataset consists of the chlorophyll-*a* data collected from the eastern Great Australian Bight (GAB) by van Ruth (2009). A point to note is that the GAB dataset was collected for purposes other than this present study, and hence the chlorophyll-*a* measurements were collected from a depth of 3 metres rather than at the immediate sea surface as with the previously examined datasets. The relationship between the GAB chlorophyll-*a* data and the MODIS chlorophyll-*a* data using all data points is rather poor with R^2 values of 0.33 or less for all the algorithms and RMS errors of 70% or greater, with the exception of the GSM01 algorithms which had an RMSE of 41% but still had a poor R^2 of 0.24 (Figure 4.11; Table 4.6). Unlike the previous datasets, where the errors have come primarily from MODIS overestimating chlorophyll-*a*, for the data collected from the GAB the majority of the errors are from MODIS underestimating the corresponding field-based chlorophyll-*a* measurement.

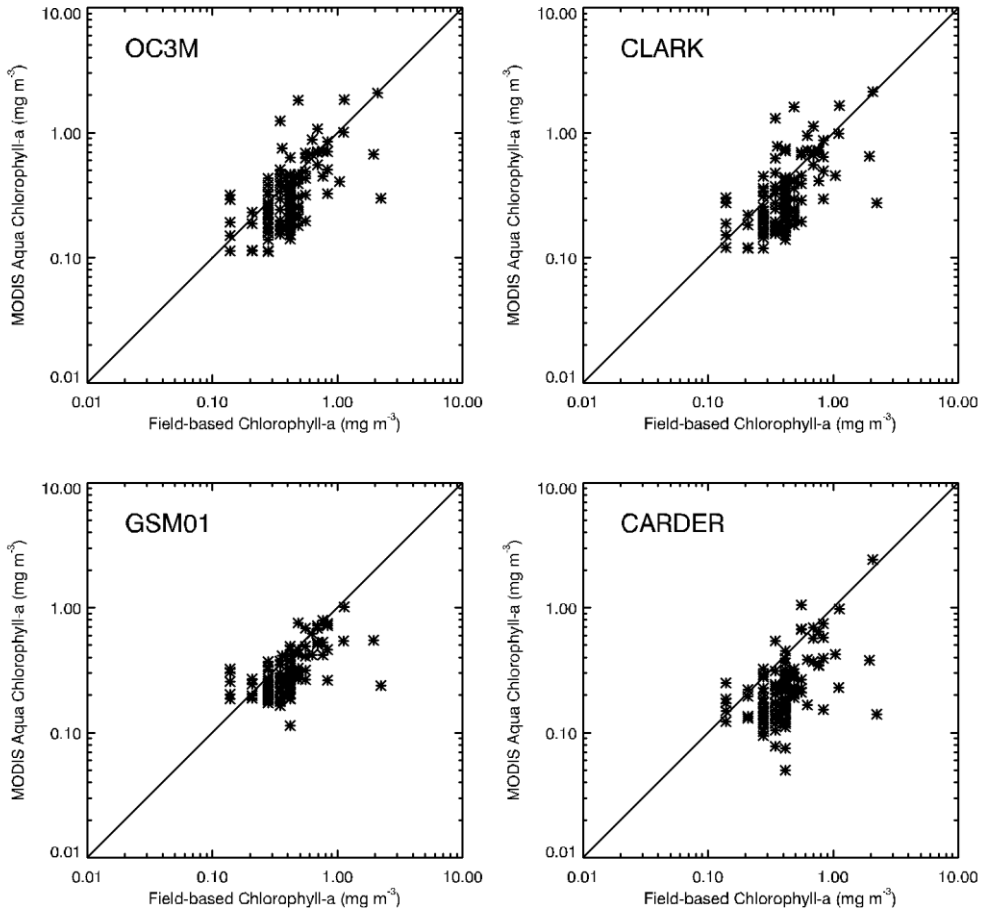

Figure 4.11: Relationship between MODIS OC3M, Clark, GSM01 and Carder chlorophyll-*a* and field-based chlorophyll-*a* data for the GAB dataset. The apparent quantisation of field-based values is due to limited precision in the field-based method.

Table 4.6: Regression statistics for MODIS OC3M, Clark, GSM01 and Carder chlorophyll-*a* and field-based chlorophyll-*a* data for the GAB dataset.

Algorithm	N	R^2	p value	Slope	Intercept	RMSE (mg m^{-3})	RMSE (%)
OC3M	127	0.31	1.4×10^{-11}	0.56	0.11	0.26	70 %
CLARK	127	0.31	1.3×10^{-11}	0.56	0.11	0.26	71 %
GSM01	120	0.24	1.3×10^{-8}	0.27	0.20	0.14	41 %
CARDER	127	0.33	1.3×10^{-12}	0.47	0.049	0.21	78 %

There may be a number of reasons why the field-based chlorophyll-*a* data from the eastern Great Australian Bight and the corresponding MODIS chlorophyll-*a* data are not matching up as well as expected. Firstly the depth at which the field data were collected was 3 m, and thus they may not reflect surface chlorophyll-*a* concentrations. With no data relating the chlorophyll-*a* at a depth of 3 m to that at the surface, it is not possible to determine what impact this may have on the comparison between MODIS and field-based chlorophyll-*a* concentrations. Large overestimates by MODIS appear to occur primarily near the coast, while large underestimates are mostly in offshore waters (Figure 4.12). Perhaps the overestimates in coastal areas are related to bottom reflectance, while the underestimates in deeper offshore waters may be related to unknown sub-surface chlorophyll-*a* profiles.

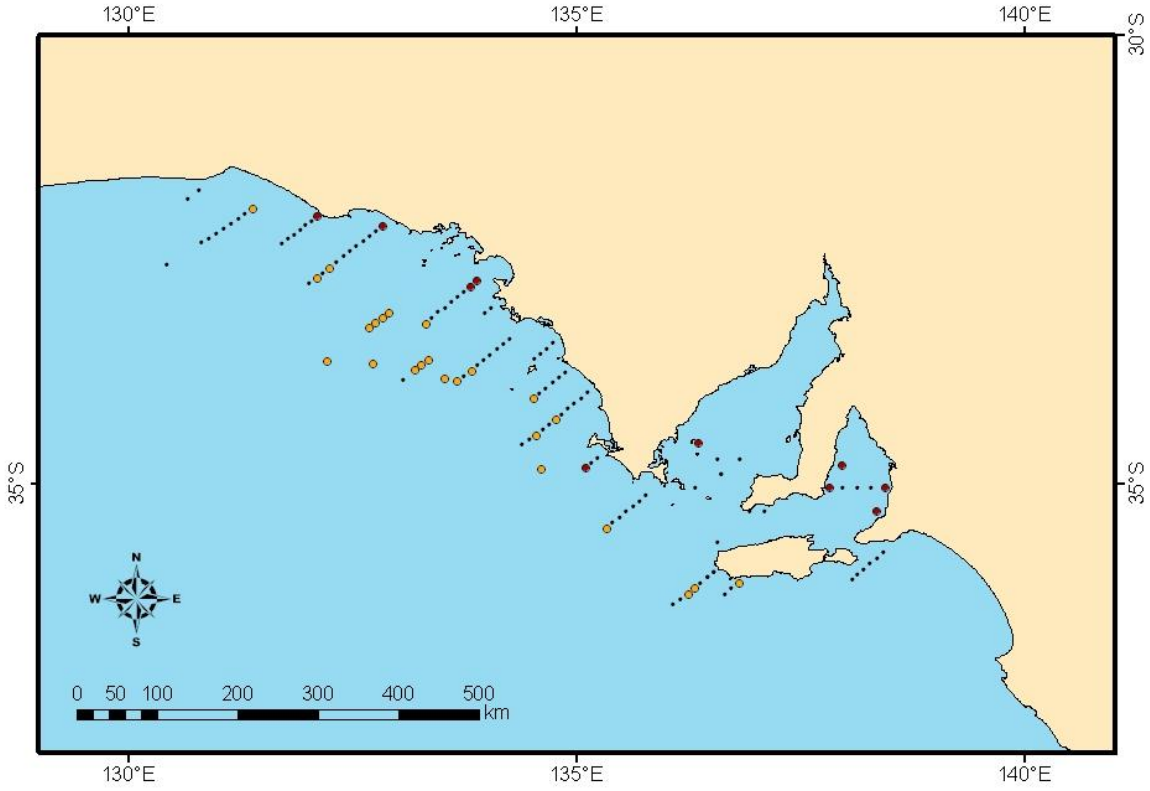

Figure 4.12: The locations of stations used in the GAB dataset, coloured stations show where the errors between the MODIS and field-based datasets are greater than 50%. Yellow stations are where MODIS underestimated, and red stations are where MODIS overestimated.

The GAB dataset was collected over three years, in February/March of 2004, 2005 and 2006. There are considerable differences in the relationship between MODIS OC3M and the field-based chlorophyll-*a* between years (Figure 4.13; Table 4.7). The only year where a significant relationship is observed is 2005, with very poor relationships for 2004 and 2006. For the measurements where there was greater than a 50% error between MODIS OC3M and field-based chlorophyll-*a*, 22 out of the 24 underestimates by MODIS OC3M occurred in either 2004 or 2006. No annual dependence was observed for the overestimated data. Reasons why there were such large errors between the data sources in 2004 and 2006, are unknown, but perhaps related to variations in the sub-surface chlorophyll-*a* profiles.

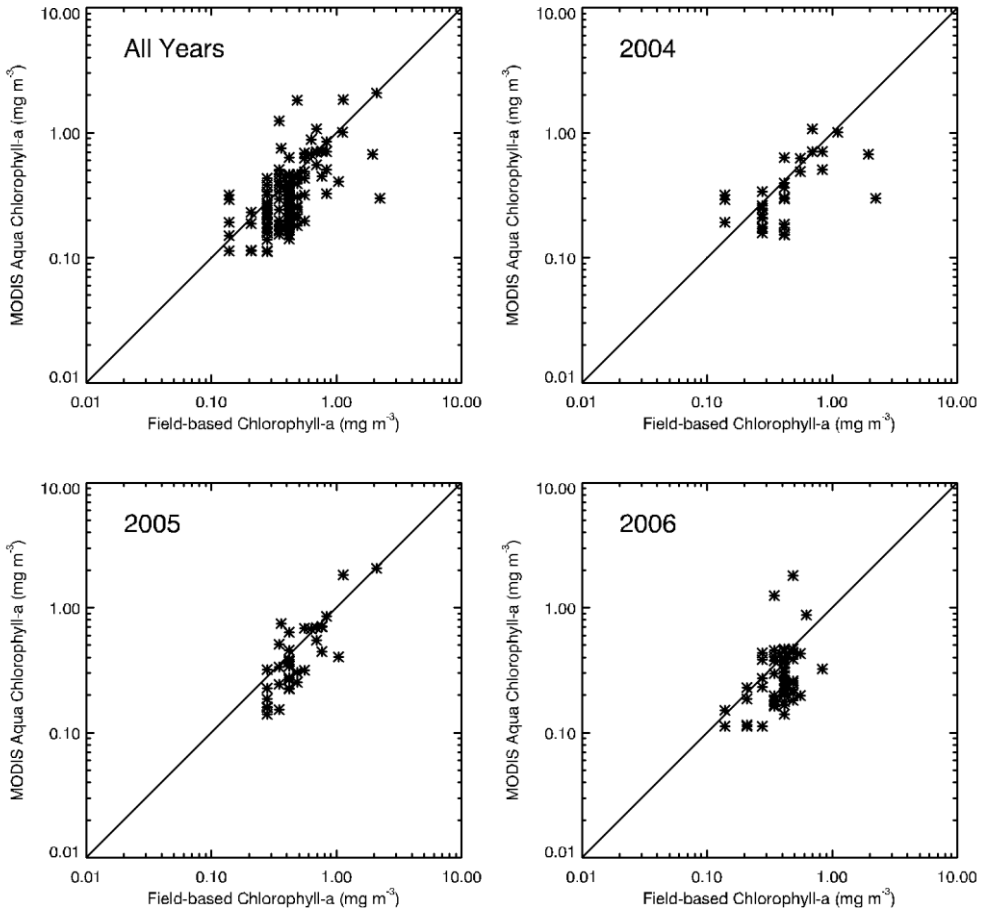

Figure 4.13: Relationship between MODIS OC3M chlorophyll-*a* and field-based chlorophyll-*a* data for the GAB data separated by year.

Table 4.7: Regression statistics for MODIS OC3M chlorophyll-*a* and field-based chlorophyll-*a* data for the GAB dataset separated by year.

OC3M	N	R^2	p value	Slope	Intercept	RMSE (mg m^{-3})	RMSE (%)
All Years	127	0.31	1.4×10^{-11}	0.56	0.11	0.26	71 %
2004	33	0.21	0.0071	0.24	0.24	0.21	60 %
2005	36	0.74	2.1×10^{-11}	1.0	-0.077	0.21	44 %
2006	58	0.071	0.043	0.62	0.070	0.26	84 %

4.3.2 MODIS v Field-based Sea Surface Temperature

The relationship between MODIS Aqua standard day-time (11 µm) sea surface temperature imagery and temperature measurements taken in the field around the tuna farming region east of Port Lincoln from the Risk and Response dataset was strong (R^2 = 0.94, RMSE 2.8%) (Figure 4.14; Table 4.8). MODIS SST measurements followed the field-based measurements well, with the exception of a few samples where there was some over-estimation by MODIS. The slight differences that are observed may be a result of the

satellite-based SST measurement coming from the immediate surface of the ocean, whereas the field-based CTD temperature measurement was taken at approximately 1 m below the surface. The regression shows a positive bias towards MODIS of 0.92 °C, this is likely to be influenced by just a few measurement points where MODIS over-estimated by a significant amount.

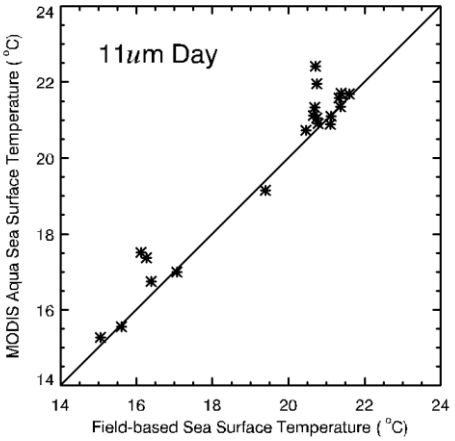

Figure 4.14: Relationship between MODIS Aqua standard day-time SST estimations and SST measurements obtained in the field at a depth of ~1 metre.

Table 4.8: Regression statistics for MODIS Aqua standard day-time SST estimations and SST measurements obtained in the field at a depth of ~1 metre.

MODIS SST	N	R^2	p value	Slope	Intercept	RMSE (ºC)	RMSE (%)
Day SST (11μm)	20	0.94	9.0×10^{-13}	0.97	0.92	0.56	2.8 %

MODIS Aqua and Terra day-time 11 μm, night-time 11 μm and night-time 4 μm sea surface temperatures were compared to field-based CTD temperatures from a depth of between 1 and 3 metres collected from the IMOS cruises. MODIS day-time SST shows good agreement with the CTD temperature data ($R^2 = 0.95$, RMSE = 2.27%) (Figure 4.15; Table 4.9). While the MODIS temperatures followed the field-based dataset well, there was slight overestimation by MODIS relative to the CTD-based temperatures, which is likely due to the sampling depth of the CTD measurements used. Night-time MODIS SST measured at 11 μm also compared well against the CTD data ($R^2 = 0.92$, RMSE = 2.01%). The night-time 4 μm SST performed the best out of the three methods ($R^2 = 0.96$, RMSE = 1.48%). All three methods show some overestimation of the MODIS SST relative to the CTD-measured temperature, which is particularly evident at the warmer end of the temperature range observed, but this may be a symptom of more data being available from the summer months.

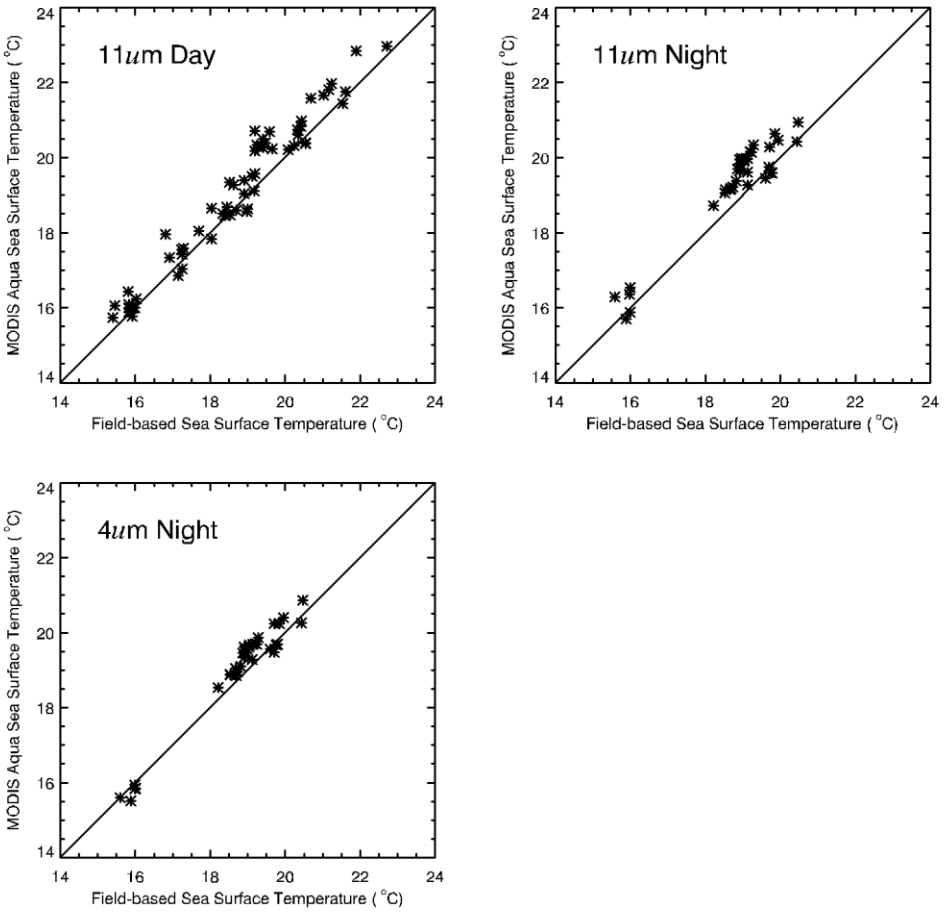

Figure 4.15: Relationship between MODIS day-time SST at 11 µm, night-time SST at 11 µm, night-time SST at 4 µm and field-based CTD temperature measurements.

Table 4.9: Regression statistics for MODIS day-time SST at 11 µm, night-time SST at 11 µm, night-time SST at 4 µm and field-based CTD temperature measurements.

MODIS SST	N	R^2	p value	Slope	Intercept	RMSE (ºC)	RMSE (%)
Day SST (11µm)	61	0.95	5.6×10^{-41}	1.1	-0.56	0.43	2.3 %
Night SST (11µm)	36	0.92	2.4×10^{-20}	1.0	-0.079	0.39	2.0 %
Night SST (4µm)	36	0.96	1.1×10^{-25}	1.1	-1.6	0.28	1.5 %

4.3.3 Spatial and Temporal Variability in Chlorophyll-*a*

Surface chlorophyll-*a* variability showed large variations in concentrations within areas less than the instantaneous field of view (IFOV) of the MODIS sensor of approximately 1 km. Along the transect conducted on the 8th May 2007 the chlorophyll-*a* concentrations of the 65 measurements ranged from 0.83 up to 1.95 µg L^{-1} (mean = 1.45 µg L^{-1}, SD = 0.29 µg L^{-1}). The range of over 1 µg L^{-1} within a distance of only 5.5 km indicates the highly variable nature of chlorophyll-*a* concentrations on a localised-scale (Figure 4.16). The transect sampled on 13th May 2008 confirmed the findings from 2007, again with a large range in concentrations observed over a small area. On this occasion concentrations of the 32 measurements ranged from 0.87 up to 1.49 µg L^{-1} (mean = 1.14 µg L^{-1}, SD = 0.16 µg L^{-1}) (Figure 4.17). The range of values observed on this occasion was not as large as the previous transect, but the distance covered of 2.4 km was less. If we consider a small section of the 2007 transect covering an area of just 500 m, we observe a range of chlorophyll-*a* concentrations from 0.83 up to 1.88 µg L^{-1} (Figure 4.18). Therefore a very large range in values is observed in an area less than the MODIS IFOV and this is likely to have a large impact on the validation of MODIS measurements.

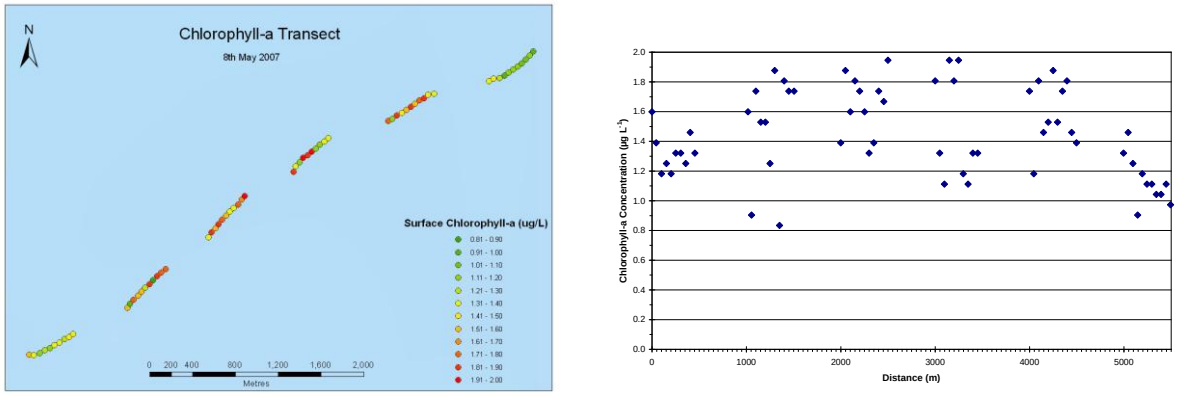

Figure 4.16: Fine-scale surface field-based chlorophyll-*a* transect on 8/5/07 nearby to Port Lincoln in Spencer Gulf showing the high spatial variability in surface chlorophyll-*a*.

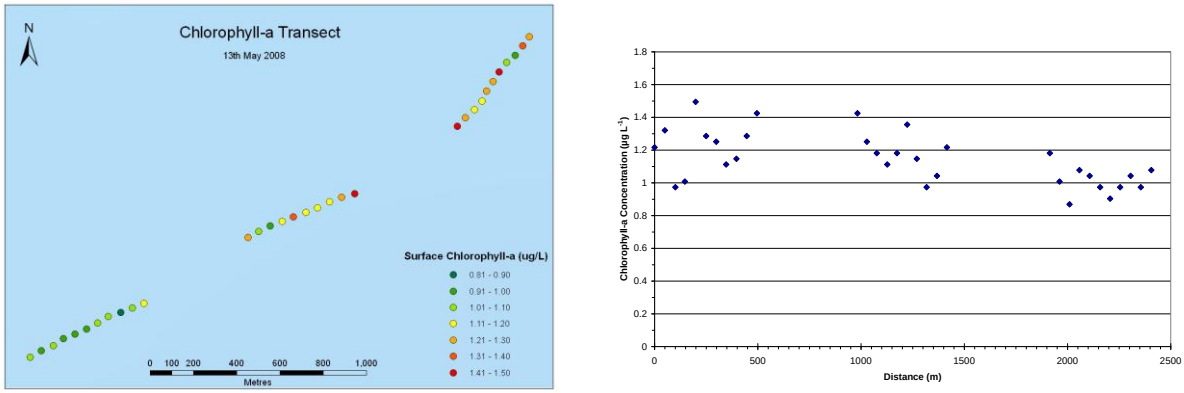

Figure 4.17: Fine-scale surface field-based chlorophyll-*a* transect on 13/5/08 nearby to Port Lincoln in Spencer Gulf showing the high spatial variability in surface chlorophyll-*a*.

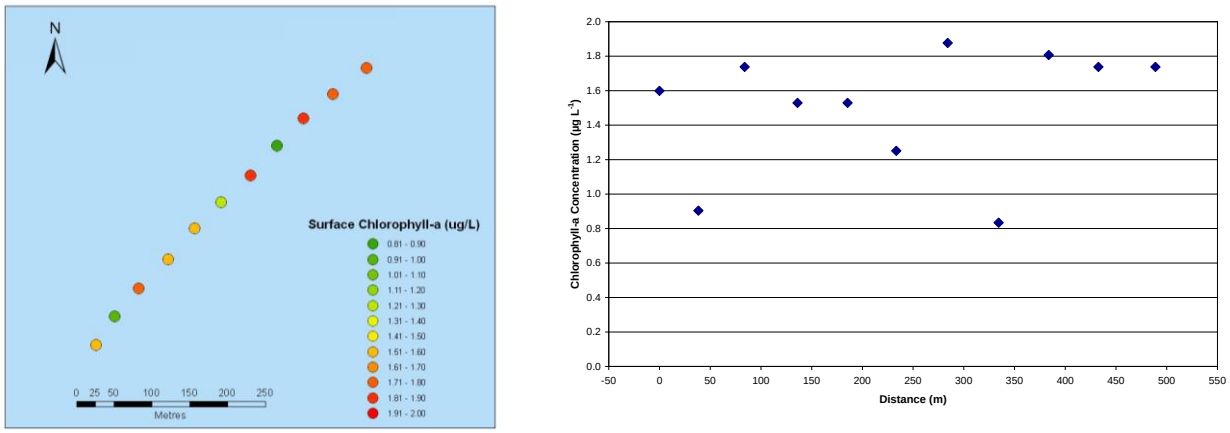

Figure 4.18: A portion of the fine-scale surface field-based chlorophyll-*a* transect on 8/5/07 showing the high spatial variability in surface chlorophyll-*a* over a small distance of just 500m.

Temporal variation in field-based surface chlorophyll-*a* concentrations was measured on 17th October 2008 in northern Spencer Gulf over 7 hours (only slightly longer than the 6 hour window allowed for each MODIS image). Concentrations measured between 9:30 am and 4:30 pm range from 0.17 up to 0.31 µg L^{-1}, (mean = 0.24 µg L^{-1}, SD = 0.05 µg L^{-1}) (Figure 4.19). The range of values on this occasion is small, but considering the low concentrations on this date shows that the variation over a day can be significant. Therefore considering the temporal gap between field-based and MODIS measurements when conducting a validation may be important when interpreting results.

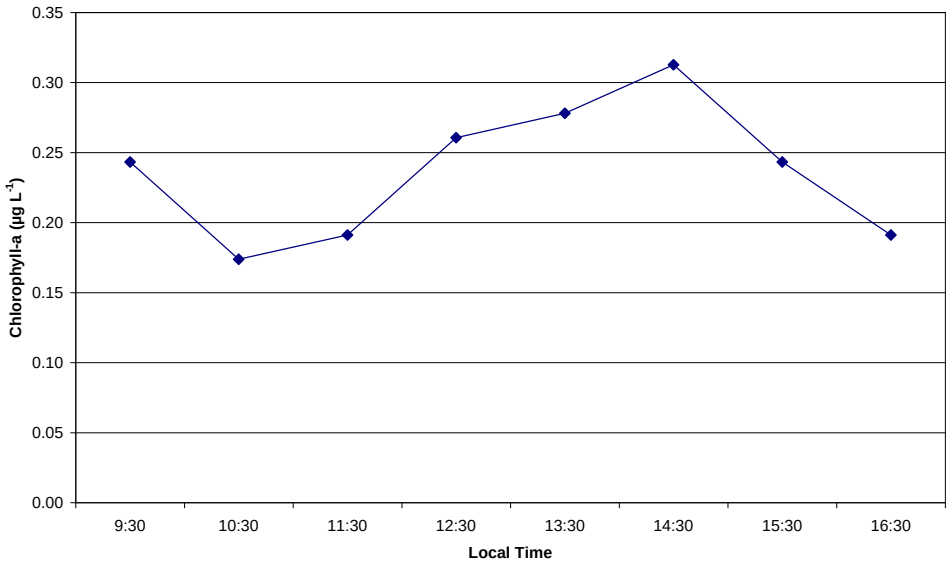

Figure 4.19: Surface field-based chlorophyll-*a* measurements at the same location in northern Spencer Gulf on 17/10/08 showing the variability in chlorophyll-*a* within a day.

4.4 Discussion

4.4.1 Chlorophyll-*a*

MODIS chlorophyll-*a* products have been assessed by previous studies in other parts of the world. Pinkerton et al. (2005) investigated the performance of a number of band-ratio chlorophyll-*a* algorithms developed for different platforms in the waters around New Zealand. They considered algorithms for MODIS, SeaWiFS, CZCS, OCTS, MERIS and GLI and tested how well different algorithms for each of these satellite sensors compared to *in situ* chlorophyll-*a* data collected from a number of regions including the New Zealand continental shelf, the subantarctic waters east of New Zealand and the subtropical front. They applied the ocean colour algorithms to measurements of surface reflectance to compare with the *in situ* HPLC-derived chlorophyll-*a* concentrations, rather than using satellite-derived chlorophyll-*a* estimates, thus they only assessed the performance of the algorithm, and not errors arising from sensor performance and calibration or inaccurate atmospheric correction procedures. Of the algorithms evaluated, only the empirical Clark algorithm was assessed for MODIS, with the OC3M MODIS algorithm not considered to be independent of the SeaWiFS OC4v4, which was tested. Overall it was considered that all the algorithms in question agreed well with the *in situ* measurements of chlorophyll-*a*. The MODIS Clark algorithm produced root mean square errors (RMSE) of 5.4%, 9.0%, 11.9% and 14.4% for the subtropical waters, subantarctic waters, shelf waters and subtropical front waters respectively. The larger errors in the sub tropical front region were as a result of an underestimation by all of the algorithms compared to *in situ* chlorophyll-*a*. In comparison, the OC4v4 algorithm showed RMSE very similar to the MODIS Clark algorithm, with an exception in the shelf waters where the RMSE was reduced to just 4.3% for OC4v4 compared to 11.9% for Clark. The performance of the OC4v4 algorithm in the shelf waters was the best of all of the eight algorithms in each of the four regions.

Pinkerton et al. (2005) showed promising results for chlorophyll-*a* algorithms in the Case 1 waters of New Zealand, but the results of Darecki and Stramski (2004) for the complex Case 2 waters of the Baltic Sea were rather poor. They assessed the performance of the CZCS pigment algorithm for MODIS, the Clark empirical MODIS algorithm, the OC3M MODIS algorithm, the Carder semi-analytical MODIS algorithm and the OC4v4 SeaWiFS algorithm. They applied the algorithms to in-water and above-water radiometric measurements and compared the outputs to *in situ* chlorophyll-*a* concentrations and found

that the MODIS and SeaWiFS pigment algorithms significantly overestimated chlorophyll-*a* concentrations. Very poor results, with RMS errors well in excess of 100%, were obtained for all the algorithms. It was concluded that all of the algorithms tested were unacceptable for use in the complex waters of the Baltic Sea due to the influences of coloured dissolved organic matter (CDOM).

Garcia et al. (2006) tested the performance of the empirical OC4v4 algorithm and the semi-analytical GSM01 and Carder algorithms in the south-western Atlantic off the eastern coast of South America. Algorithm-derived chlorophyll-*a* was produced from ship-borne measurements of upwelling radiances and compared to *in situ* chlorophyll-*a* measurements. The GSM01 algorithm performed the best against *in situ* data with an R^2 of 0.86, although chlorophyll-*a* was overestimated in turbid waters. The Carder algorithm showed the greatest errors, with an R^2 of just 0.39, while the empirical OC4v4 performed reasonably well with R^2 of 0.82. Garcia et al. (2006) also compared *in situ* chlorophyll-*a* measurements with actual satellite-derived chlorophyll-*a* estimations from SeaWiFS for summer and winter datasets. In winter, OC4v4 and Carder performed well, while GSM01 underestimated chlorophyll-*a*. In summer though, Carder continued to perform well and GSM01 performed better while OC4v4 overestimated chlorophyll-*a*. Neither of the algorithms tested performed consistently well against the *in situ* data, with the Carder algorithm performing well in both seasons but producing many outliers when the ship-borne radiance data was used.

Carder et al. (2004) assessed the performance of the Carder MODIS semi-analytical chlorophyll-*a* algorithm and the OC3M empirical algorithm by comparing MODIS/Terra chlorophyll-*a* estimates with *in situ* chlorophyll-*a* concentrations from SeaWiFS SeaBASS data archive collected in the Antarctic, Equatorial Pacific, Californian Current, western mid-pacific, and the West Florida Shelf (Werdell and Bailey 2005). RMS error results for the OC3M empirical and Carder semi-analytical algorithms for the whole dataset are 41% and 40% respectively, with the accuracy of the Carder algorithm improving to 21% by removal of data from continental shelves. The results of this study indicate that continental shelf waters may be a potential source of error in the Carder algorithm, which may help explain the poor results obtained in the present study for the Carder algorithm.

These and other previous studies have identified some potential sources of error within satellite-derived chlorophyll-*a* measurements. For example Darecki and Stramski (2004)

identified that large concentrations of coloured dissolved organic matter (CDOM) are likely to be responsible for frequent over-estimations of MODIS chlorophyll-*a* in the Baltic Sea, as did Tang et al. (2008) for the South China Sea. Garcia et al. (2005) suggested continental river discharge as a source of error in MODIS chlorophyll-*a* estimates in the southwest Atlantic. Gregg and Casey (2004) suggested that CDOM from tropical river discharge and also dust in the atmosphere may be responsible for poor performance of SeaWiFS chlorophyll-*a* in the equatorial Atlantic and Indian oceans.

One of the likely sources of apparent error between the MODIS and field-based chlorophyll-*a* datasets examined in this study is spatial variability in chlorophyll-*a* concentrations. Results from both of the fine-scale transects of chlorophyll-*a* near Port Lincoln identified considerable variation in field-based surface chlorophyll-*a* measurements over small distances. MODIS chlorophyll-*a* imagery calculates an average chlorophyll-*a* estimate for an area of 1 km^2. Furthermore, in this study an array of 3 by 3 pixels was used to give an average over 9 km^2. In contrast the field-based chlorophyll-*a* data comes from a single point measurement. Thus, where considerable spatial variability in chlorophyll-*a* occurs, as observed near Port Lincoln, there is likely to be greater observed error between the datasets when the field-based measurement is not representative of the surrounding area. This variation in the scale of the measurements being compared will result in observed discrepancies between the datasets, but this does not equate to an error in the MODIS chlorophyll-*a* estimate. Yuan et al. (2005) also investigated in-pixel variability in chlorophyll-*a* in the Gulf of Mexico and demonstrated how large in-pixel variability can increase the apparent error between *in situ* and satellite data. Temporal variability in surface chlorophyll-*a* would also result in increased apparent errors when large changes in concentration occur between the time of field sample collection and the satellite overpass. Attempts to minimise the influence of temporal variability were made in this study by using a window of ±3 hours between sample collection and satellite overpass as suggested by Bailey and Werdell (2006).

Another source of error that could arise between the field-based and MODIS chlorophyll-*a* estimates are errors in the field-based chlorophyll-*a* method. In the analysis of the performance of MODIS chlorophyll-*a* we have taken our field-based datasets to be our „ground-truth" measurements. But errors in this dataset can lead to apparent errors in the MODIS-derived chlorophyll-*a*. Unfortunately, insufficient data has been collected to assess the variability in the methodology to identify erroneous measurements in the field-

based datasets. But it must be recognised that errors in the field data will result in apparent errors in MODIS chlorophyll-*a* when the datasets are compared. Measurement error could also contribute to the apparent variation in chlorophyll-*a* over small distances, and as such the fine-scale chlorophyll-*a* variability may not be as large as the results suggest. One of the known limitations to the chlorophyll-*a* analysis method used for the majority of the field-based data used in this study is the precision of the spectrophotometer. The spectrophotometer used here records the absorbance to just three decimal places, and as a result is unable to resolve small variations in concentration. The influence of this can be seen in Figure 4.11, where there are large numbers of measurements with the same field-based chlorophyll-*a* values but different MODIS chlorophyll-*a* values. Hence the precision or sensitivity of the field-based chlorophyll-*a* method may also result in more apparent errors in the MODIS chlorophyll-*a* when the field-based data is assumed to be truth.

Errors in the MODIS estimates can arise due to other constituents of the water such as coloured dissolved organic matter (CDOM) and suspended particulate matter (SPM). A number of studies have identified CDOM as a contributing factor for poor performance of satellite chlorophyll-*a* estimates (Darecki and Stramski 2004; Gregg and Casey 2004; Tang et al. 2008). CDOM has been shown to have considerable impacts on the absorption of light in the visible wavelengths where the chlorophyll-*a* absorption features occur and therefore absorption due to CDOM can have significant impacts on satellite measurements of chlorophyll-*a* (Bricaud et al. 1981; Carder et al. 1989; Nieke et al. 1997). The source of CDOM in ocean waters is either from terrestrial runoff in coastal waters or from the degradation of phytoplankton. In the region of interest for this study there is very little terrestrial runoff, thus we could expect that CDOM from these sources is likely to be minimal. However, there is no information regarding CDOM concentrations in the area and thus we are not able to quantify the impact of CDOM on MODIS chlorophyll-*a* estimates in the region. Suspended particulate matter (SPM), either terrestrially-derived sediments from river discharge or wind-borne dust or seafloor sediments stirred up by the action of wind and waves, can also impact upon satellite estimates of chlorophyll-*a* due to changes in absorption and scattering in the water column (Stramski et al. 2004). Particulates from different sources, such as terrestrially derived clays and resuspended sand from the seafloor, will have different influences upon satellite observations. Tzortziou et al. (2007) showed how non-algal particles contributed to poor performance of MODIS chlorophyll-*a* algorithms due to high backscattering of the suspended particulates. The influence of suspended material on MODIS imagery in our study regions is unknown, but

likely to be a contributing source of error, at least in the shallow waters near Port Lincoln where fine seafloor sediments can potentially be mobilised given winds and swell of sufficient energy (Fernandes et al. 2006). Wind-borne dust may also be a potential source of SPM, due to the dry semi-arid regions to the north of Spencer Gulf.

Another consideration is the depth penetration of light in the upper ocean. Gordon and McCluney (1975) define the penetration depth of light in the sea as „the depth above which 90% of the diffusely reflected irradiance (excluding specular reflectance) originated", which for a homogeneous ocean is the depth at which the downwelling in-water irradiance falls to 1/e (~36.8%) of its value at the surface; also known as the first optical depth. This depth is dependant upon the wavelength of the light and the water clarity. The penetration depth influences satellite estimates of chlorophyll-*a* in two ways. Firstly, where the penetration depth (or apparent optical depth, AOD) is greater than the physical depth of water the water can be described as „optically shallow" (Bailey and Werdell 2006) and the satellite-observed water-leaving radiances may include a contribution of reflected radiance from the seafloor (Spitzer and Dirks 1987; Estep 1994; Maritorena et al. 1994). The contribution of seafloor reflectance to measurements of water-leaving radiance will depend upon the combined influences of the water depth, the depth of light penetration and the albedo of the seafloor (Estep 1994; Maritorena et al. 1994). The maximum penetration depth is inversely proportional to the absorption coefficient of the water (Gordon and McCluney 1975). Bailey and Werdell (2006) showed that the apparent optical depth (AOD) in metres can be estimated from MODIS observations of the diffuse attenuation coefficient at 490 nm (K_{490}) via Equation 4.2:

$$AOD = 1.3 / K_{490} \tag{4.2}$$

The MODIS Aqua K_{490} monthly climatology imagery shows that for the Port Lincoln, region where shallow water depth has been identified as a contributing factor to MODIS chlorophyll-*a* accuracies, the downwelling diffuse attenuation coefficient values range between approximately 0.06 and 0.11 m^{-1}. From Equation (4.2) and these mean K_{490} values for the region we see that the approximate apparent optical depths are between 11.82 and 21.67 m. The greater optical depths occur in spring and summer where chlorophyll-*a* concentrations are a minimum in the region and shallower optical depths in autumn and winter when the concentrations of chlorophyll-*a* are greater (See Chapter 5 on seasonal variability). Thus with water depths of between 15 and 25 m, it is evident that bottom reflectance can occur in the region offshore from Port Lincoln, particularly in periods when

chlorophyll-*a* is lower and thus the water is clearer, causing overestimation of MODIS chlorophyll-*a*.

The second way in which light penetration in the ocean influences satellite chlorophyll-*a* estimates is where chlorophyll-*a* is not vertically homogeneous in the water column. Gordon and Clark (1980) demonstrate that the satellite estimates of chlorophyll-*a* concentration are related to the vertical profile of chlorophyll-*a* in the water column by Equation 4.3:

$$C_{sat} = \frac{\int_0^{Z_{90}} C(Z).g(Z).dZ}{\int_0^{Z_{90}} g(Z).dZ} \tag{4.3}$$

where C_{sat} is the satellite observed chlorophyll-*a*, C(Z) is the chlorophyll-*a* concentration as a function of depth, Z_{90} is the light penetration depth, and g(Z) is a weighting term related to the attenuation coefficient. Thus the satellite observations of chlorophyll-*a* are not equal to the surface concentration, but a weighted mean over the light penetrating depth of the water column. Smith (1981) has discussed how significant changes to a vertical chlorophyll-*a* profile below depths of a few attenuation lengths without a corresponding change in the surface concentration will be overlooked by satellite estimates due to the weighting as a function of light attenuation in the water column favouring shallow depths. Xiu et al. (2008) were able to show that two areas of ocean with the same surface chlorophyll-*a*, but different vertical chlorophyll-*a* profiles, can produce different satellite-based estimations of chlorophyll-*a*.

Another potential source of error in the validation process may be differences in the range of concentrations for which the algorithms were designed and the concentrations observed in the study region. Oceanic waters can be classified as either oligotrophic, where chlorophyll-*a* is less than 0.1 mg m^{-3}, mesotrophic, where chlorophyll-*a* is between 0.1 and 1.0 mg m^{-3}, or eutrophic, when chlorophyll-*a* is greater than 1.0 mg m^{-3} (Antoine et al. 1996). In the region of interest for this study, Spencer Gulf and nearby coastal waters of South Australia, surface chlorophyll-*a* concentrations are typically within the mesotrophic classification. From the combined field-based chlorophyll-*a* datasets used in this study, 90.6% of the samples are within the mesotrophic classification, while only 2.5% are oligotrophic and 6.9% are eutrophic. The *in situ* dataset used to calibrate the OC4v4 algorithm consists of chlorophyll-*a* concentrations across all three classifications and the

range of values observed in this region are well represented in the dataset (O'Reilly et al. 2000). Thus, at least for the case of the OC4v4/OC3M algorithm, the observed chlorophyll-*a* concentrations are within the range for which the method was designed and hence we would not expect this to result in errors of the satellite-based chlorophyll-*a* estimates.

The atmospheric correction of the upwelled radiances is a necessary step to determine accurate chlorophyll-*a* concentrations from space. Of the upwelled radiance signal observed by a satellite sensor, the water-leaving signal we are interested in for chlorophyll-*a* estimations is less than 10% of the total signal (Gordon and Morel 1983; cited in Esaias et al. 1998). The majority of the signal, which originates from the atmosphere, needs to be filtered out via atmospheric correction to leave behind just the ocean signal as would be observed immediately below the sea surface. Gordon and Wang (1994) and Gordon (1997) review the concepts of atmospheric correction for ocean colour imagery and Gordon and Voss (1999) describe in detail the algorithms applied for atmospheric correction of MODIS ocean imagery as processed in SeaDAS. Atmospheric influences that are not taken into account correctly, such as scattering by aerosols or absorption by gases, will escalate into errors in the satellite-based chlorophyll-*a* estimate. Bailey and Werdell (2006) conducted a validation of SeaWiFS water-leaving radiances to assess the performance of atmospheric correction and found that uncertainties in the order of 9 to 19% occur with slightly better results (6 – 12%) for the deep ocean compared to coastal regions. Wang et al. (2009) showed that the overall correlation coefficient between *in situ* water-leaving radiances and MODIS atmospherically corrected satellite-derived water-leaving radiances was 0.910, equivalent to an R^2 of 0.828. Thus, while the atmospheric correction procedures to calculate normalised water-leaving radiances work reasonably well, errors do exist that can manifest into errors in the calculations of chlorophyll-*a* that rely upon these measurements.

The various algorithms, whilst designed to estimate the same properties, employ different methods and therefore will likely vary in performance due to their ability to incorporate potential sources of error. The results presented do not show a clear superiority of one algorithm in the region. The GSM01 algorithm showed promising results for the Risk and Response dataset in the shallow waters near Port Lincoln, but was unable to be applied to some of the other datasets due to complications in the image processing, and despite generating the smallest errors for the GAB dataset still showed poor results. The Carder

algorithm showed strong results for the deep water dataset from the January 2009 IMOS cruise, but performed poorly in the shallow waters and also failed to produce results for some of the dates required. The empirical algorithms, OC3M and Clark, did not suffer the same processing problems as the other algorithms and were applied to all of the datasets. The Clark algorithm performed slightly better than OC3M in the Risk and Response dataset from the shallow waters near Port Lincoln, a surprising result since the Clark algorithm is designed for use in open ocean waters. However the OC3M algorithm showed better results than Clark for the May 2008 data in the same location and both the IMOS datasets. Thus the OC3M algorithm, due to its consistent performance against our field-based datasets and due to it being the standard chlorophyll-*a* algorithm distributed by the GSFC, is recommended for future applications of MODIS chlorophyll-*a* imagery in South Australia.

4.4.2 Sea Surface Temperature

Barton and Pearce (2006) used *in situ* sea surface temperature measurements collected from a commercial ferry operating between Rottnest Island and the mainland coast near Perth in Western Australia in an assessment of satellite-based SST measurements. Along with GLI, AVHRR and AATSR, they investigated MODIS Terra and Aqua SST measurements for day-time SST only, since the ferry did not operate at night. They showed that the biases for MODIS Terra and Aqua SST were -0.32 and -0.23 ºC respectively, for measurements within 2 hours of satellite overpass time. It was also shown that low wind speeds contributed to greater biases between satellite SST measurements and *in situ* SST due to solar heating in the upper ocean layer and a lack of vertical mixing producing vertical temperature gradients. The study also identified improved SST accuracies for sensors with 12-bit radiometric resolution (MODIS) compared to those with only 10-bit resolution (AVHRR). Likewise Barton (2007) compared satellite-based SST measurements with *in situ* SST collected in the Gulf of Carpentaria in northern Australia. Satellite-based SST measurements from nine different sensors were compared to *in situ* temperature measurements from a depth of 3 metres. MODIS SST measurements performed within an accuracy of 0.5 K with biases of -0.15 K and 0.05 K for Terra and Aqua respectively and standard deviations of 0.43 and 0.41 K. The MODIS instruments performed better than the NOAA AVHRR sensor and the geostationary MSI GOES-9 sensor, due to the improved 12-bit digitization of MODIS, as was also observed by Barton and Pearce (2006).

Comparison between surface and satellite measurements of SST may be influenced by the variability of the surface temperature relative to the spatial resolution of the satellite image, as observed for chlorophyll-*a*. Fine-scale *in situ* measurements of SST were not obtained to assess the within-pixel SST variability in this study, but localised variation in SST is assumed to be small and thus have minimal influence on satellite to *in situ* SST comparisons. Minnett (1991) did, however, investigate the influence of scale on satellite and *in situ* SST measurements. The separation distances and temporal differences at which the RMS difference between *in situ* and satellite SST measurements was greater than 0.2 K were assessed for a number of datasets. It was concluded that a maximum displacement of 10 km and 2 hours between *in situ* and satellite SST measurements should be tolerated. In this study the distance between the measurements was much less than 10 km, while a temporal window of up to 3 hours between *in situ* and satellite measurements was permitted.

A known source of difference between satellite radiometer-based SST measurements and *in situ* SST measurements is the skin temperature effect (Schluessel et al. 1990; Donlon et al. 2002). The satellite-based measurements of SST, such as the MODIS SST examined in this study, are a measure of the temperature of the immediate skin of the sea surface, a layer less than 1 mm deep, while the *in situ* measurements are a measure of the bulk surface temperature, typically at a depth of between 1 and 3 metres. Schluessel et al. (1990) and Donlon et al. (2002) describe in detail the fine-scale vertical temperature profiles of the sea surface and the implications for remote sensing SST measurements. Differences between the temperature of the immediate sea surface and the temperature at a given depth are a combination of the latent heat flux due to evaporation at the surface, sensible heat flux from direct transfer of heat between the air and water, the turbulent heat flux of the upper layers of the sea, and radiative heat flux from absorbed shortwave and longwave radiance and emitted longwave radiance. During day-time with low wind conditions, absorption of incoming shortwave radiance will result in an increase in surface temperature relative to the deeper waters, thus the satellite-based measurements may overestimate relative to the *in situ* measurements. During the day-time with strong mixing in the surface layers, however, the well mixed layer will have uniform temperatures with the exception of the immediate surface skin which may be cooler due to latent heat flux at the sea-air interface, thus the satellite will appear to underestimate. Likewise at night the longwave radiance heat flux of the immediate surface will result in a surface cooling and thus the temperature as measured by the sensor may be cooler than the measured

temperature at depth. However the temperature difference between the surface skin and the temperature at depth is strongly dependant upon local atmospheric and oceanic conditions and the associated heat fluxes, thus it is not possible to account for the difference in temperatures on the attempted validation of MODIS SST. It is realised, however, that the different depths of the two measurements will result in observed differences. Schluessel et al. (1990) observed differences between skin SST as measured by satellite sensors and bulk SST as measured by *in situ* instruments in the North Atlantic typically between ± 1.0 K, with the average difference of the observed day-time and night-time measurements of 0.11 K and 0.30 K respectively. The influence of the difference in temperature at the immediate surface, as measured by MODIS, and the temperature at depth as measured by the CTD is likely to make a considerable contribution to the errors observed between the datasets in this study.

Satellite measurements of SST are influenced by the emission of infrared radiation from the sea surface and the transfer of this outgoing radiance through the earth‟s atmosphere. The emissivity of the surface is the ability of the surface to emit radiation relative to a pure black-body and where a surface has an emissivity of less than 1 in the infrared wavelengths used to measure surface temperature the surface will appear cooler. When the surface emissivity is known, however, its influence on measured temperature can be accounted for. The sea surface emissivity in the infrared spectrum is high and relatively stable under usual environmental conditions, and the influence of variations of emissivity due to viewing angle are accounted for in the algorithms (Brown and Minnett 1999). Surface roughness as influenced by wind speed can alter the surface emissivity at high viewing angles (Masuda et al. 1988; Wu and Smith 1997), but at the observation angles experienced by MODIS this influence is likely to be minimal (Brown and Minnett 1999). Atmospheric absorption by water vapour and other gases in the atmosphere can significantly influence the outgoing radiance emitted by the ocean surface. The influence of water vapour absorption, however, is corrected for by using a combination of two bands with different absorption characteristics (Anding and Kauth 1970; McMillin 1975; McMillin and Crosby 1984). This split-window technique is utilised by the MODIS SST algorithms to account for water vapour absorption using the difference in temperature between close spectral bands (Brown and Minnett 1999). While water vapour is the most important absorbing gas in the atmosphere for SST measurements, carbon dioxide also significantly absorbs in the infrared wavelengths, along with smaller contributions from nitrogen, ozone, nitric acid, ammonia, carbonyl sulphide, nitrous oxide, methane, trichloromethane and

dichlorofluoromethane (Zavody et al. 1995). Atmospheric radiative transfer modelling is used to remove the effects of absorption by atmospheric gases on the upwelled radiance from the sea surface as it passes through the atmosphere (see Zavody et al. 1995). Aerosols are another atmospheric property that can influence satellite infrared SST measurements by absorbing the outgoing longwave radiance emitted by the sea surface. Vazquez-Cuervo et al. (2004) showed that atmospheric dust can play a significant role in underestimating SST due to the absorption of outgoing infrared radiation by the aerosols. Arbelo et al. (2005) also showed that the difference between AVHRR and *in situ* SST measurements increased as the aerosol optical thickness, as measured by SeaWiFS, increased as a result of Saharan dust over the North Atlantic. As with atmospheric correction of the visible wavelengths for the chlorophyll-*a* estimations, atmospheric correction of the infrared wavelengths for SST estimations is a complex task and sources of error that are not correctly accounted for in the atmospheric correction process will lead to errors in the satellite-based SST measurements.

The MODIS SST methods that have been assessed in this study vary slightly in their approaches, and thus may perform differently against *in situ* SST data. The results of this study on MODIS SST accuracies show only subtle differences between the methods, with all three showing very good results. Overall the night-time 4 μm SST performed the best with R^2 of 0.95 and RMSE of only 1.5%, but the 11 μm day-time and night-time SST also compared well with the field-based temperature data with R^2 values of greater than 0.92 and RMSE less than 2.3%. The slight advantage of the 4 μm SST may be due to the 4 μm wavelengths being less affected by water vapour and having greater temperature sensitivity than the 11 μm wavelengths. All SST datasets often overestimate against the field-based temperature measurements, but this is likely due to the difference in depth of measurement between the satellite, at the immediate sea surface, and the CTD measurement, between 1 and 3 metres below the surface.

4.5 Conclusion

The purpose of this chapter has been to assess the accuracy of MODIS chlorophyll-*a* and sea surface temperature imagery in South Australian coastal waters, to assure the satellite-based method is valid in the region and applicable for future use. MODIS Aqua chlorophyll-*a* estimates were compared to field-based measurements collected across several regions from different projects. With a few exceptions, MODIS chlorophyll-*a*

estimates have shown good results for the region with errors generally within 35%, which is the generally accepted accuracy goal for chlorophyll-*a* in the open ocean (McClain 2009). Overestimation by MODIS compared to the field-based method has been detected in shallow waters, as a result of seafloor reflection. Measurements from the SBT aquaculture region near Port Lincoln show that a water depth of 20 m appears to be critical and MODIS estimates from areas shallower than 20 m are likely to be erroneous. This water depth is not absolute and will vary depending on a number of factors including the clarity of the water, the type of seafloor substrate, and also the time of year and the location. It is also known that MODIS chlorophyll-*a* estimates are influenced by suspended particulate matter and coloured dissolved organic matter in the water column. No data is available to quantify these influences; although they are likely to be a contributing source of error in the MODIS chlorophyll-*a* estimates. The sub-pixel variability in chlorophyll-*a* has been shown to be a contributing source of apparent error between MODIS and field-based chlorophyll-*a*, with surface chlorophyll-*a* around the SBT aquaculture region highly variable over short distances. Sub-surface chlorophyll-*a* profiles are also likely to contribute to apparent errors between the two methods. Despite the number of potential errors within the MODIS chlorophyll-*a* estimates and the limitations to the comparison methodology applied, the MODIS chlorophyll-*a* estimates perform well against the field-based method. Thus they can be applied to understand chlorophyll-*a* and phytoplankton variability in the region as long as the limitations are understood. The standard OC3M chlorophyll-*a* algorithm was the most accurate and consistent of the four algorithms assessed and thus will be the preferred algorithm for further application of MODIS chlorophyll-*a* imagery.

MODIS sea surface temperature imagery has also performed well in the study area. While the SST measurements are not affected by shallow water depth or constituents of the water column, as is chlorophyll-*a*, they are influenced by variations in temperature at different depths. It is well known that satellite-based SST measurements are temperature measurements of the immediate skin of the sea surface. This potentially leads to differences between satellite and field-based temperatures. This temperature-depth influence can be seen in the present data as apparent over-estimation by MODIS compared to the deeper CTD temperatures. Despite this, the results of SST validation in this chapter have shown very promising results for further application of MODIS SST imagery in South Australia. Statistically, the night-time 4 µm SST shows the best relationship with the field-based measurements, although it was only slightly better than the day and night 11

μm SST, which both performed very well also. The day-time 11 μm SST has been chosen for future application.

This chapter has assessed MODIS chlorophyll-*a* and SST imagery in South Australia and has shown that the satellite-based methods are suitable for future application. There are limitations that this chapter has identified, but as long as these limitations are understood in future applications then they can be used with confidence to increase understanding of chlorophyll-*a* and temperature variability in the SBT aquaculture region, Spencer Gulf and South Australia. The standard OC3M chlorophyll-*a* and 11 μm day-time SST have been selected as the most suitable products for further applications.

Chapter 5: Seasonal Variability of Chlorophyll-*a* and Sea Surface Temperature in and around Spencer Gulf

5.1 Introduction

As described in Chapter 2, Spencer Gulf is an inverse estuary whereby the salinity within the gulf is greater than outside of the gulf as a result of an excess in evaporation over precipitation. The gulf is also characterised by a greater annual temperature range than waters outside of the gulf. Across the mouth of Spencer Gulf during summer there is a sea surface temperature front, where the warm gulf waters meet the cooler ocean waters; this leads to reduced exchange between the gulf and other nearby water masses. In winter, however, cooling of the high salinity gulf water generates high density water in the northern gulf that then flows southwards, exiting the gulf on the east and being replaced by an inflow of ocean water to the west. A number of past studies have investigated these processes, leading to a well developed understanding of the oceanography of Spencer Gulf (Nunes and Lennon 1986; Lennon et al. 1987; Nunes and Lennon 1987; Nunes Vas et al. 1990; Petrusevics 1993; Corlis et al. 2003). Recent modelling simulations also confirm the general circulation features of Spencer Gulf with a clockwise gyre in the southern gulf (Herzfeld et al. 2009). While the knowledge of the physical oceanography of Spencer Gulf is well developed, we still have a poor understanding of how this is related to biological processes in the water column. For example, there exists little information regarding how phytoplankton abundance varies on broad scales, how different regions are connected with respect to phytoplankton assemblages, and how temporal variation is related to geographic location.

One possible reason why there is limited understanding of these topics is the availability of suitable data. Often datasets of chlorophyll-*a,* and sea surface temperature, are spatially or temporally restricted and therefore do not cover the large areas and long time periods required to study patterns over an area as large as Spencer Gulf. Satellite remote sensing allows information on chlorophyll-*a* concentrations and sea surface temperature to be collected at moderate resolution, over vast regions, over long periods of time, with reasonable accuracy and at low cost. The Moderate Resolution Imaging Spectroradiometer (MODIS) is one instrument that can produce such data. A background on the MODIS

instrument and imagery have been provided in earlier chapters, and the previous chapter has shown how MODIS chlorophyll-*a* and sea surface temperature imagery performs with acceptable accuracy within and around Spencer Gulf, as long as care is taken when interpreting the outputs. Due to the large area covered by the MODIS imagery, the frequency of the image collection, and the multiyear coverage, MODIS is an ideal platform to investigate the seasonal variations of chlorophyll-*a* and sea surface temperature in and around Spencer Gulf.

Therefore the aim of this chapter is to apply MODIS remotely sensed imagery to develop a better understanding of the seasonal chlorophyll-*a* and sea surface temperature variations within and around Spencer Gulf, and investigate how the seasonal variations change with geographic location. Knowledge of the seasonal variability in chlorophyll-*a* and sea surface temperature assists in developing a more comprehensive understanding of the dynamic environment of Spencer Gulf, and thus aids in better understanding the interactions between southern bluefin tuna aquaculture and its immediate environment.

5.2 Methods

5.2.1 MODIS Imagery

MODIS satellite-based imagery was used to investigate annual and inter-annual chlorophyll-*a* and sea surface temperature (SST) variability within and around Spencer Gulf, South Australia. Monthly averaged level 3 MODIS Aqua imagery at 4 km spatial resolution was obtained from the Goddard Space Flight Centre. Sixty monthly images were obtained, representing each month over a 5-year period from July 2002 up to and including June 2007. Also obtained were 12 climatology images, consisting of a 5-year average for each calendar month. The standard OC3M chlorophyll-*a* and day-time (11 μm) SST imagery were chosen. The hierarchical data format (HDF) files were imported into ENVI version 4.3 (RSI 2006) using the ENVI plug-in for ocean colour (White undated). The global images were subset to the study area from 30 ºS to 40 ºS and from 132 ºE to 142 ºE. Images were then stacked together to create 4 layered files: the 60 monthly chlorophyll-*a* images from July 2002 to June 2007, the 60 monthly SST images, the 12 chlorophyll-*a* climatology images, and the 12 SST climatology images.

5.2.2 Analysis

To compare the seasonal variability of chlorophyll-*a* and SST at different locations inside and outside Spencer Gulf, 14 stations were established (Figure 5.1; Table 5.1). To show how seasonal patterns vary with position along the gulf, stations A through G were placed on a transect that runs down the centre of Spencer Gulf from near the head to well offshore near the edge of the continental shelf. Station H was placed near the southern bluefin tuna (SBT) farming zone to show how this region compares to the rest of the gulf, while station I was placed on the opposite side of the gulf, at approximately the same distance from the coast, as a reference for station H. Stations J, K and L were placed on the western side of Eyre Peninsula, and finally stations M and N were placed on the southwest corner of Kangaroo Island in order to possibly detect the effects of coastal upwelling.

At each of the 14 stations, the values of an array of 3 by 3 pixels from each MODIS chlorophyll-*a* and SST image were extracted and averaged to enable a temporal profile to be determined for each station. Since the monthly imagery consists of 4 km pixels, the area averaged around each station was 12 by 12 km. The temporal profiles were compared and the correlation between stations assessed with the Pearson correlation statistic. To assess similarity between the temporal profiles at different stations, a hierarchical cluster analysis was applied. Each station was treated as an individual case, with each month considered a variable. Hierarchical cluster analysis was performed in SPSS version 15.0 (SPSS 2006) using Ward‟s method with squared Euclidean distance to produce a dendrogram visually showing degrees of similarity between the stations. To identify the modes of variability within the imagery and identify characteristics of the dataset responsible for the majority of the variability, principal components analysis (PCA) was used. PCA was performed in ENVI on the 5-years of monthly chlorophyll-*a* and SST imagery. The principal components were calculated using the covariance matrix and the eigenvalues of each extracted component used to calculate the percentage of variance explained by each component. The component loadings were also examined to determine the contribution of each monthly image to the principal components. Finally, to assess broader scale variation in the temporal profiles of chlorophyll-*a* and SST, unsupervised classification (non-hierarchical cluster analysis) was applied over the entire study area covered by the MODIS imagery. K-means unsupervised classification was performed in ENVI on the 5-year series of monthly MODIS imagery with 10 iterations and 6 groups selected for chlorophyll-*a* and 7 groups for SST.

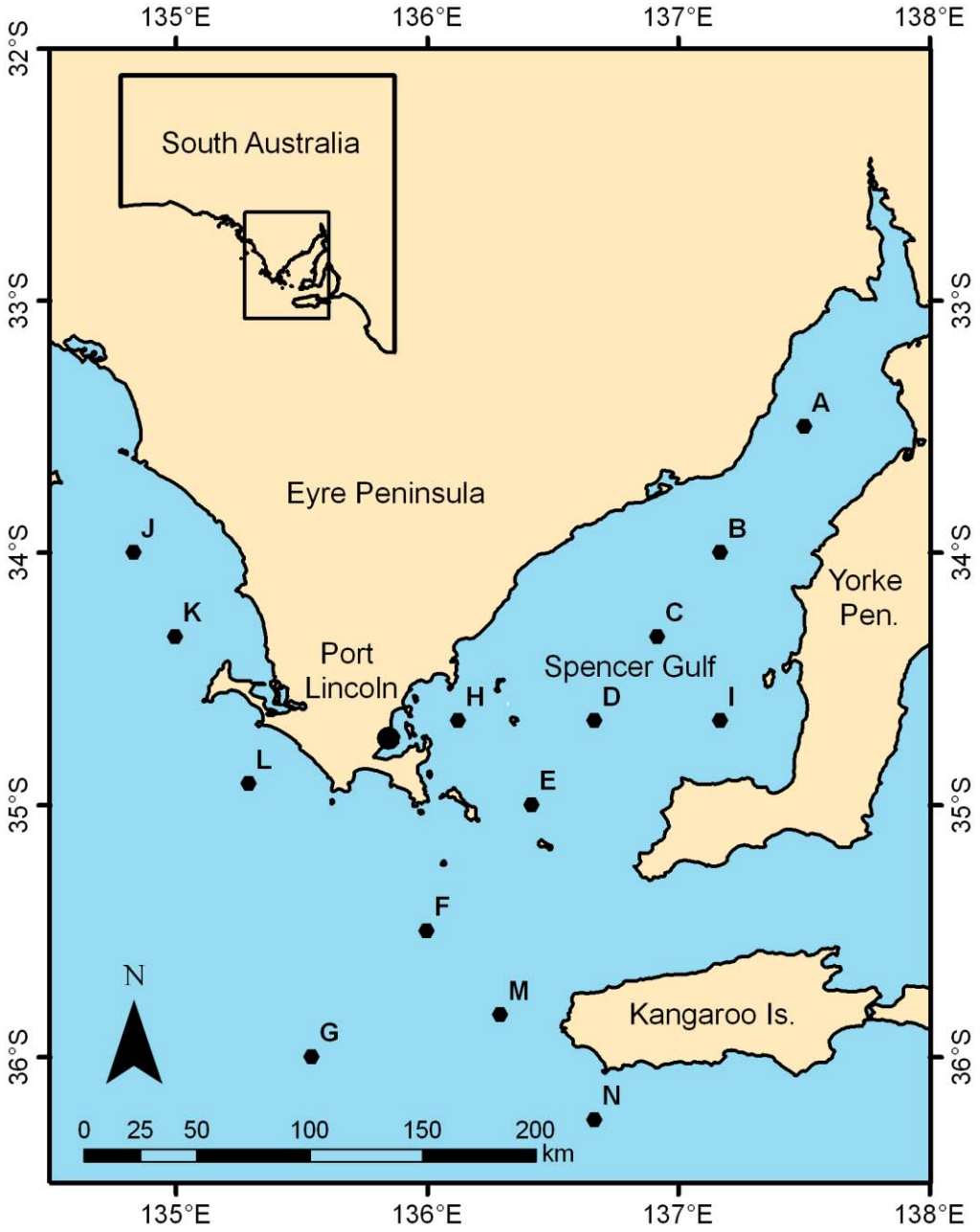

Figure 5.1: The location of stations A to N used to investigate the seasonal chlorophyll-*a* and SST variability within and around Spencer Gulf, South Australia (co-ordinates are given in Table 5.1).

Table 5.1: The co-ordinates of the stations used to assess spatial variability in chlorophyll-*a* and SST.

Station ID	Latitude (ºS)	Longitude (ºE)
A	33.50	137.53
B	34.00	137.17
C	34.33	136.92
D	34.67	136.67
E	35.00	136.40
F	35.50	136.00
G	36.00	135.55
H	34.67	136.13
I	34.67	137.17
J	34.00	134.83
K	34.33	135.00
L	34.92	135.30
M	35.83	136.30
N	36.25	136.67

5.3 Results

5.3.1 Chlorophyll-*a*

Differences in the magnitude of the MODIS chlorophyll-*a* concentrations were observed, and the timing of the seasonal patterns varied between locations in and around Spencer Gulf (Figure 5.2; Figure 5.3). MODIS monthly averaged chlorophyll-*a* concentrations ranged from a minimum of < 0.1 mg m^{-3} at station G outside the mouth of Spencer Gulf on several occasions, up to a maximum of almost 2.0 mg m^{-3} at station A in northern Spencer Gulf in March 2007.

Station A, in northern Spencer Gulf, showed the highest MODIS-derived chlorophyll-*a* concentrations, between 0.58 and 1.97 mg m^{-3}, and also the largest seasonal differences. It is possible that the MODIS chlorophyll-*a* at this location is influenced by shallow water depth and seafloor reflectance, which was shown in the previous chapter to result in over-estimates of MODIS chlorophyll-*a*. The maximum of the MODIS chlorophyll-*a* estimates in northern Spencer Gulf occurred between January and May, while minimum chlorophyll-*a* was observed between August and November. The 5-year averaged monthly climatology imagery showed an average annual range from a minimum of 0.69 mg m^{-3} in October up to a maximum of 1.67 mg m^{-3} in April (Figure 5.3).

The magnitude of chlorophyll-*a* concentrations decreased further south in the gulf. At station D, in southern Spencer Gulf, concentrations ranged from 0.19 up to 0.93 mg m^{-3}, with maximum concentrations between April and July, and minimum concentrations between September and November. The 5-year average annual range was from just 0.22 mg m^{-3} in October up to 0.60 mg m^{-3} in July (Figure 5.3). Further south, outside Spencer Gulf at station G, concentrations ranged from just 0.08 up to 0.42 mg m^{-3}. At station G the maximum chlorophyll-*a* occurred between August and October with minimum chlorophyll-*a* between December and March. The 5-year average annual range at station G was very small, between 0.10 mg m^{-3} in March and 0.27 mg m^{-3} in October (Figure 5.3). The seasonal pattern in chlorophyll-*a* south of Spencer Gulf was almost the opposite of that in northern Spencer Gulf at station A, as indicated by the negative correlation of -0.58 (Table 5.2), although the concentrations at G are much lower than at A (Figure 5.3). The differences in chlorophyll-*a* patterns in and around Spencer Gulf throughout the year can be observed in the climatology images for each month (Figure 5.2).

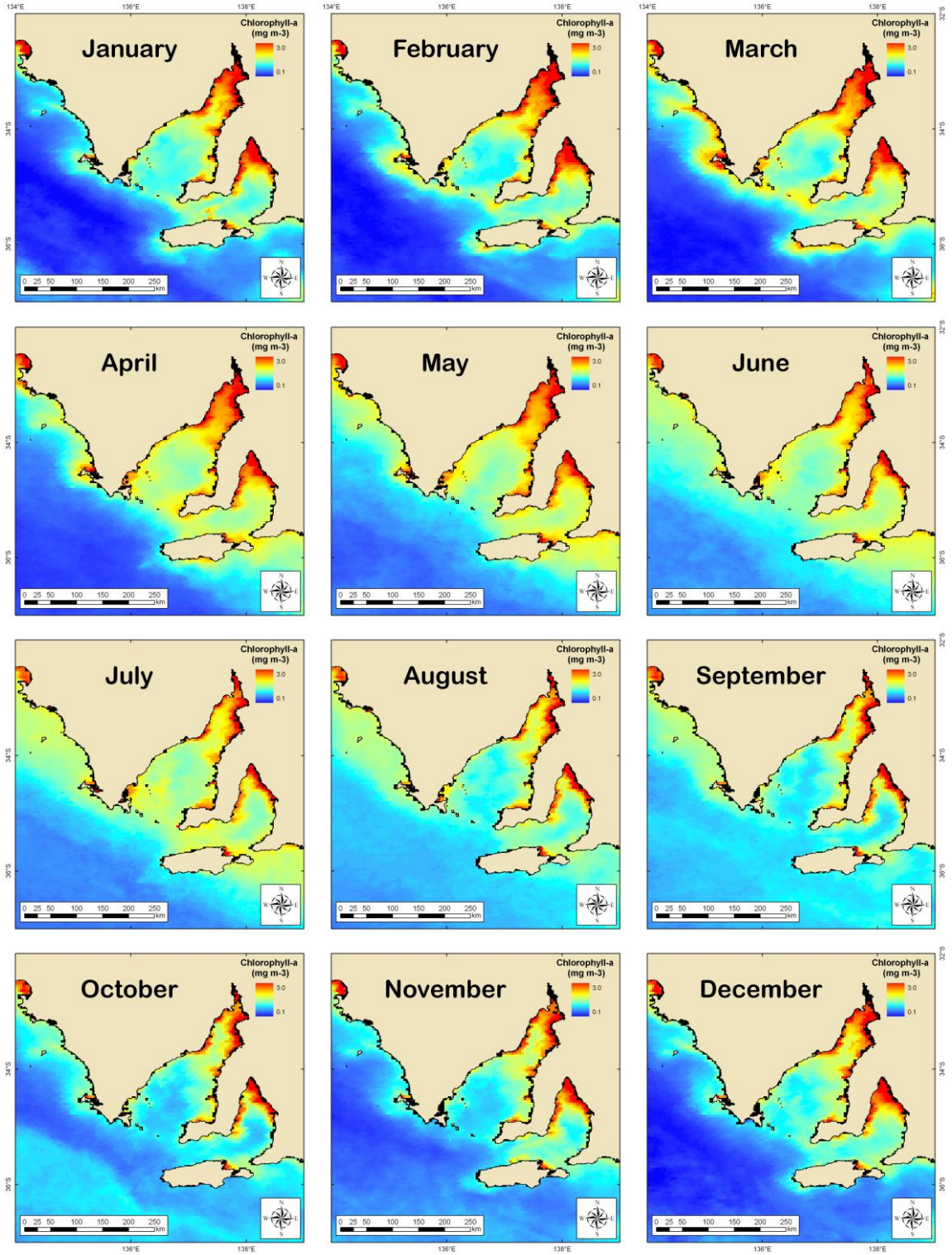

Figure 5.2: Monthly chlorophyll-*a* climatology (mg m^{-3}) from MODIS/Aqua between 2002 and 2007.

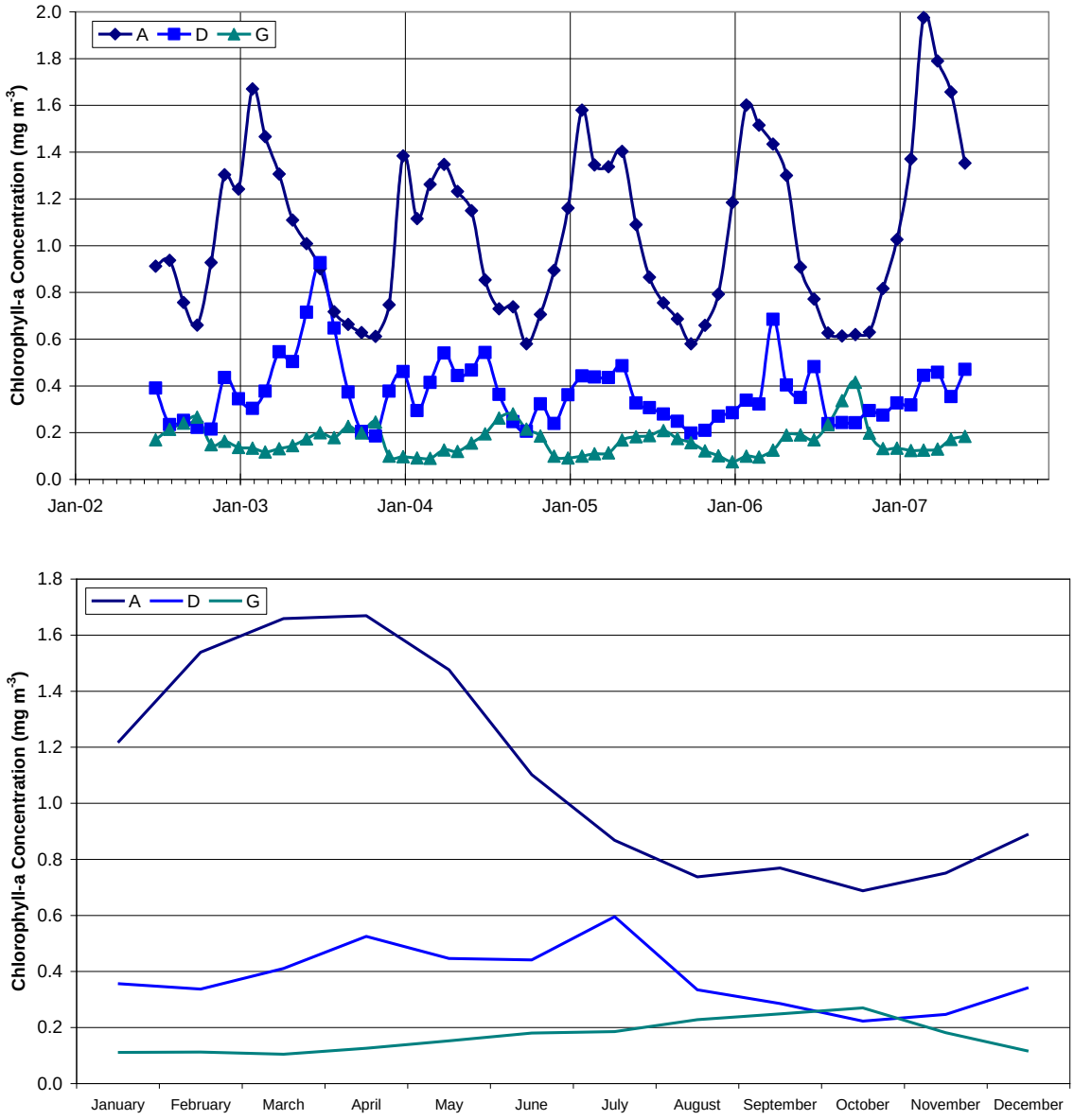

Figure 5.3: The monthly chlorophyll-*a* concentrations at stations A, D and G from July 2002 to June 2007 and the monthly climatology averaged over the 5-year period.

Table 5.2: Correlation matrix for the temporal chlorophyll-*a* profiles at each station from 5 years of monthly MODIS imagery.

	A	B	C	D	E	F	G	H	I	J	K	L	M	N
A	1													
B	0.76	1												
C	0.47	0.51	1											
D	0.37	0.35	0.81	1										
E	0.55	0.42	0.60	0.76	1									
F	-0.16	-0.26	0.10	0.23	0.25	1								
G	-0.58	-0.49	-0.33	-0.22	-0.29	0.42	1							
H	0.44	0.29	0.67	0.82	0.75	0.36	-0.18	1						
I	0.00	0.02	0.60	0.53	0.32	0.23	-0.14	0.42	1					
J	-0.12	-0.30	0.13	0.25	0.32	0.77	0.35	0.42	0.17	1				
K	0.22	0.03	0.22	0.22	0.48	0.37	-0.02	0.38	-0.06	0.65	1			
L	0.06	-0.17	0.05	0.15	0.42	0.67	0.10	0.27	0.04	0.72	0.65	1		
M	0.00	-0.11	-0.10	-0.06	0.10	0.52	0.17	-0.01	-0.11	0.31	0.31	0.57	1	
N	0.00	-0.21	-0.07	0.05	0.19	0.67	0.31	0.17	-0.03	0.58	0.46	0.58	0.57	1

Station H is located near the tuna farming zone in the southwest of the gulf. The chlorophyll-*a* at station H ranged from 0.29 mg m^{-3} up to 1.42 mg m^{-3}, with maximum concentrations between March and July and minimum concentrations between September and January (Figure 5.4). The 5-year average annual range was from 0.35 mg m^{-3} in November up to 1.02 mg m^{-3} in July (Figure 5.4). The chlorophyll-*a* characteristics at station H were similar to station D, which lies directly east of H in the centre of the gulf, shown by a Pearson correlation coefficient of 0.82 (Table 5.2). However, the concentrations at H were consistently higher than at D. On average the chlorophyll-*a* observed at station H was 0.18 mg m^{-3} greater than at station D, but consistently up to 0.4 mg m^{-3} greater between March and July. Station I was placed on the opposite side of the gulf to H, at a similar distance offshore. Station I also showed the same seasonal patterns as H and D. Station I showed higher concentrations than D during some periods of the year, although not as high as station H (Figure 5.4).

Station J on the western side of Eyre Peninsula showed a range of chlorophyll-*a* concentrations between 0.14 and 0.69 mg m^{-3}, with the minimum concentrations between November and February and maximum between June and September. The 5-year average annual range was between a minimum of 0.18 mg m^{-3} in January and a maximum of 0.55 mg m^{-3} in July (Figure 5.5). The seasonal chlorophyll-*a* cycle at station J showed two periods of elevated concentrations throughout the year, a primary peak between June and September, with a smaller peak evident in March. The chlorophyll-*a* seasonal trends were similar at nearby stations K and L, although at K the peak in March was larger than the peak between July and September. The pattern on the west of Eyre Peninsula is similar to the stations inside Spencer Gulf, with the exception of the second peak in March and the continued higher chlorophyll-*a* until September.

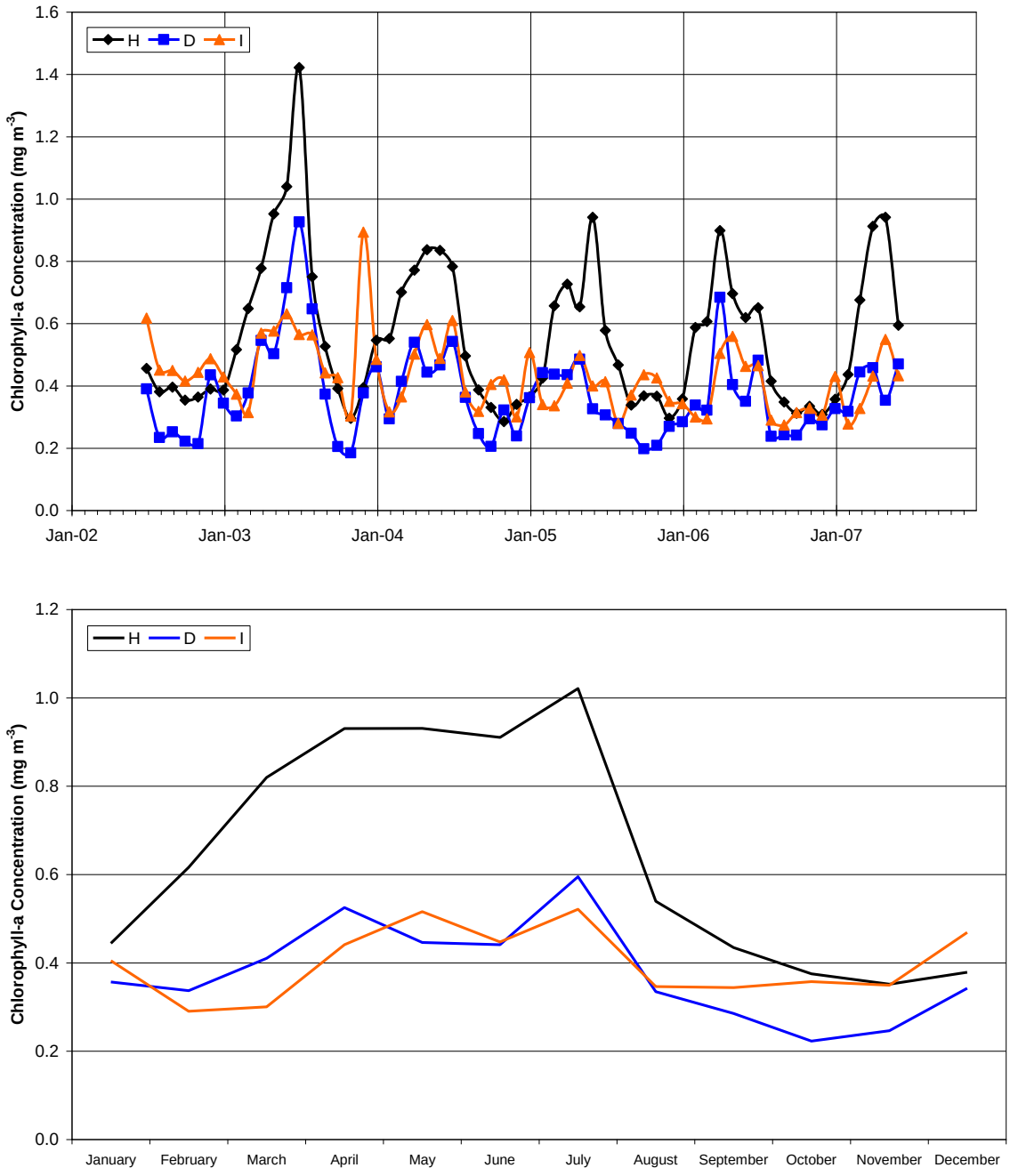

Figure 5.4: The monthly chlorophyll-*a* concentrations at stations H, D and I from July 2002 to June 2007 and the monthly climatology averaged over the 5-year period.

Station M, on the west coast of Kangaroo Island, showed chlorophyll-*a* concentrations between 0.12 mg m^{-3} and 0.46 mg m^{-3}, with minimum values between October and January and maximum between June and September (Figure 5.5). The 5-year average annual chlorophyll-*a* at station M ranged from 0.17 mg m^{-3} in January to 0.27 mg m^{-3} in June. The nearby station N, on the southern coast of Kangaroo Island, showed similar patterns and chlorophyll-*a* concentrations as M. The seasonal cycle at M and N was less pronounced than at other stations where a dominant seasonal pattern was observed. However, there is evidence of a biannual cycle with peaks in chlorophyll-*a* occurring in both March and

between June and September, as was seen on the west of Eyre Peninsula. The March peaks may be related to upwelling. The images in Figure 5.2 show that the entire offshore region is relatively high in chlorophyll-*a* between June and September, but during March only areas along the coastlines are higher in chlorophyll-*a*, while the offshore regions remain low.

As mentioned, the magnitude of the chlorophyll-*a* concentrations varied with distance from the head of the gulf, therefore the monthly climatology images of chlorophyll-*a* concentration were used to show how they change along the transect that runs along the centre of the gulf in each month of the year (Figure 5.6). In all months, station A had the highest chlorophyll-*a*, and there was a clear decrease from the head towards the mouth. The high chlorophyll-*a* observed at station A is most likely due to combined influences of shallow water depth, proximity to land and suspended particulate matter in the water column, and not solely an increase in phytoplankton. The lowest concentration was at station G in all months except October and November, when station F was lower. The decrease in chlorophyll-*a* concentration from A to F or G was not linear, however. The concentration decreased rapidly from A to C in all months, and there was a slight increase at station E in a few months before the concentration decreased further at stations F and G.

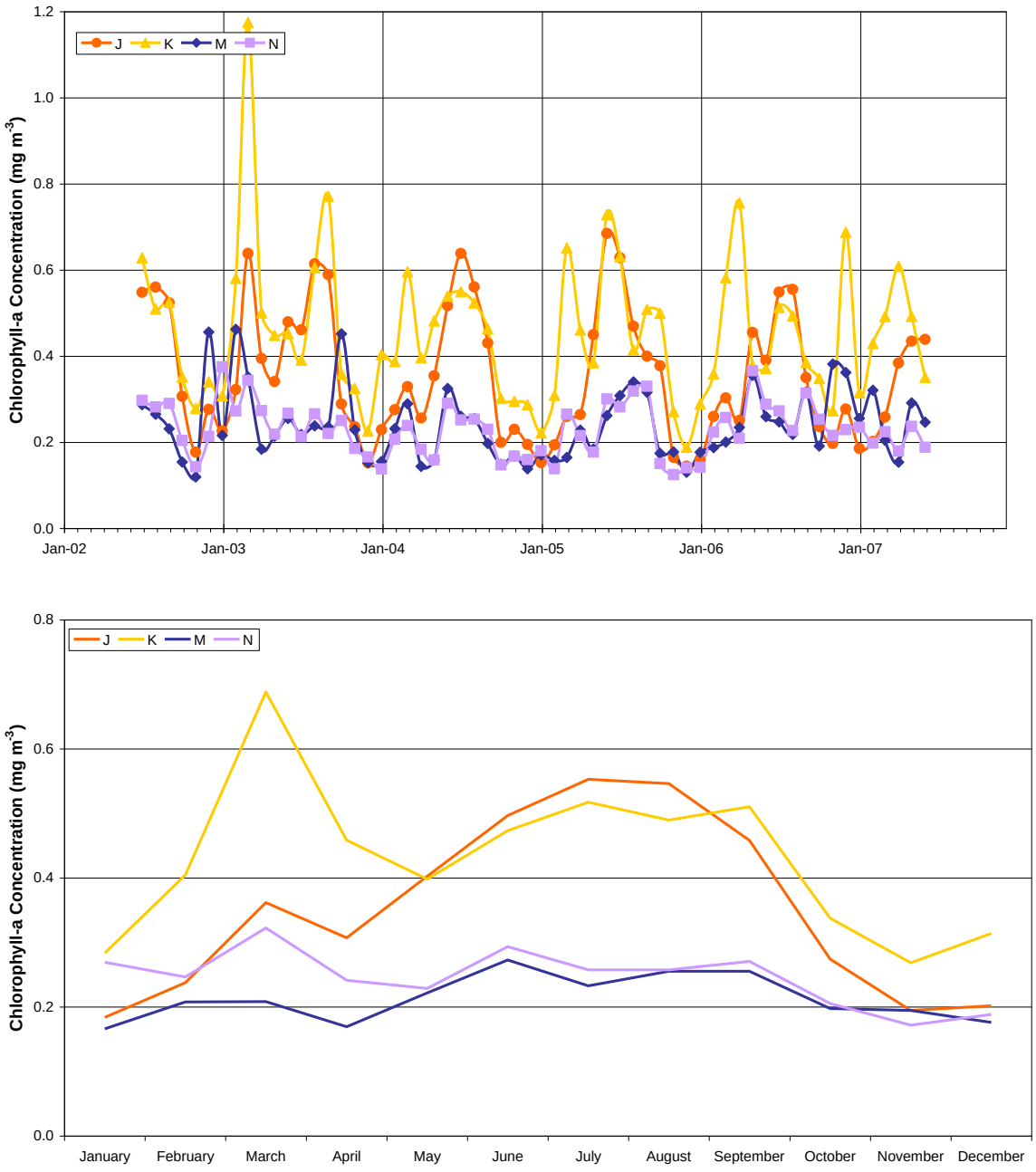

Figure 5.5: The monthly chlorophyll-*a* concentrations at stations J, K, M and N from July 2002 to June 2007 and the monthly climatology averaged over the 5-year period.

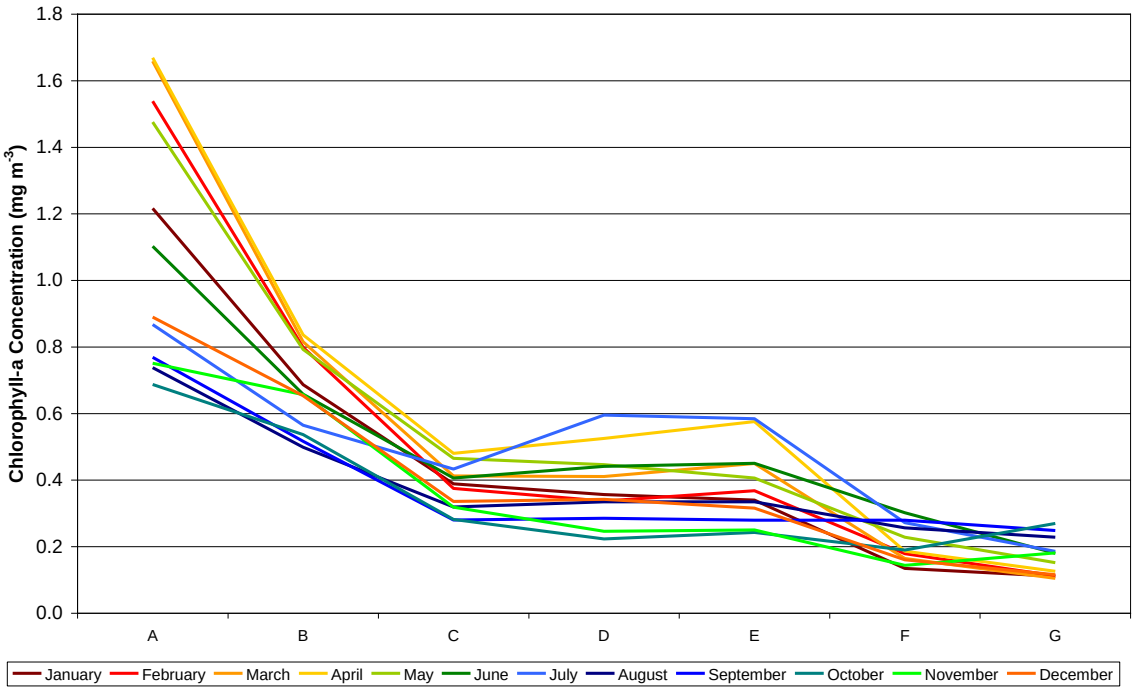

Figure 5.6: The chlorophyll-*a* climatology in each month of the year at stations along the transect from A in the northern Spencer Gulf to G outside the mouth of the gulf.

Hierarchical cluster analysis of chlorophyll-*a* showed that stations F, N, M and G outside the mouth of Spencer Gulf are similar to each other, as are C, D, E and I in the southern gulf (Figure 5.7). Stations J, K and L on the western side of Eyre Peninsula are more similar to the southern gulf than they are to the other stations outside of the gulf. Station H, near the tuna farming zone, is more similar to station B further north in Spencer Gulf than it is to any of the nearby stations, and stations A, B and H are all very dissimilar to the other stations in the study area. Interestingly, station H is grouped with stations A and B in the hierarchical cluster analysis despite having a higher correlation with nearby station D (Table 5.2).

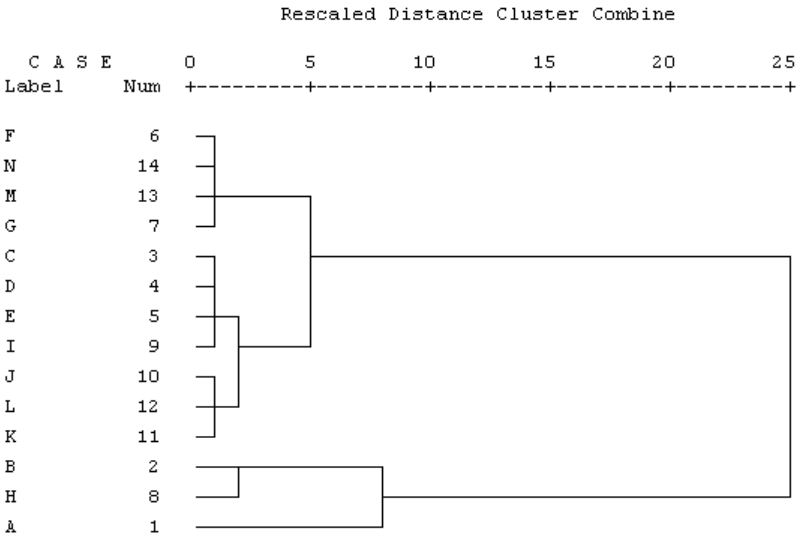

Figure 5.7: Dendrogram from hierarchical cluster analysis using Ward's method showing the similarities between stations based on chlorophyll-*a*.

The first axis of the principal components analysis accounted for 82.7% of the variance, and separates the overall high and low chlorophyll-*a* areas of the region. It identifies the areas where chlorophyll-*a* concentrations are relatively high in all months, within the gulfs and along the coastline, and the offshore waters with relatively low chlorophyll-*a* in all months (Figure 5.8). Principal component 2 accounted for just 3.96% of the variance, showing negative values throughout the Great Australian Bight (GAB) and the gulfs and positive values offshore and in the far north of the gulfs (Figure 5.8). The plots of component loadings indicate that this pattern represents a seasonal contrast identifying the areas with a peak in chlorophyll-*a* in summer with areas with peak chlorophyll-*a* in winter (Figure 5.9). The following PCs 3 and 4, which represent 2.48% and 1.63% of the variance, also appear to be related to seasonal cycles and contrast the gulfs and coastal regions with the rest of the study area (Figure 5.8; Figure 5.9). The following components that account for the remaining 9.23% of the variance represent features that are more localised, in either space or time.

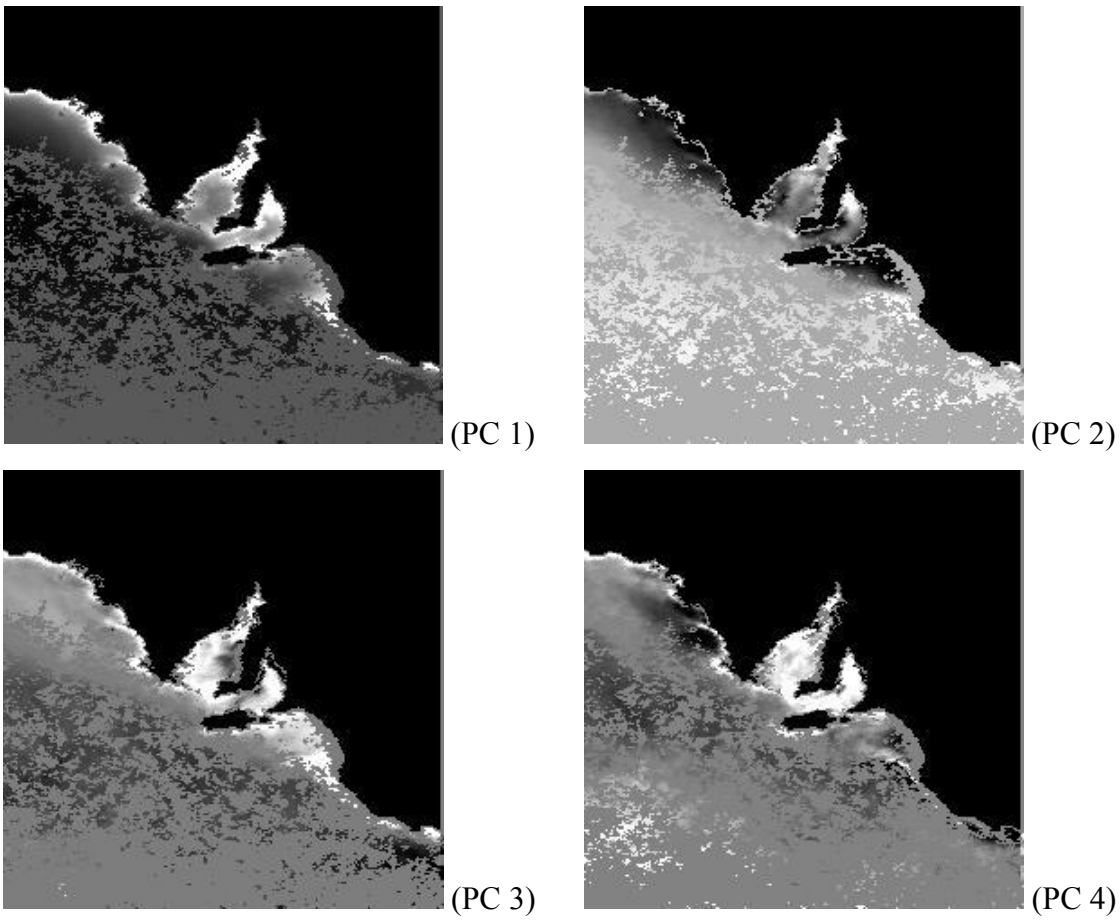

Figure 5.8: Components 1 - 4 from PCA upon the monthly chlorophyll-*a* imagery. PC1 represents 82.7% of variability and shows the overall high and low chlorophyll-*a* areas, while PCs 2 (3.96%), 3 (2.48%) and 4 (1.63%) represent different features of the seasonal chlorophyll-*a* variability. White areas indicate positive PC values, while black areas are negative.

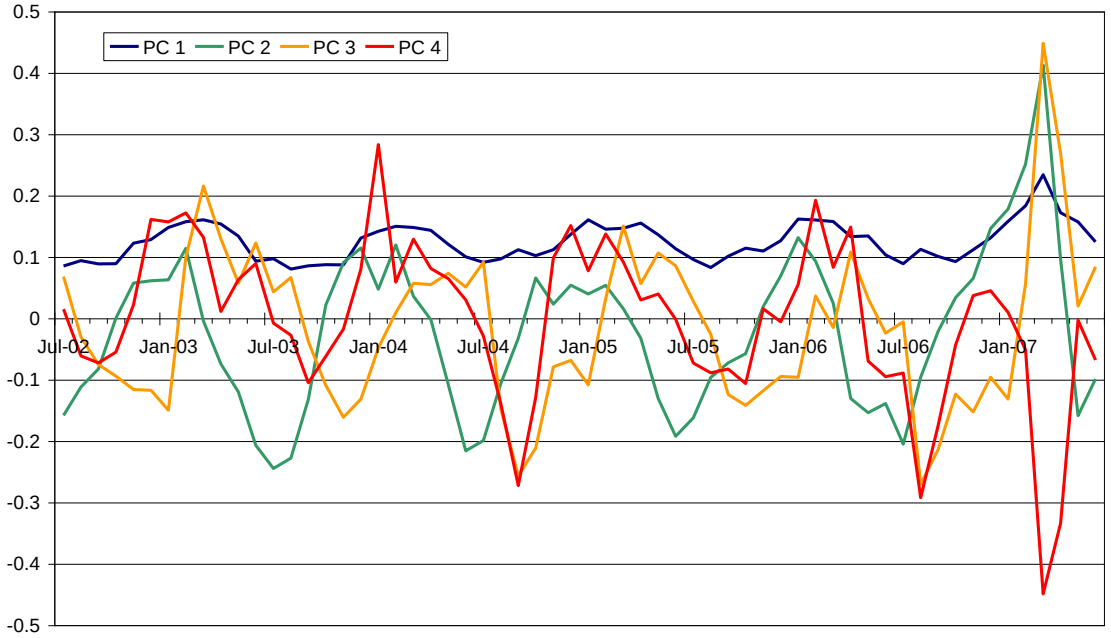

Figure 5.9: Principal component band loading for PCs 1 – 4, identifying which monthly input images most influence the resulting principal components.

The waters of the study area were classified into one of four groups using unsupervised classification of the monthly chlorophyll-*a* images. The four groups were interpreted to represent oceanic, shelf, coastal and shallow water. The area of the scene covered by each class is approximately 143,539 km^2 (13.7%) for oceanic waters, 47,111 km^2 (4.5%) for shelf waters, 26,123 km^2 (2.5%) for coastal waters and just 3,807 km^2 (0.4%) for the shallow waters. The land and unclassifiable pixels (where cloud cover has affected the imagery) covered 46.7% and 32.3% of the scene and are masked out in the classification image (Figure 5.10). It can be seen that the classification of the 14 stations is mostly consistent with the hierarchical cluster analysis. Stations F, G, M and N all fall within the open ocean region, stations J, L, C, D, E and I within the shelf region, while stations A, B, H and K are in the coastal water region (Figure 5.10).

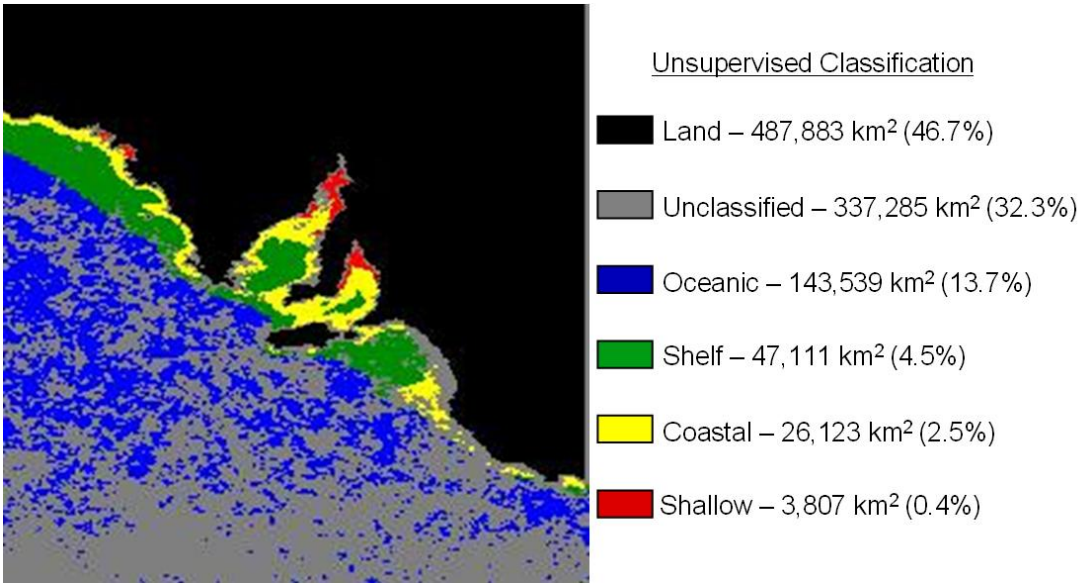

Figure 5.10: Results of an unsupervised classification upon 60 MODIS monthly chlorophyll-*a* images between July 2002 and June 2007.

5.3.2 Sea Surface Temperature

The monthly averaged SST ranged from a minimum of just under 13 ºC at station A in August 2003 up to a maximum of just over 24 ºC, also at station A in February 2007 (Figure 5.11; Figure 5.12). The range of temperatures experienced at A is greater than at any other station, 11.3 ºC compared with the smallest range of just 4.4 ºC at station L. Stations inside Spencer Gulf showed a greater average annual range in temperature than stations outside the gulf. As a result, the waters of Spencer Gulf are warmer than nearby ocean waters during summer, but cooler during winter, resulting in a temperature gradient that reverses in direction between summer and winter (Figure 5.11; Figure 5.14).

The 5-year average annual range in northern Spencer Gulf at A was from a minimum of 13.5 ºC in August up to 22.9 ºC in February. Further south at station C the SST ranged from 13.9 ºC in August to 21.9 ºC in February. Along the mouth of Spencer Gulf at station E, SST ranged from 14.8 ºC in August to 20.1 ºC in February. Outside Spencer Gulf at station G, the range was from 14.4 ºC September to 18.7 ºC in March (Figure 5.12).

Around the tuna farming zone at station H, the average annual SST range was between a minimum of 14.3 ºC in August up to 21.2 ºC in February. The seasonal temperature cycle at station H was very similar to nearby station D, as one would expect, with a correlation of 0.99 (Table 5.3). However, station H was slightly cooler than the central station D during summer and autumn. The difference between H and D was over 1 ºC in May. The SST at H was very different to K on the west of Eyre Peninsula, with K over 3 ºC cooler than H on average in February and March, but warmer than H by almost 1 ºC in July (Figure 5.13). The Pearson correlation coefficients for SST show very high correlations (0.80 or greater) between all stations, indicating a high degree of similarity in seasonal temperature patterns throughout the region (Table 5.3).

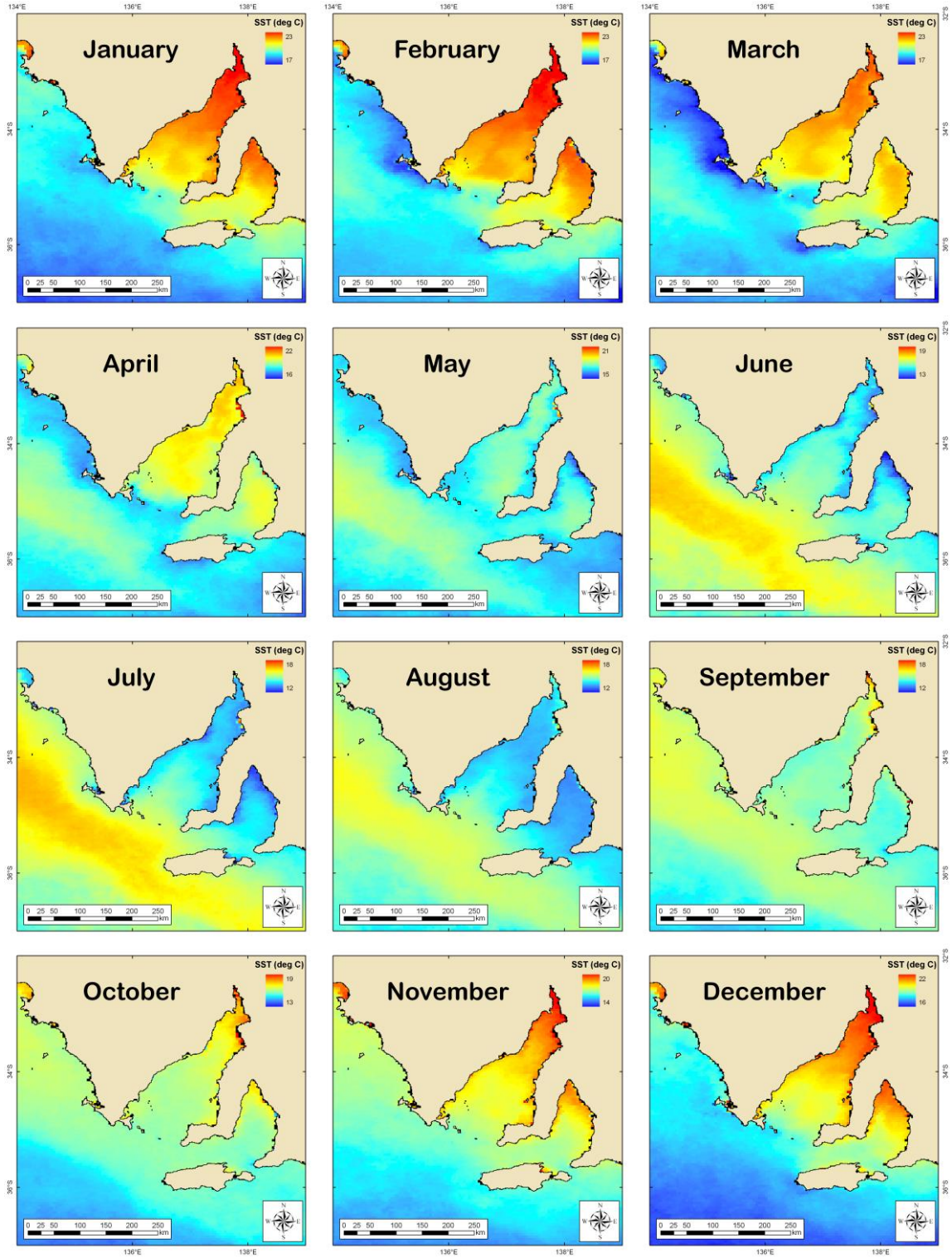

Figure 5.11: Monthly SST climatology (°C) from MODIS/Aqua between 2002 and 2007.

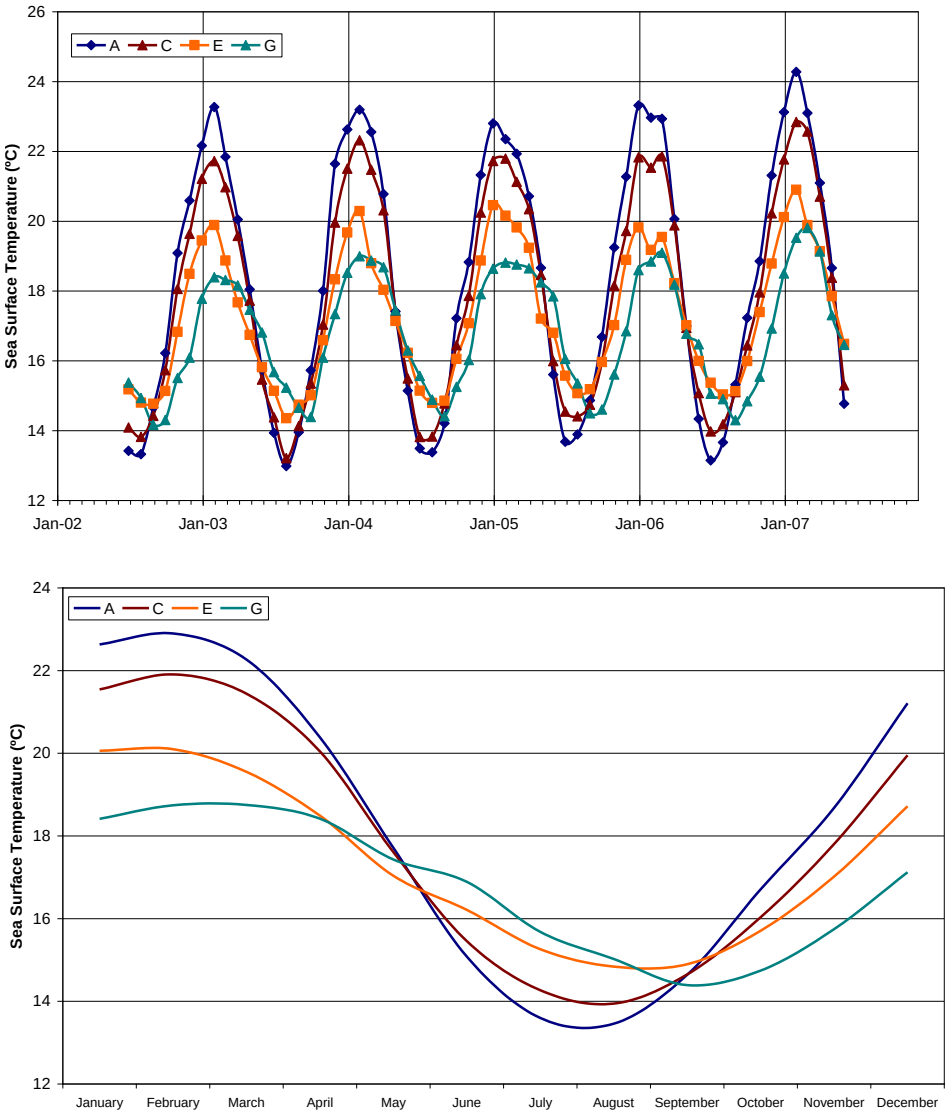

Figure 5.12: Monthly average SST and monthly SST climatology at stations A, C, E and G highlighting the decrease in range of temperatures experienced with distance from northern Spencer Gulf.

Table 5.3: Correlation matrix for the temporal SST profiles at each station from 5 years of monthly MODIS imagery.

	A	B	C	D	E	F	G	H	I	J	K	L	M	N
A	1													
B	1.00	1												
C	0.99	1.00	1											
D	0.99	0.99	1.00	1										
E	0.96	0.97	0.98	0.98	1									
F	0.87	0.88	0.91	0.92	0.94	1								
G	0.83	0.85	0.88	0.89	0.90	0.97	1							
H	0.99	0.99	0.99	0.99	0.97	0.90	0.85	1						
I	0.99	0.99	1.00	1.00	0.98	0.91	0.88	0.99	1					
J	0.94	0.94	0.94	0.94	0.96	0.89	0.84	0.93	0.95	1				
K	0.92	0.93	0.93	0.92	0.94	0.87	0.81	0.91	0.93	0.99	1			
L	0.90	0.92	0.94	0.94	0.95	0.97	0.94	0.91	0.94	0.95	0.93	1		
M	0.85	0.87	0.90	0.91	0.92	0.99	0.98	0.88	0.90	0.89	0.86	0.97	1	
N	0.87	0.88	0.90	0.92	0.93	0.99	0.97	0.90	0.91	0.88	0.85	0.95	0.98	1

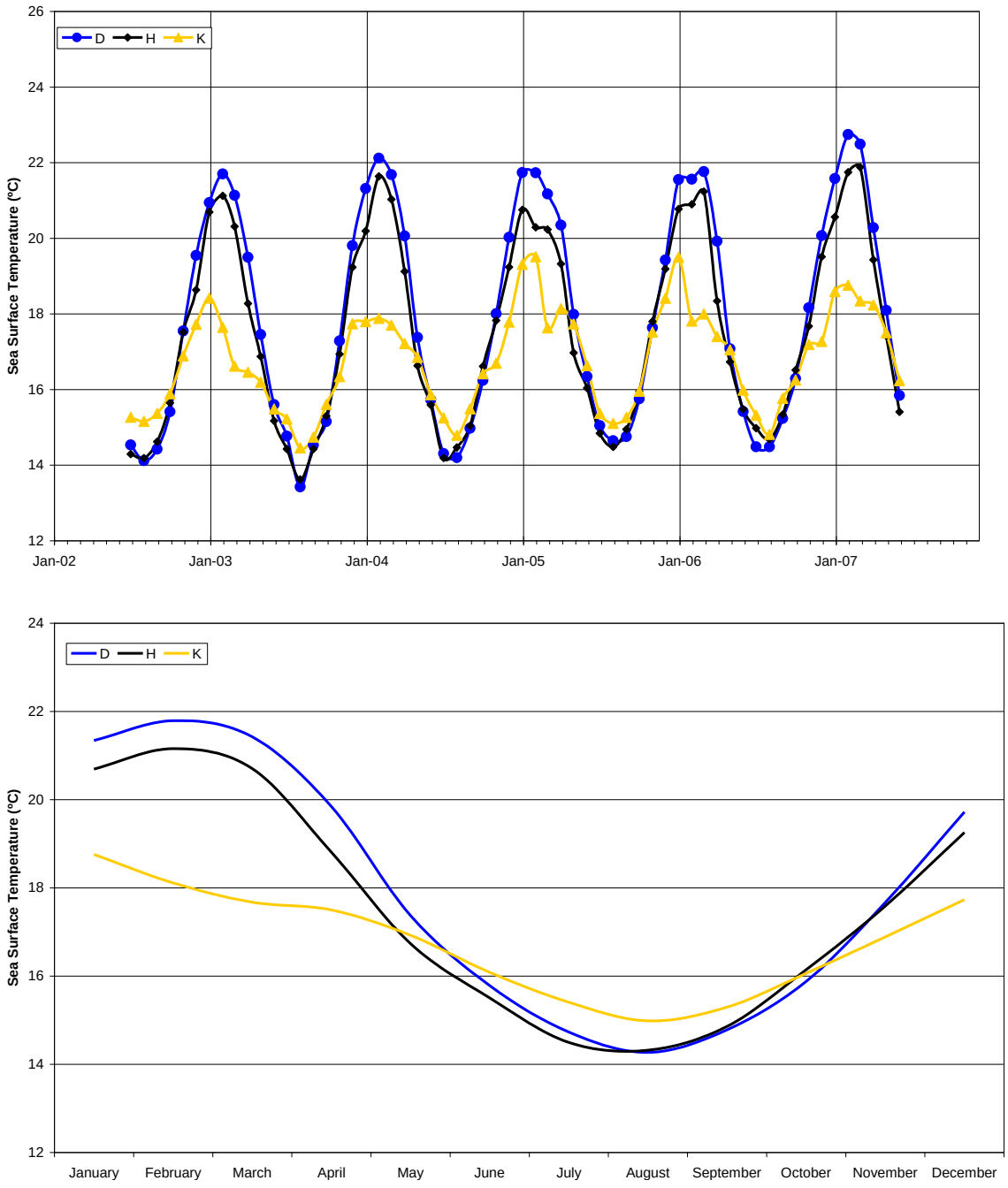

Figure 5.13: Monthly average SST and monthly SST climatology at stations D, H and K showing the slight difference in SST between H and D, and the larger difference in SST between K and D and H.

The monthly climatology SST images were used to observe the changes in temperature along the Spencer Gulf transect in each month of the year (Figure 5.14). From October through to April there was a decrease in temperature with distance from the northern gulf, when gulf waters were warmer than ocean water. During June, July and August there was an increase in temperature towards the south, when the ocean waters were warmer than the gulf. During September and May there was very little difference along the transect. Station A was over 4 ºC warmer than G from December to February while station G was just over 2 ºC warmer than A in July.

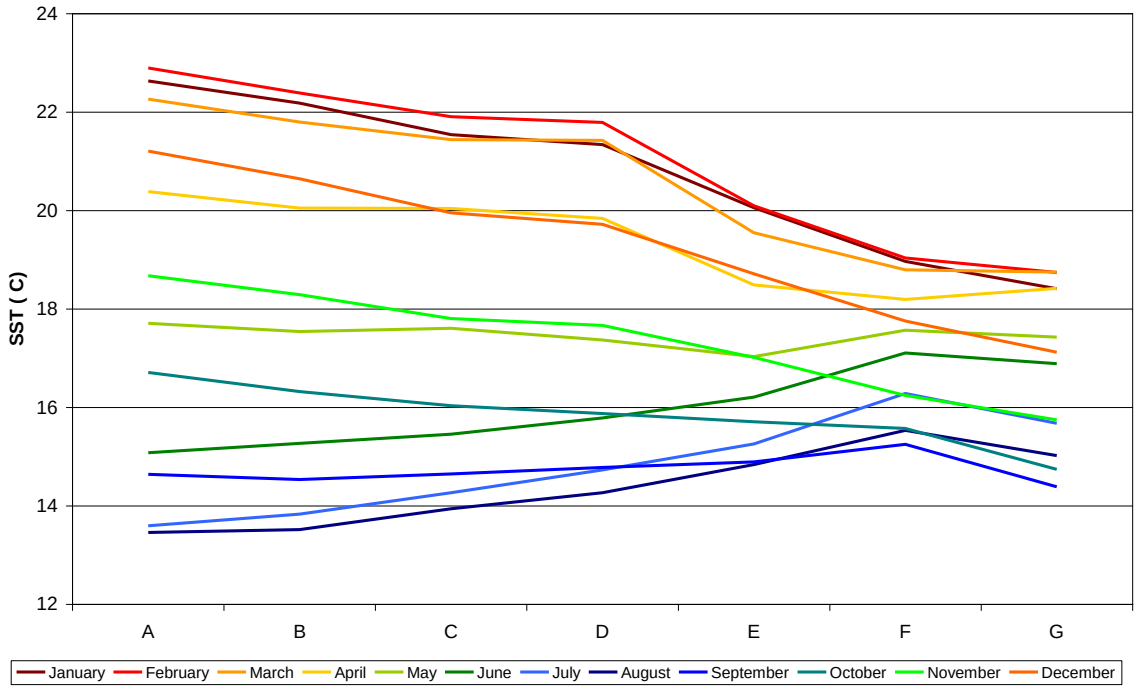

Figure 5.14: The SST climatology at stations along the transect from station A in northern Spencer Gulf and G outside the mouth of the gulf.

A hierarchical cluster analysis of SST showed that the stations within the gulf (A, B, C, D, H and I) and those outside formed two distinct groups (Figure 5.15). Station E, at the mouth of Spencer Gulf, was grouped with the outside stations and was most similar to stations J and K off western Eyre Peninsula. This grouping is similar to what we would expect from the observations of the stations inside the gulf with their large annual range in SST. There is generally greater similarity between the stations within each grouping for SST than there was for chlorophyll-*a*. Extremely high correlation exist between all the stations that form the Spencer Gulf group in the hierarchical cluster analysis (A, B, C, D, H and I), with correlation coefficients equal to 0.99 (Table 5.3).

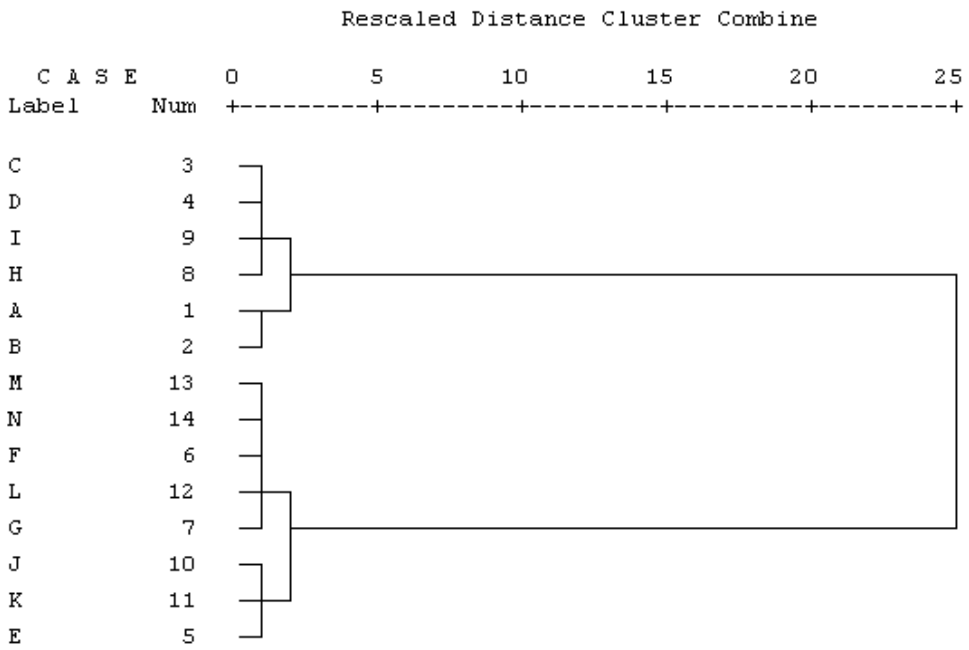

Figure 5.15: Dendrogram from hierarchical cluster analysis using Ward's method showing the similarities between stations based on SST.

Three principal components were identified representing the majority of the variability in SST (Figure 5.16; Figure 5.17). Principal component 1, which represented 78.7% of the variability, appears to be a contrast between inshore and offshore waters. Principal component 2, which represented 11.0% of the variance, is a seasonal cycle. PC 2 clearly shows a contrast between Spencer Gulf waters and the water outside of the mouth in response to the large seasonal SST range within the gulf and the small annual range immediately outside the mouth. This is also observable in the graph of band loadings for PC 2, with positive eigenvector values over summer leading to the positive PC values inside the gulf, and the negative eigenvector values in winter leading to the negative PC values just outside the gulf (Figure 5.17). PC 3, which accounted for just 3.2%, is also a seasonal cycle and appears to be related to upwelling, showing a clear contrast between the areas where upwelling is known to occur, in the south east of SA and on the western side of Eyre Peninsula, with the rest of the region. Three principal components for SST accounted for more variability than the first four components from chlorophyll-*a*, indicating that there is greater variability in chlorophyll-*a* than SST, possibly due a greater number of localised factors.

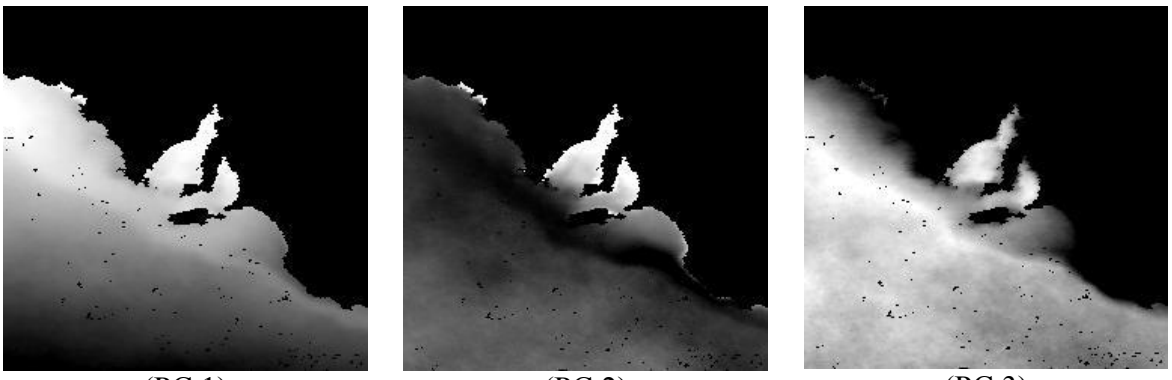

(PC 1) (PC 2) (PC 3)

Figure 5.16: Components 1, 2 and 3 from PCA upon monthly SST imagery, white areas indicate positive PC values and dark areas indicate negative.

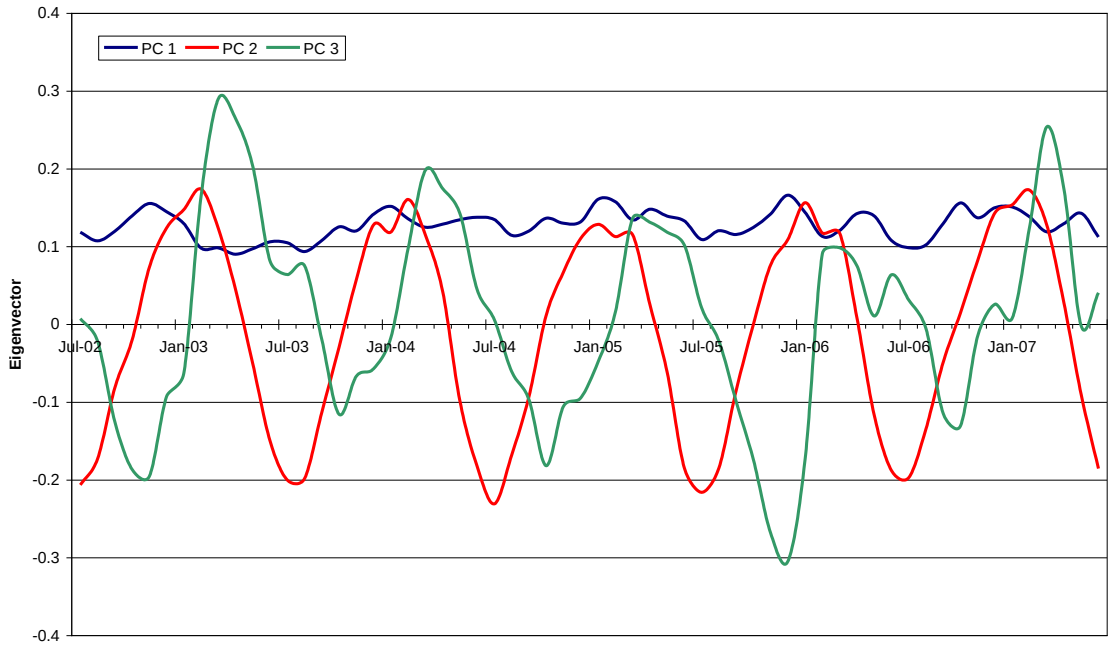

Figure 5.17: Principal component band loading for PCs 1 – 3, identifying which monthly input SST images most influence the resulting principal components.

The waters of the study area were grouped into one of five groups from the unsupervised classification. The waters of Spencer Gulf and Gulf St Vincent formed one group, distinct from the rest of the region, but only accounted for 3.0% of the area of the image. The remaining 4 ocean groups formed bands from the coastline towards the open ocean, accounting for 8.9%, 10.1%, 15.3% and 14.6% of the area respectively (Figure 5.18). The land and unclassifiable pixels accounted for 46.7% and 1.4% of the area. The fact that the classification places gulf waters into a distinct group further emphasises that the waters inside Spencer Gulf are different from waters outside the gulf. The classification also showed waters of the upwelling regions as belonging to a class found further offshore than would normally be the case without the affects of upwelling on the water temperature (Figure 5.18). The classification map based on SST images (Figure 5.18) differs from the

map produced from chlorophyll-*a* (Figure 5.10), indicating that chlorophyll-*a* and SST behave differently and independently in the region.

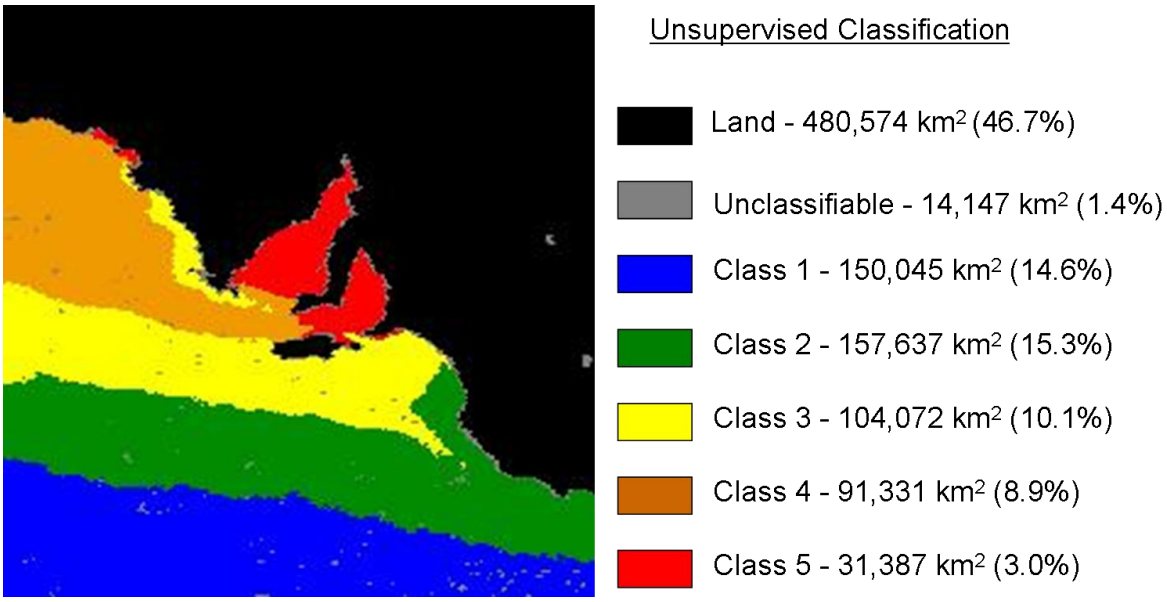

Figure 5.18: Results of an unsupervised classification upon 60 MODIS monthly SST images between July 2002 and June 2007.

5.4 Discussion

In the present chapter the seasonal characteristics of chlorophyll-*a* and sea surface temperature in and around Spencer Gulf were investigated using MODIS satellite imagery. Throughout the study area a large range of chlorophyll-*a* and SST values was observed. Chlorophyll-*a* values differed greatly with location. The chlorophyll-*a* values observed for the far northern Spencer Gulf were considerably higher than at any other location, likely as a result of shallow water depth and interference of bottom reflectance, which has been shown to result in overestimated MODIS chlorophyll-*a* in shallow areas (Chapter 4). The average depth around station A is 20.45 m, although the depth does range from as little as 9 m up to 31 m within the 12 by 12 km area around the station that was avereged. Results from the MODIS chlorophyll-*a* validation in Chapter 4 showed that the relationship between MODIS and field-based chlorophyll-*a* measurements was much stronger when the water depth is greater than 20 metres.

Another interesting feature observed in the MODIS chlorophyll-*a* measurements is an apparent increase in chlorophyll-*a* in the waters east of Port Lincoln in the tuna farming zone compared to the centre of the gulf. As shown in Figure 5.4, the monthly chlorophyll-*a*

observations at station H, near the SBT aquaculture, were noticeably higher than at station D, located in the centre of the gulf at the same latitude, with the greatest discrepancies occurring during the period from March to July. The first consideration is whether the MODIS chlorophyll-*a* estimate is affected by the water depth. Water depth at station H is approximately 21.8 metres, with the majority of the region greater than 20 m, suggesting that water depth may not be a major issue. Despite this, the observed critical depth of 20 m observed in Chapter 4 is unlikely to be absolute and the depth at which bottom reflectance may occur will vary with the clarity of the water. Chapter 4 indicates that the apparent optical depth (AOD) in the region around station H may be between approximately 12 and 22 metres, thus for areas where the physical depth of water is less than the AOD seafloor reflection is likely. It is also possible that the area is influenced by suspended matter or organic matter that are known to also cause overestimates of chlorophyll-*a*, as discussed in Chapter 4.

Another possibility is that the waters of the Port Lincoln area are actually higher in chlorophyll-*a* as a result of processes occurring in this area that are not occurring in nearby areas of Spencer Gulf, such as increased nutrients from aquaculture or other industries in the region, or from naturally occurring processes. Sea cage aquaculture is known to release nutrients into the water column as a result of waste products, uneaten feed and faecal material (Gowen and Bradbury 1987). Fernandes et al. (2007) modelled the nitrogen released from the southern bluefin tuna aquaculture and suggested that more than 85% of nitrogen in the baitfish fed to the tuna is expected to be lost to the environment. Recently it has been determined that nitrogen is the most important limiting nutrient in the aquaculture region, and that nutrient inputs from the SBT aquaculture activities could cause considerable changes to the availability of nutrients for phytoplankton growth (Thompson et al. 2009). The period of greatest increase in chlorophyll-*a* was observed between March and July, which does correspond to the SBT farming season. Thus perhaps the slightly elevated chlorophyll-*a* concentrations of the area of the SBT aquaculture are related to the nutrient release from aquaculture.

The hierarchical cluster analysis and unsupervised classification of chlorophyll-*a* measurements showed that station H was more similar to stations A and B in the north of Spencer Gulf, than the closer stations C, D and E. This finding indicates that coastal influences, to which A and B are also exposed, influence the chlorophyll-*a* at station H. The Pearson correlation, however, indicates that the chlorophyll-*a* at H is more highly

correlated with that at the closer stations in the southern gulf. This is because the correlation coefficient is only related to the timing of the seasonal chlorophyll-*a* cycle while the cluster analysis and unsupervised classification are also related to the magnitude of the concentrations. The principal components analysis showed that the majority of variability in the chlorophyll-*a* dataset (82.7%) was associated with the higher chlorophyll-*a* coastal areas differing from the lower chlorophyll-*a* offshore waters. From PCA and the unsupervised classification it can be seen that H is within the coastal class. Since the remaining principal components were small compared to the spatial pattern, the affect of seasonal changes upon differences between station H and other stations is small. Thus, the differences between H and other stations are as a result of its location near to the coast, and not a characteristic of its temporal chlorophyll-*a* variability.

SST imagery has identified a temperature gradient through Spencer Gulf that reverses in direction during the year (Figure 5.14). In summer, gulf waters are much warmer than offshore waters and as a result SST decreases from the northern gulf towards the shelf. In winter, gulf waters cool down further than the offshore waters, thus the temperature increases from the gulf towards the shelf. The relative increase in SST outside the mouth of Spencer Gulf is also related to a plume of relatively warm water extending from the Great Australian Bight (GAB), which spans across the mouth of Spencer Gulf (Figure 5.19). Although the wintertime GAB plume is of cooler water than is present during summer, it is significantly warmer than surrounding waters at the same time of year. This plume has previously been described by Herzfeld (1997) who investigated the annual cycle of SST in the Great Australian Bight using satellite SST imagery. The warm waters form in the shallow waters of the GAB during summer and autumn and spread eastwards to form a tongue of warm water extending eastwards of 136ºE (Herzfeld 1997), past the mouth of Spencer Gulf. During late autumn the warm GAB plume joins up with the warm Leeuwin Current, which flows into the GAB from the Western Australian coastline, to produce a continuous band of warm water along the southern Australian coastline during winter (Herzfeld 1997). Thus, the increase in SST observed from stations E through to G (Figure 5.14) observed during June, July and August is a result of this warm GAB surface water extending across the mouth of Spencer Gulf (Figure 5.19).

Another oceanographic feature of Spencer Gulf, identified in the MODIS imagery, which plays an important role in the circulation of the gulf during summer, is the sea surface temperature front (Figure 5.19). This front marks the boundary between the shallow, warm

waters of Spencer Gulf, and the deeper, cooler oceanic waters. Previous work using daily AVHRR SST imagery by Petrusevics (1993) has shown that the front begins to develop in November, as summertime solar heating intensifies, and persists until May, with the greatest temperature difference of 4 ºC occurring in April. CTD surveys by Petrusevics (1993) showed that the SST front is also a density minimum, where currents from Spencer Gulf and the shelf converge, generating upwelling that isolates gulf and shelf waters. SST in Spencer Gulf can be seen to decrease between stations D and E from December through to April (Figure 5.14) as a result of this SST front. The front appears to be a key factor accounting for the pattern seen in the unsupervised classification of the SST. The classification image separated the gulf waters from nearby ocean waters at a location where the SST front is known to occur (Figure 5.18; Figure 5.19). In addition the hierarchical cluster analysis separated stations inside the gulf from those outside Spencer Gulf (Figure 5.15); the SST front divides these two regions.

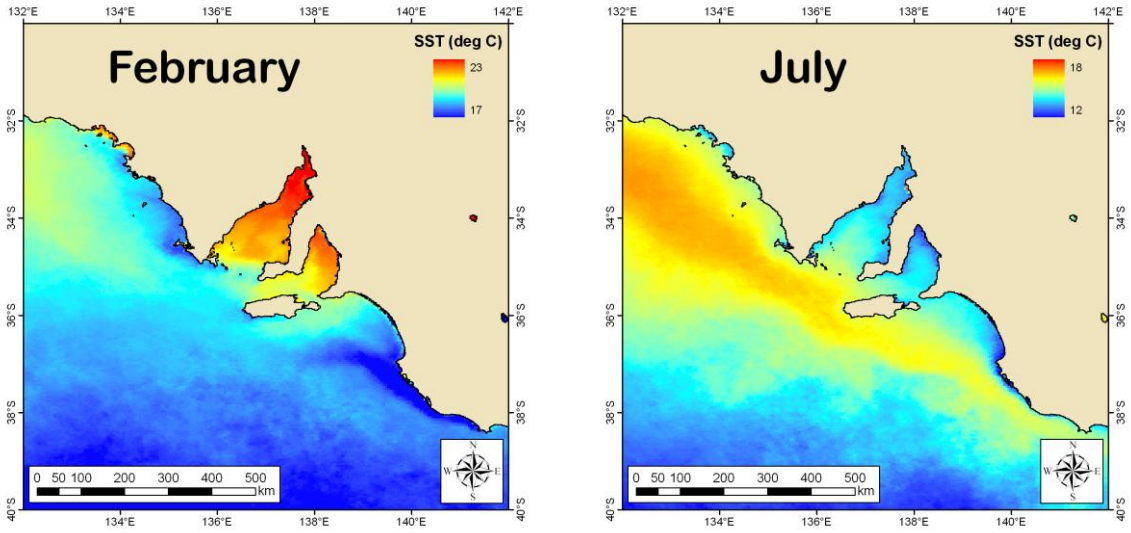

Figure 5.19: Monthly SST climatology during February, showing the warm gulf waters isolated from the adjacent shelf waters by the SST front during summer and the monthly SST climatology during July, showing the tongue of warm GAB water extending past the mouth of Spencer Gulf during winter. Note the different scales on the colour bars.

Coastal upwelling is also observable in the MODIS satellite imagery of South Australia. Upwelling has been observed at three locations along the South Australian coast: the Bonney coast in the southeast of the state; the southwestern coast of Kangaroo Island; and the western coast of Eyre Peninsula. Approximately 2 or 3 upwelling events occur simultaneously at these locations each summer, each lasting approximately 1 week and resulting in decreases in SST of 2 – 3 ºC and increases in chlorophyll-*a* up to 4 mg m^{-3} (Kampf et al. 2004). McClatchie et al. (2006) showed that the Eyre Peninsula upwelling is

not independent from the Kangaroo Island upwelling, but rather the Kangaroo Island upwelling draws water up to form a subsurface pool and the water is later drawn to the shallow waters of the eastern GAB. Although the short time span of each event, ~ 1 week, is masked within monthly composite imagery, evidence of the occurrence of upwelling is available within the monthly MODIS imagery, particularly during months when multiple upwelling events have occurred. March 2003 is one month where the effects of coastal upwelling are visible in monthly MODIS imagery (Figure 5.20). Cooler surface waters are evident along the Bonney Coast, Kangaroo Island and Eyre Peninsula where upwelled water is 2 – 3 ºC cooler. Chlorophyll-*a* concentrations are also elevated in corresponding locations to the cooler waters. Upwelling in these regions is a common occurrence and is detected by the unsupervised classification of the SST imagery, which shows the water in these regions as belonging to a class that is cooler (Figure 5.18). There is also some evidence for upwelling in the temporal profiles of chlorophyll-*a* at the locations along the western coast of Eyre Peninsula and the southwest of Kangaroo Island. Particularly evident at station K, but also noticeable at other stations, is a peak in chlorophyll-*a* in March that is inconsistent with the annual cycle of chlorophyll-*a* in the surrounding regions (Figure 5.5).

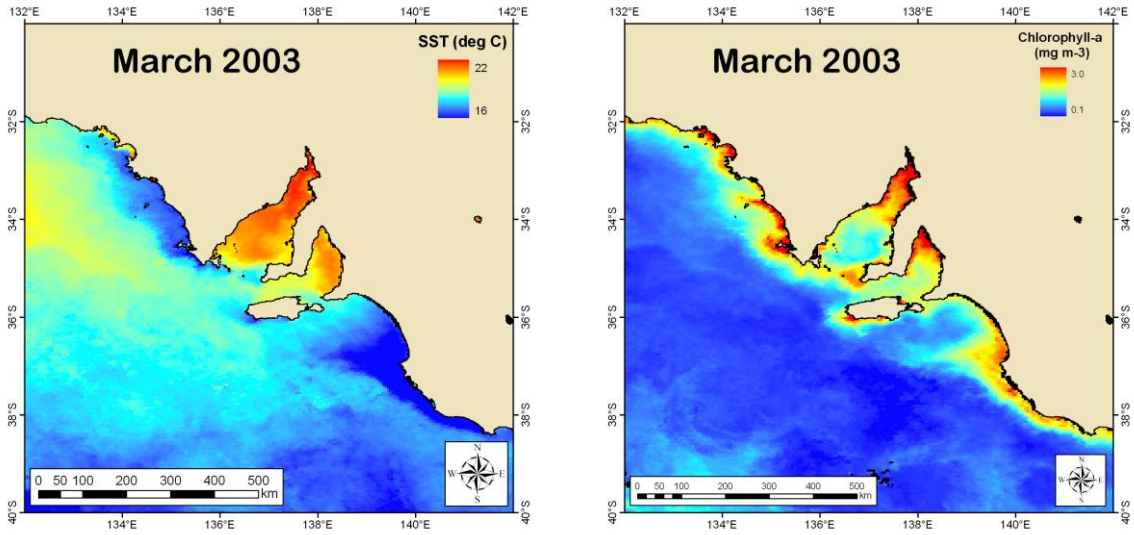

Figure 5.20: Monthly SST and monthly chlorophyll-*a* of March 2003 showing upwelling in the southeast of SA, on southwestern Kangaroo Island and on western Eyre Peninsula as indicated by cooler surface temperatures and increased chlorophyll-*a*.

5.5 Conclusion

MODIS monthly composite imagery has allowed the seasonal variations in chlorophyll-*a* and sea surface temperature to be described. Seasonal chlorophyll-*a* variations differed greatly between locations in and around Spencer Gulf. The observed MODIS chlorophyll-*a* estimates in the northern gulf were higher than at any other location, with the peak occurring from January to May and minimum from August to November. The MODIS chlorophyll-*a* estimates from the northern gulf are likely to be influenced by the adjacent land as a result of shallow water depth, reflection from the land, and suspended matter, resulting in an overestimation of chlorophyll-*a*. Thus the results derived from MODIS chlorophyll-*a* observations at station A should be treated cautiously. In the southern part of the gulf, concentrations were much lower than in the north and the periods of maximum and minimum chlorophyll-*a* occurred from April to July and September to November respectively. Further south, outside the mouth of Spencer Gulf, the concentrations were lower again and the periods of maximum and minimum occurred from August to October and December to March, almost the opposite seasonal cycle to the northern gulf. The region around the SBT aquaculture showed higher MODIS chlorophyll-*a* concentrations than nearby gulf waters, possibly as a result of water depth and coastal influences, but also possibly as a result of farming practices. A hierarchical cluster analysis and unsupervised classification of the imagery have shown that the aquaculture region is more similar to the northern Spencer Gulf and other coastal areas than to the waters in the centre of Spencer Gulf, closer to the aquaculture region.

Sea surface temperature varied greatly between Spencer Gulf and nearby ocean waters. Waters within the gulf showed a greater seasonal range than waters outside the gulf. As a result the gulf waters are warmer than nearby ocean waters in summer, but cooler during winter. There is also a noticeable gradient in the seasonal temperature range through the gulf, with warmer summer temperatures and cooler winter temperatures in the northern gulf. Moving south through the gulf the summertime maximum temperatures decreased and the wintertime minimum increased resulting in an annual temperature change of only a few degrees in the waters outside of the gulf. This result is consistent with previous studies that have described the seasonal temperature characteristics of Spencer Gulf. Results from hierarchical cluster analysis, unsupervised classification and principal components analysis have all confirmed that, based on SST, Spencer Gulf and Gulf St Vincent are different from other waters of the region, as a result of the large seasonal changes in temperature.

These findings from MODIS imagery in this chapter have expanded the knowledge of the seasonal chlorophyll-*a* and SST variations of Spencer Gulf and nearby waters. There existed some previous knowledge of the variations of both chlorophyll-*a* and SST at particular locations within the study area, but the variations across the large area of Spencer Gulf had not been studied previously in detail. Knowledge gained on the seasonal variations allows an improved understanding of the ocean dynamics of the region.

Chapter 6: Variability of Chlorophyll-*a* and Sea Surface Temperature in the Tuna Farming Zone

6.1 Introduction

Southern bluefin tuna (SBT) aquaculture takes place in the southwest of Spencer Gulf offshore from Boston Island, as previously discussed. Prior to 1996 the majority of aquaculture activity took place in the rather shallow, sheltered waters within Boston Bay. Since 1996, however, the industry has moved its operations further offshore east of Boston Island to utilise the deeper waters and greater flushing that this area offers. Figure 6.1 shows the location of the Lincoln Offshore sectors of the Boston Bay and Lincoln Offshore aquaculture zone where farming of SBT takes place. An annual quota of 5,265 tonnes of juvenile SBT is caught from the eastern Great Australian Bight each summer. The SBT are then held in pens within the aquaculture zone between January and September, where they are primarily fed with frozen Australian sardines. It has been shown that a considerable amount of the nitrogen input into the system as feed is lost to the surrounding environment (Fernandes et al. 2007), and the local nutrient inputs from fish farming and recycling of nutrients from the sediments significantly increase the nutrients available for phytoplankton growth (Thompson et al. 2009).

Monthly average chlorophyll-*a* concentrations in Spencer Gulf were observed to range between 0.3 and 1.4 mg m^{-3} near the tuna farming zone (Chapter 5). The seasonal peak in chlorophyll-*a* was observed between March and July, similar to the findings of Paxinos (2007), who showed maximum chlorophyll-*a* from March to June, and van Ruth et al. (2009) who showed a peak in May. These previous studies of chlorophyll-*a* in the tuna farming zone identify the broad seasonal patterns of chlorophyll-*a*, but are unable to resolve temporal variability on timescales finer than one month, nor are they able to show detailed spatial variability within the tuna farming zone. Chlorophyll-*a* variability can be studied at finer temporal and spatial scales than the previous field-based studies using daily MODIS chlorophyll-*a* imagery.

While temperature variation within Spencer Gulf and nearby coastal waters of South Australia has previously been investigated (Nunes and Lennon 1986; Nunes Vas et al. 1990; Petrusevics 1993), few studies have examined temperature around Port Lincoln or

the tuna farming zone. Chapter 5 showed that the warmest temperatures (~21.2 °C) were observed in February, with temperatures decreasing to a minimum of around 14.3 °C in August. It was also shown that the waters inside Spencer Gulf, including those in the tuna farming zone (TFZ), undergo a larger annual range in SST compared to outside the gulf.

The previous chapter, and some studies already mentioned, have investigated variability of chlorophyll-*a* and SST around the Port Lincoln tuna farming zone. However, these investigations have been limited in their ability to describe the variability over short temporal and fine spatial scales. Therefore, the aim of this chapter is to describe the fine-scale spatial and temporal variability of chlorophyll-*a* and SST in the TFZ with daily MODIS imagery.

6.2 Methods

6.2.1 Study Area

The region of interest in this study is the southwest of Spencer Gulf, and in particular the waters of the TFZ. To facilitate investigation of MODIS chlorophyll-*a* and SST variability of the TFZ, a subset area covering where the majority of the SBT aquaculture activity takes place was defined. The TFZ subset covers the area from 34º 34‟ 55.08” S to 34º 42‟ 27.81” S, and from 135º 59‟ 49.88” E to 136º 8‟ 27.20” E (Figure 6.1). The TFZ subset was also designed to avoid the shallowest areas of the region where bottom reflectance is likely to have considerable impact on chlorophyll-*a* estimates (Chapter 4). The average depth within the TFZ subset is 20.7 m, but varies between 16 and 25 m and is generally shallowest in the west and deepest towards the east.

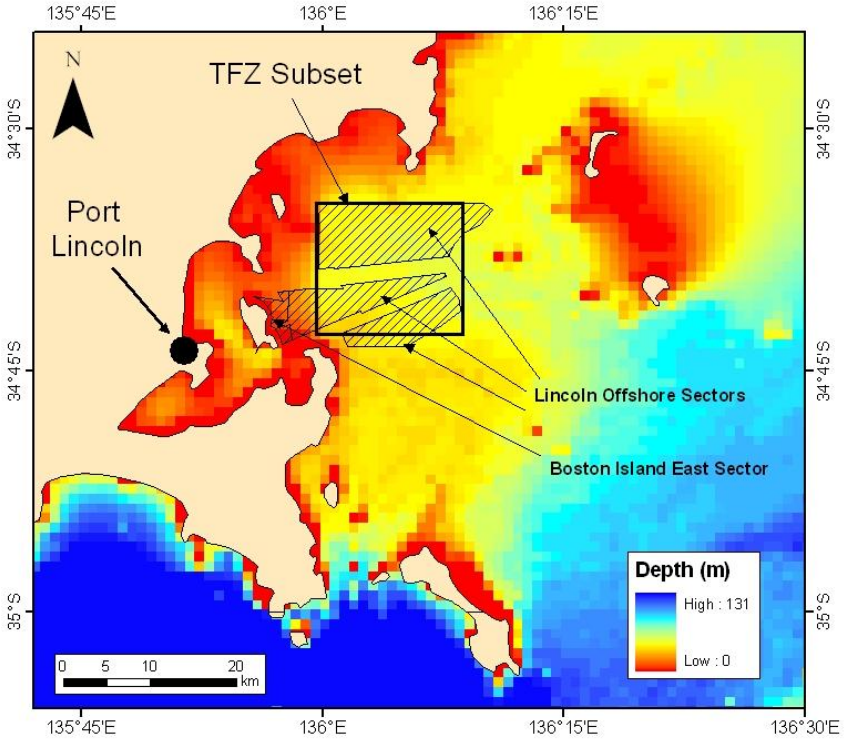

Figure 6.1: The tuna farming zone subset, the aquaculture zones, and the bathymetry of the region.

6.2.2 MODIS Imagery

To investigate the daily variability around the TFZ, MODIS daily level 2 chlorophyll-*a* and SST images were used. MODIS Aqua level 2 standard OC3M chlorophyll-*a* images and day-time 11 μm SST images at 1 km spatial resolution were obtained from the Goddard Space Flight Centre. Daily images were obtained for a 6-year period between July 2002 and June 2008. Images were initially subset to an area from 30ºS to 40ºS and from 132ºE to 142ºE. The HDF (hierarchical data format) files were imported into ENVI version 4.3 (RSI 2006) using the ENVI plug-in for ocean colour (White undated). The images were stacked together into a single layered file, with the daily files placed as bands in a multiple band image file. A subset of the images was then created for the TFZ subset. In creating the TFZ subset, the images were processed via the nearest neighbour method so that each of the images had corresponding pixels and the resulting images were 15 pixels wide by 17 pixels high, approximately 14 km by 15 km, and an area of 209 km^2. Many of the images were influenced by cloud cover and masking of image pixels. When one or more of the 255 pixels of the TFZ subset were masked, the images were removed from the dataset. Images with masked pixels were removed from the layered file using the spectral subset tool in ENVI. This resulted in 475 clear and cloud-free images of the TFZ between July

2002 and June 2008. The daily images were not uniformly distributed throughout the year, but biased towards the summer months when cloud cover was less prevalent. Figure 6.2 shows the number of cloud-free images per month.

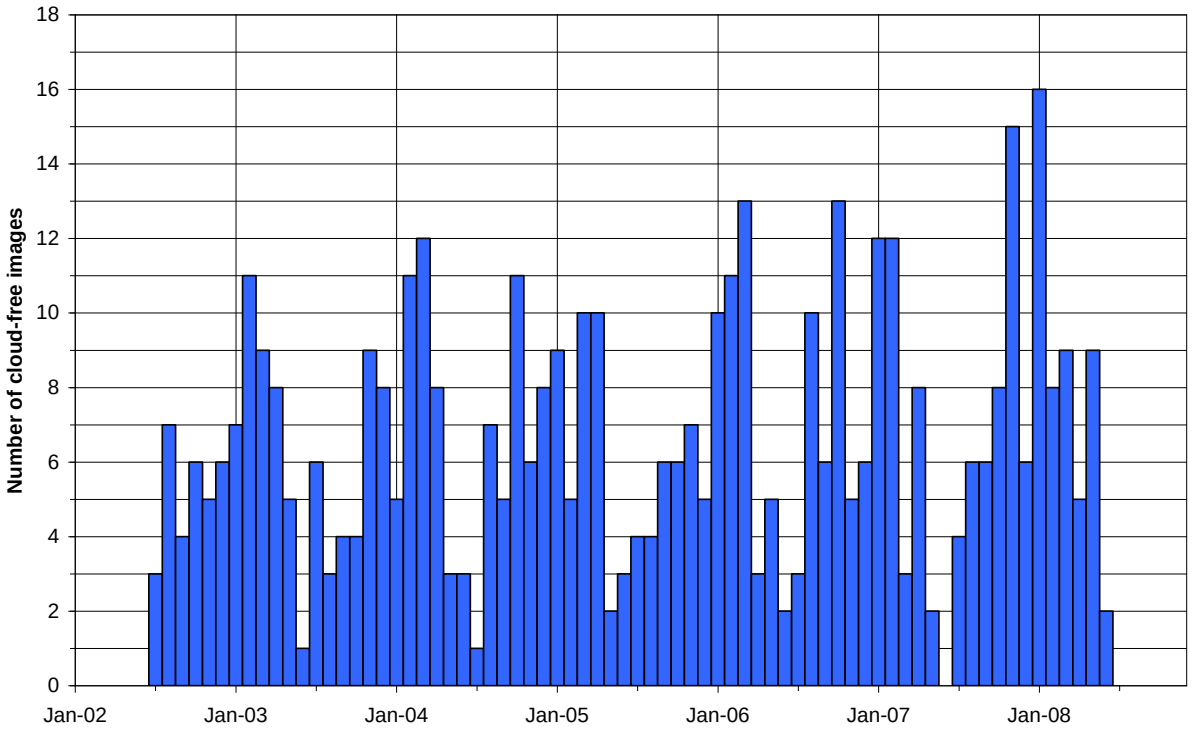

Figure 6.2: The number of cloud-free MODIS Aqua images over the tuna farming zone per month.

6.2.3 Analysis

For both the chlorophyll-*a* and SST images, the mean, minimum, maximum and standard deviation of the values within the TFZ subset were calculated for each of the 475 daily images. The temporal variation in each of these statistics was observed over the 6-year period. For each month a monthly mean image of the TFZ subset was calculated by averaging all of the daily images within that month. Furthermore a long-term mean image of the 6 years was calculated by averaging all of the monthly images. The temporal variability at selected locations was compared to help explain variations across the region.

6.3 Results

6.3.1 Chlorophyll-*a*

There was a distinct temporal pattern in the spatial mean chlorophyll-*a* for the TFZ, with maximum concentrations during autumn and winter (March to July) and lowest concentrations in spring and summer (September to January) (Figure 6.3). The lowest spatially averaged concentration observed for the TFZ was 0.27 mg m^{-3} on 11/11/2007, and the maximum was 2.39 mg m^{-3} on 22/7/2003. Daily spatial means typically ranged between 0.3 and 0.6 mg m^{-3} during the spring and summer and between 0.7 and 1.3 mg m^{-3} during autumn and winter. This seasonal variability is comparable to that observed in Chapter 5 for a similar location using the monthly composite imagery; although the results from the monthly images provided no indication of the variability on shorter time scales. There is greater absolute day-to-day temporal variability during periods of higher concentration than periods of lower chlorophyll-*a* concentration (Figure 6.3), with the standard deviation showing a seasonal pattern that follows the seasonal cycle of chlorophyll-*a* concentration (Figure 6.4). Hence the region is more variable on short timescales during the period when chlorophyll-*a* concentrations are high, autumn and winter, and less variable during periods of low chlorophyll-*a*, spring and summer.

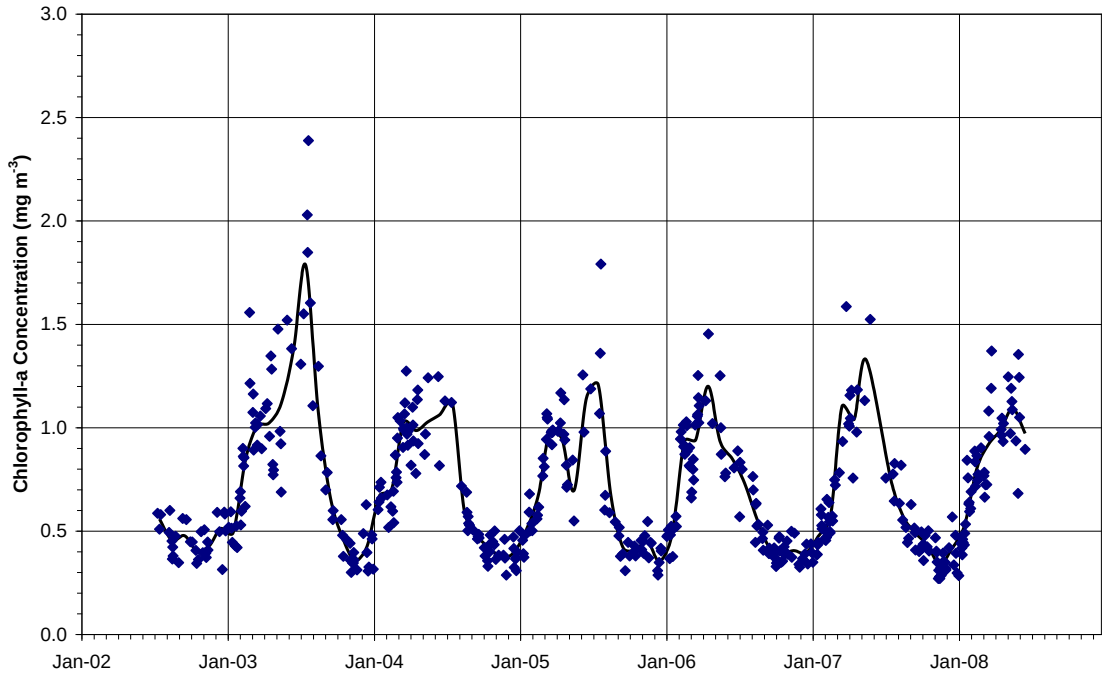

Figure 6.3: The daily spatial mean chlorophyll-*a* for the tuna farming zone (diamonds), with the monthly average curve from averaging the daily images in each month.

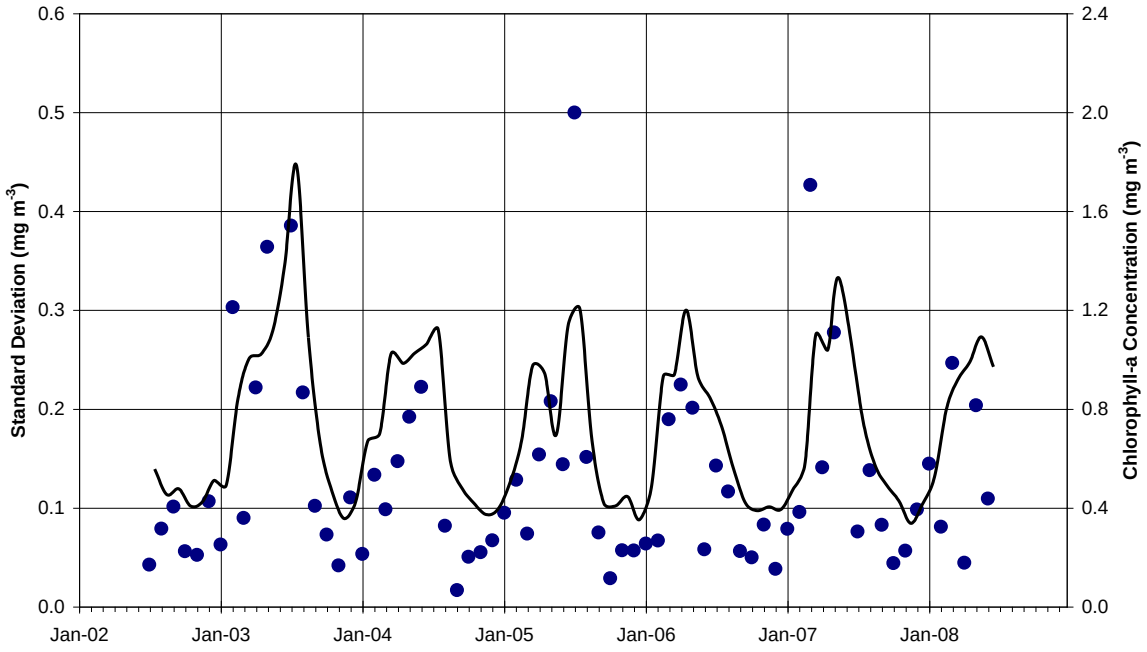

Figure 6.4: Standard deviation of the daily spatial mean chlorophyll-*a* for the tuna farming zone within each month (circles), and the curve of the monthly average chlorophyll-*a*.

Along with the seasonal cycle observed for the daily spatial mean chlorophyll-*a* of the TFZ, there is also a seasonal cycle in the spatial variability. The standard deviation varied seasonally following a similar pattern to the mean. During periods of the year when chlorophyll-*a* is low the spatial variability is also low, and when chlorophyll-*a* is greater there is also greater spatial variability (Figure 6.5, Figure 6.6). Thus while the minimum

concentration within the TFZ varied only between ~ 0.2 and 1.2 mg m^{-3} over all seasons, the maximum ranged from 0.5 up to as high as 5.6 mg m^{-3} (Figure 6.7). The combination of the high spatial variability across the TFZ and the high temporal variability during the autumn and winter months indicates the possibility that small blooms of chlorophyll-*a* occur in and around the TFZ at this time.

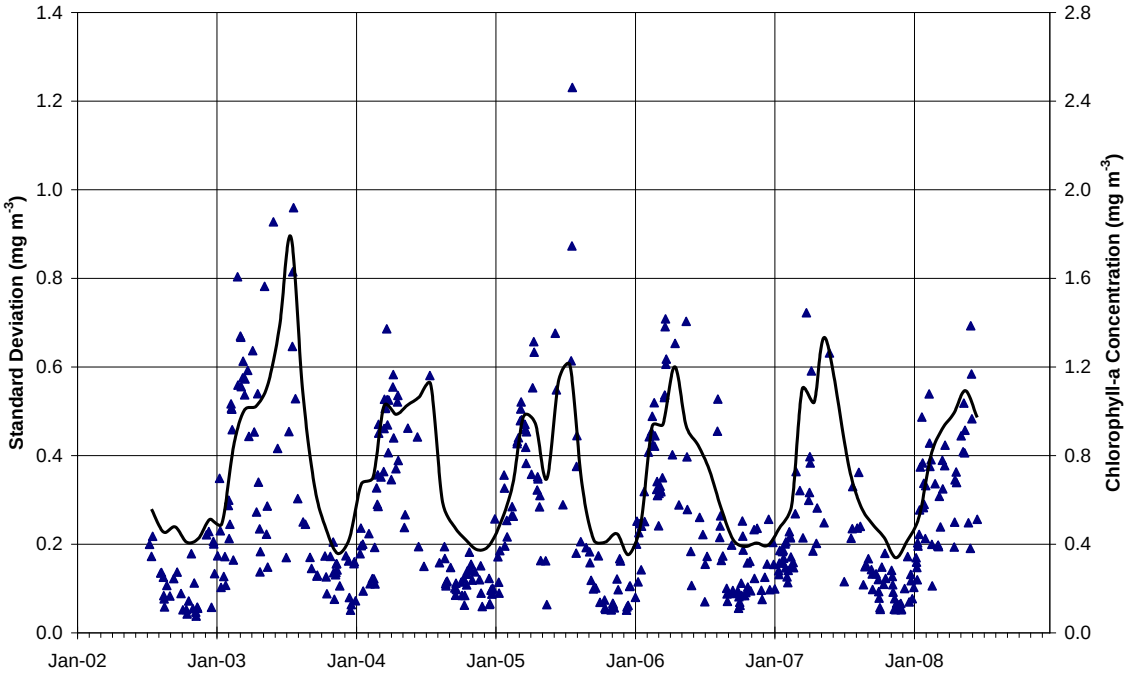

Figure 6.5: The spatial standard deviation of chlorophyll-*a* across the TFZ for each daily MODIS image (triangles), along with the curve of the monthly average chlorophyll-*a*.

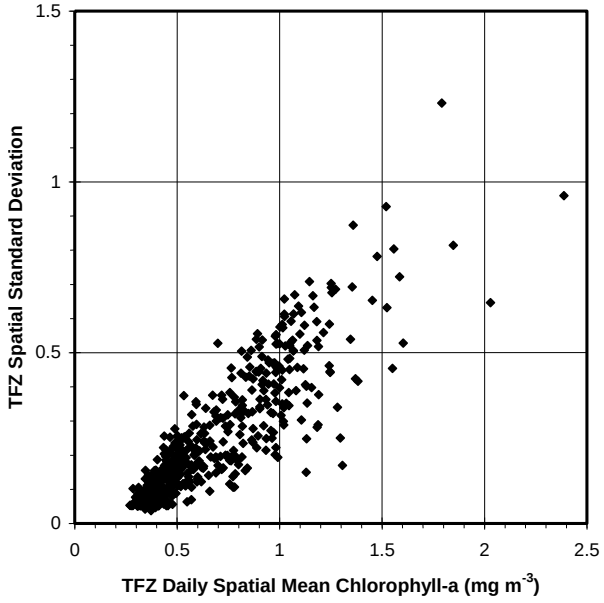

Figure 6.6: Scatter plot of the daily spatial mean chlorophyll-*a* across the TFZ against the standard deviation of chlorophyll-*a*.

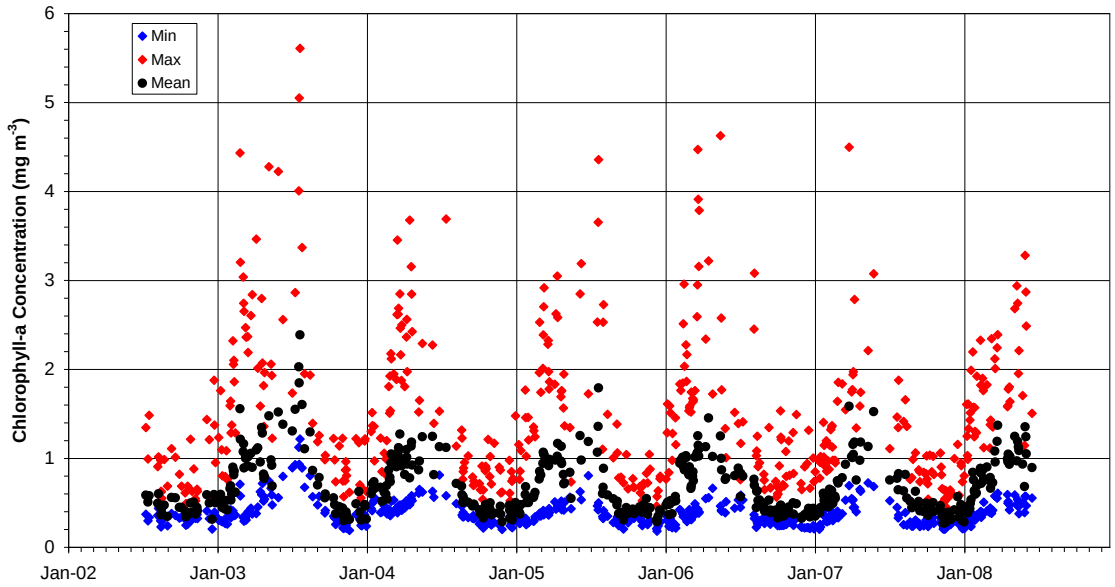

Figure 6.7: The minimum, maximum and mean chlorophyll-*a* within the TFZ subset for each daily MODIS image.

The long-term mean chlorophyll-*a* of the TFZ over the six years shows a contrast between the northwest and southeast, with higher levels towards the northwest and lower in the southeast (Figure 6.8). The daily chlorophyll-*a* in these two areas shows quite different temporal profiles (Figure 6.9). Chlorophyll-*a* in the northwest is higher than in the southeast all year, but particularly during the annual peak in the autumn and winter months. The northwest also appears to peak slightly earlier in the year and is much more variable on shorter temporal scales. The graph of daily chlorophyll-*a* in the northwest and southeast (Figure 6.9) is similar to that of the minimum and maximum chlorophyll-*a* across the TFZ (Figure 6.7).

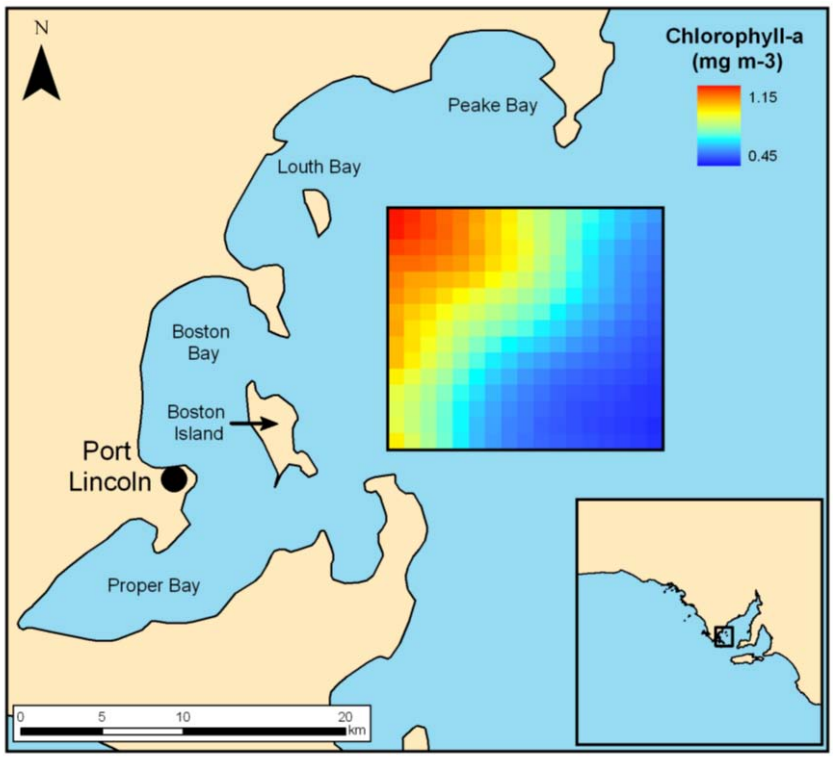

Figure 6.8: The long-term average chlorophyll-*a* image of the TFZ subset, showing the contrast between the northwest and the southeast.

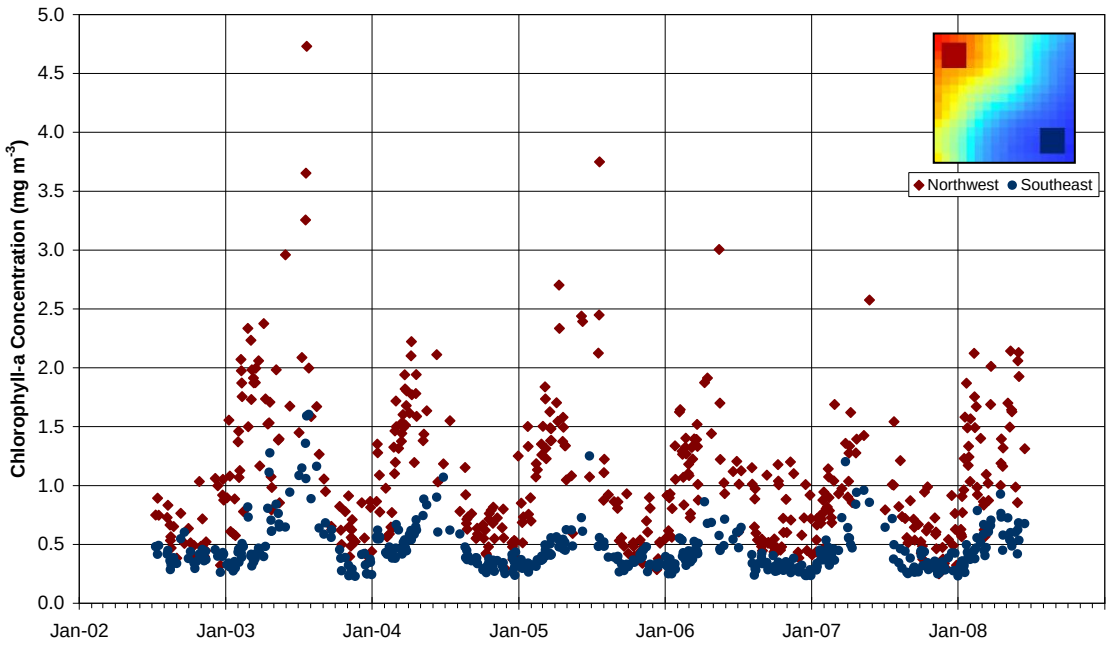

Figure 6.9: The daily chlorophyll-*a* in the northwest and southeast of the TFZ.

6.3.2 Sea Surface Temperature

There was a very clear seasonal cycle in mean SST of the TFZ, with maximum temperatures from January to March, and minimum temperatures between July and September (Figure 6.10). The lowest temperature averaged over the TFZ was 13.15 ºC on 22/08/2003 and the maximum was 24.11 ºC on 10/01/2005. The winter-time minimum SST was typically between 14 and 15 ºC, while the summer-time maximum was typically 21 – 23 ºC. The daily SST follows the monthly average SST reasonably closely, but there are periods when there are noticeable differences between the daily value and the monthly average. These differences predominantly occur at the maximum of the seasonal cycle in summer, but this is likely to be due to a greater number of images per month in the summer months compared to other periods of the year. Unlike with chlorophyll-*a*, the SST showed no clear seasonal trend in the day-to-day temporal variability within each month. The spatial variability of SST across the TFZ for each daily image showed some signs of a seasonal pattern, although not as clear as the pattern observed for chlorophyll-*a*. The greatest spatial standard deviation was observed for the warmer summer months, while the cooler winter months generally showed lower standard deviations (Figure 6.11). The long-term mean SST over the TFZ (not shown) showed no spatial pattern.

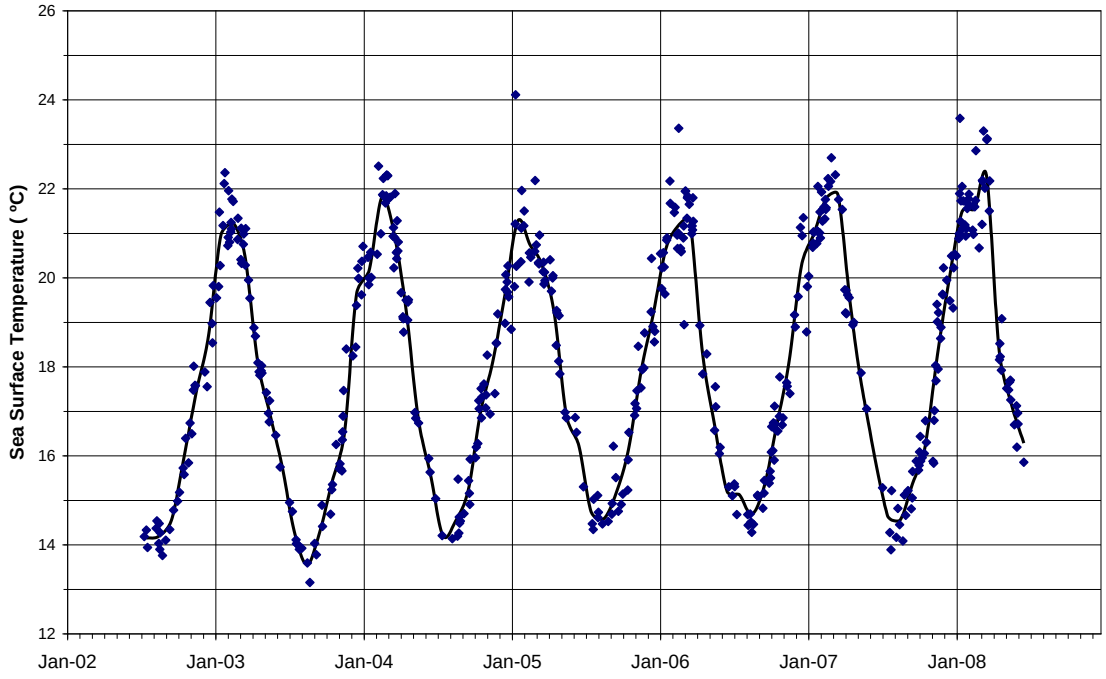

Figure 6.10: The daily spatial mean SST for the TFZ (diamonds), with the monthly average curve from averaging the daily images in each month.

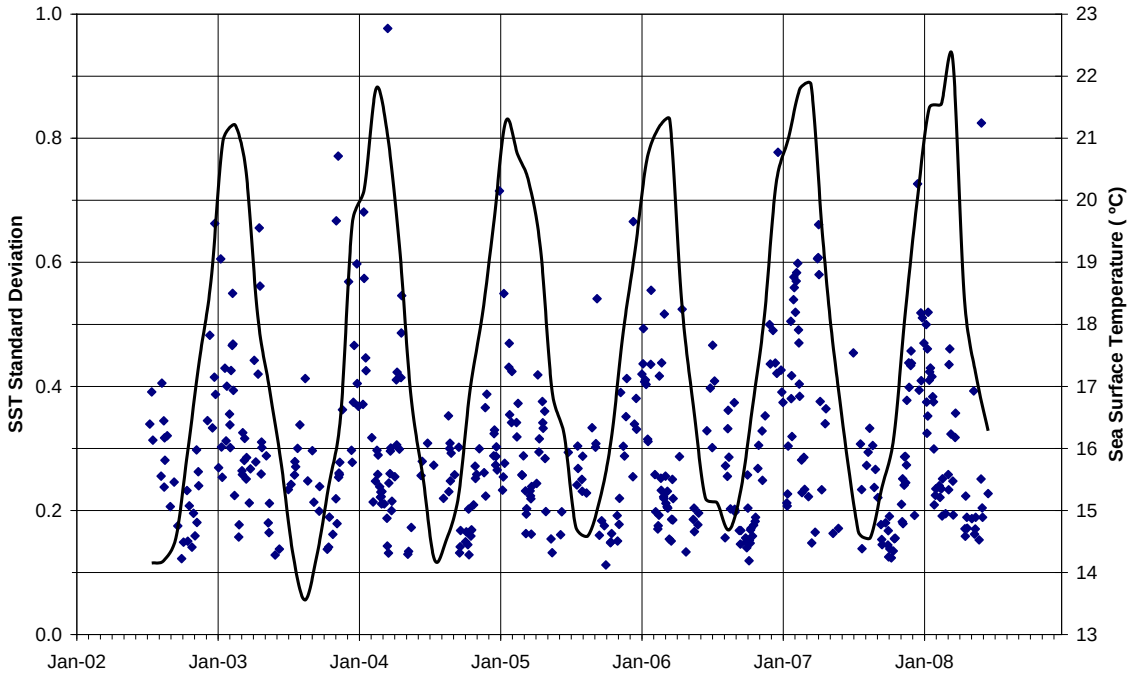

Figure 6.11: The spatial standard deviation of SST across the TFZ for each daily MODIS SST image (diamonds), along with the curve of the monthly average SST.

6.4 Discussion

The temporal pattern of the spatial average chlorophyll-*a* over the TFZ for the 6-year period studied agrees well with the seasonal patterns observed based upon the monthly composite imagery at a similar location in Chapter 5 with minimum chlorophyll-*a* between September and January and maximum chlorophyll-*a* between March and July. This seasonal pattern is also in agreement with the field-based studies of Paxinos (2007), who showed an annual maximum between March and June, and van Ruth et al. (2009) who observed peak chlorophyll-*a* in May. van Ruth et al. (2009) also show that the seasonal cycle in chlorophyll-*a* is strongly influenced by the seasonal dynamics of diatoms which may respond to a peak in silica that was measured in February. This study has further expanded the understanding of the temporal variability in chlorophyll-*a* in the tuna farming zone by observing the variability on shorter time scales. It was observed that day-to-day variability over the TFZ can be considerable, particularly during periods of the year when the average chlorophyll-*a* in the region is high. However, this may be related to the number of images within each month, which was not constant.

This study also shows that the spatial variability in chlorophyll-*a* across the TFZ can be considerable, and that it is dependant upon the time of year. Chapter 4 showed that field-

based surface chlorophyll-*a* measurements were highly variable over very small distances within the TFZ, and this chapter has confirmed that this variability is also observable within the much coarser MODIS imagery. It was observed that there is large variability across the TFZ during the periods of the year when the average chlorophyll-*a* of the region is large, and that the high average chlorophyll-*a* observed for the TFZ may be related to small blooms within the TFZ and not high concentrations across the entire region.

This study has enabled a more comprehensive understanding of the spatial variability to be developed than previous studies. For example Paxinos (2007) showed differences in chlorophyll-*a* between different regions within the southwest Spencer Gulf, with the lower Spencer Gulf region, where no aquaculture activity takes place, very different from all other areas. But she was not able to show spatial variability within the TFZ. Bierman (2005) was able to observe spatial patterns in chlorophyll-*a* across the TFZ on two occasions in 2005 using a grid of field-based measurements. Observations taken between the 7th and 10th March 2005 showed an area of higher concentration immediately east of Boston Island, surrounded by much lower concentrations to the east and north (Figure 6.12). These measurements were taken over a period of 4 days, thus the pattern observed is likely to be affected by short-term temporal variation. The results of the present study indicate that the TFZ may be variable on such timescales. MODIS chlorophyll-*a* images of the TFZ over consecutive days between the 7th and 10th March 2005 show changing spatial patterns over this short time period (Figure 6.13). The images show patterns with patches of higher chlorophyll-*a* concentrations within the relatively small area of the TFZ, and sequential images show how these patterns change over time. The images from the 7th to 10th March 2005 show increasing concentrations in the southwest of the TFZ. Thus, while field-based measurements can allow spatial patterns to be observed, the satellite-based imagery has advantages by covering large areas simultaneously and repeatedly.

The long-term mean chlorophyll-*a* of the TFZ showed a distinct spatial trend, with greater concentrations in the northwest and lower concentrations in the southeast. This difference in chlorophyll-*a* across the TFZ could possibly be due to seafloor reflection influencing the MODIS observations in the northwest resulting in overestimated chlorophyll-*a*, which has been shown to occur in shallow regions (Chapter 4). The bathymetry of the region, as shown in Figure 6.1, does not follow the same spatial pattern as observed in the chlorophyll-*a* imagery, thus indicating that this is not the case. It is also possible that the observed patterns in the MODIS chlorophyll-*a* are a result of greater flushing of the waters

in the southeast of the TFZ and accumulation of nutrients in the northwest. Herzfeld et al. (2009) showed that the offshore waters experienced greater flushing than the inshore coastal areas. However, the study also showed that the farming region is not as well connected to the rest of the gulf as was previously believed, and that nutrients appear to accumulate in near-shore areas of Louth and Peake Bays rather than being flushed out into the southern gulf (Herzfeld et al. 2009; Tanner and Volkman 2009). This may explain the apparent trends in chlorophyll-*a* observed in the TFZ subset, with the higher long-term averaged chlorophyll-*a* concentrations in the northwest towards the bays where nutrients are suggested to be transported. If in fact the northwest is higher in chlorophyll-*a* and experiencing more frequent blooms of phytoplankton, as the results suggest, this may have implications for the SBT aquaculture industry.

The sea surface temperature imagery over the TFZ for the 6-year period shows a temporal cycle consistent with the seasonal cycle observed using the monthly composite imagery in Chapter 5. Minimum temperatures were observed between July and September and maximum temperatures between January and March. The daily average SST over the TFZ differed little from the monthly mean for the majority of the time, with the exception of a few periods, predominantly during the summer months. Figure 6.10 shows that there are days when the daily spatial average SST over the TFZ is much larger than the monthly mean, possibly as a result of local weather conditions.

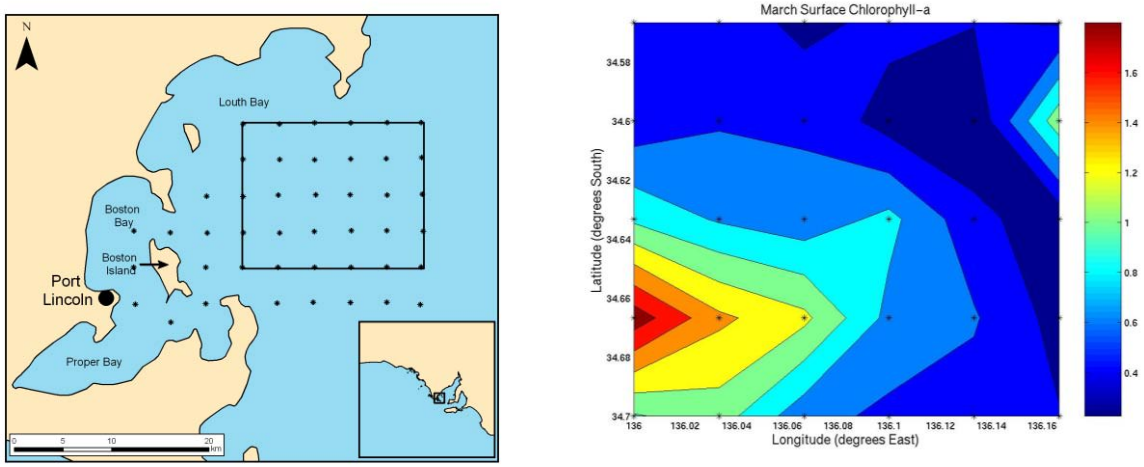

Figure 6.12: Field-based chlorophyll-*a* measurements over the tuna farming zone on the 7th – 10th March 2005 (Bierman 2005).

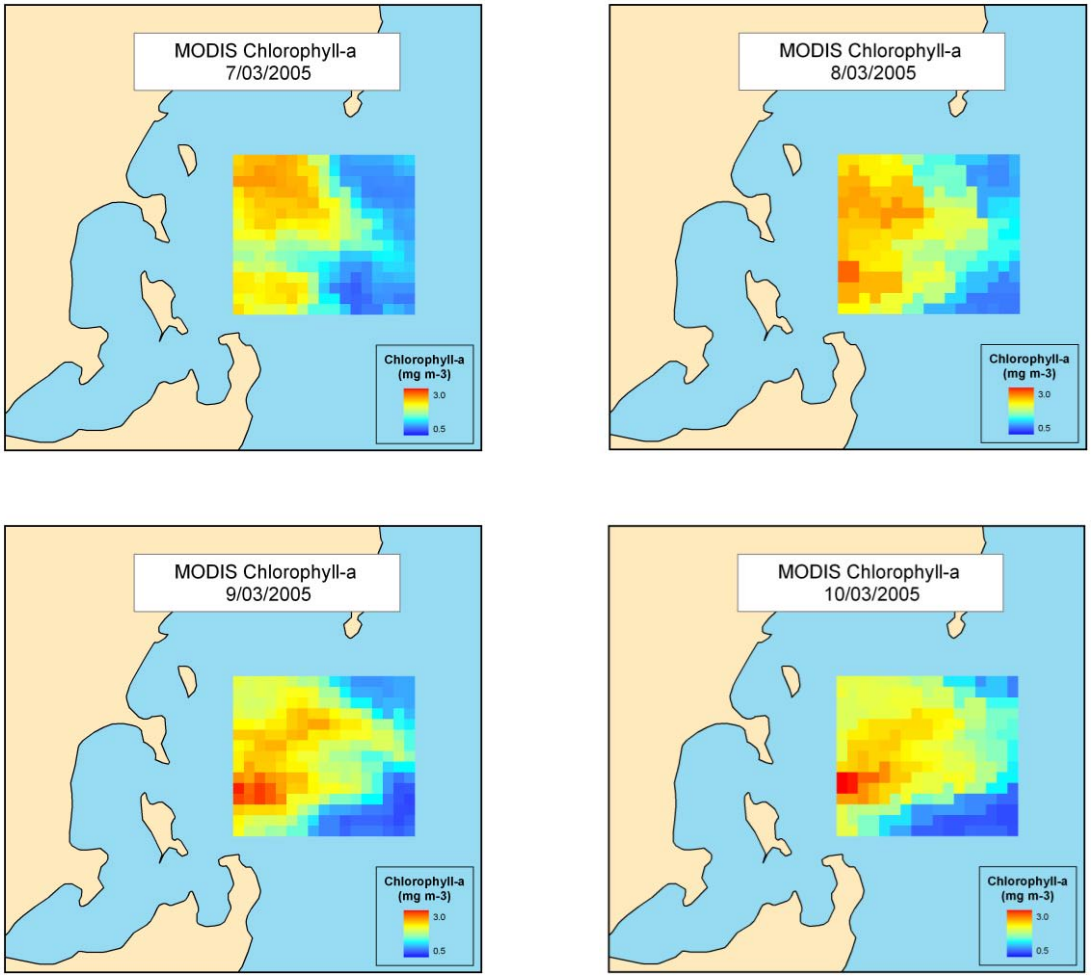

Figure 6.13: MODIS chlorophyll-*a* of the TFZ on the 7th, 8th, 9th and 10th March 2005 showing changing spatial patterns.

6.5 Conclusion

The daily MODIS chlorophyll-*a* and SST images over 6 years have enabled a greater understanding of the oceanography of the region to be developed, by allowing us to observe short-term temporal variability and fine-scale spatial variability not possible with field-based techniques alone. MODIS chlorophyll-*a* imagery has shown that the TFZ is much more variable than previously believed. The short-term temporal variability in chlorophyll-*a* averaged over the TFZ is much greater when concentrations are at their greatest, between March and July, as is spatial variability across the TFZ. It is suggested that this is related to the movement of small phytoplankton blooms throughout the TFZ during this period of the year, although the magnitude of chlorophyll-*a* does not indicate concern. The long-term spatial pattern shows that the northwest of the TFZ is higher in chlorophyll-*a* than the southeast, perhaps related to water depth and coastal influences, but also possibly related to the flushing of the region, with the southeast more exposed to the gulf-wide circulation. It may be possible that blooms of chlorophyll-*a* are more prone to occurring in the northwest of the TFZ, explaining the spatial pattern in both the mean and the variability. Since the MODIS imagery provides only an estimate of chlorophyll-*a*, field-based samples would need to be collected in this area to confirm the presence of phytoplankton blooms and determine whether they pose any threat to the aquaculture industries of the area. The SST observations from the daily MODIS images over the TFZ show a seasonal pattern consistent with that observed nearby from monthly imagery. There is some short-term temporal variability, although it is low is relation to that observed for chlorophyll-*a*. Furthermore there were no detectable temporal trends in the spatial variability or any long-term spatial patterns over the 6 years.

Chapter 7: Discussion and Conclusions

7.1 Review of Research Findings

The aim of this project was firstly to determine whether MODIS satellite-based chlorophyll-*a* and sea surface temperature imagery was suitable and valid for use in the coastal waters of South Australia. Following the assessment of the imagery, the objective was to apply MODIS imagery to increase the understanding of chlorophyll-*a* and sea surface temperature variability throughout Spencer Gulf and the southern bluefin tuna aquaculture region near Port Lincoln.

The use of satellite-based ocean colour imagery has increased dramatically in the past decade and it is now applied to many different marine applications (McClain 2009). It is known, however, that the accuracy of satellite-based chlorophyll-*a* estimates is limited in coastal regions with several factors potentially impacting upon the measurements. Coloured dissolved organic matter (CDOM) in the water column is known to have considerable impacts on the absorption of visible light (Bricaud et al. 1981; Carder et al. 1989; Nieke et al. 1997), and previous studies have shown that CDOM has contributed to poor satellite-based chlorophyll-*a* accuracy (Darecki and Stramski 2004; Gregg and Casey 2004; Tang et al. 2008). Suspended particulate matter (SPM) is also known to potentially impact upon satellite-based chlorophyll-*a* measurements by altering the characteristics of absorption and scattering in the water column (Stramski et al. 2004; Tzortziou et al. 2007). Not only can constituents of the water column influence the measurements, but the accuracy of the satellite-based chlorophyll-*a* is also dependant upon accurate atmospheric correction of the radiance received by the satellite sensor, and the algorithms that convert the radiance measures into chlorophyll-*a* concentrations. Assessment of the accuracy of the satellite-derived water leaving radiances has been conducted for SeaWiFS and MODIS (Bailey and Werdell 2006; Wang et al. 2009). These studies, whilst showing promising results, have also shown that the atmospheric correction procedures are not perfect, and that errors do exist that can potentially manifest into errors in the determination of chlorophyll-*a*. The absorbing aerosols are one of the known limitations to atmospheric correction methods (Bailey and Werdell 2006), and are likely to be responsible for the difficulties associated with the GSM01 and Carder algorithms (Chapter 4). Ocean colour algorithms have also been assessed by a number of studies in several ocean regions (Carder

et al. 2004; Pinkerton et al. 2005; Garcia et al. 2006). These studies have shown mixed results for the ocean colour algorithms tested, suggesting possible regional inconsistencies for the algorithms.

Considering the number of factors discussed above that have the potential to influence satellite-based measurements of chlorophyll-*a,* it is not surprising that the accuracy of the method is less than perfect. It is apparent that satellite-based chlorophyll-*a* estimates need to be assessed in previously untested regions, such as Spencer Gulf, to determine whether the method is valid for such regions and the accuracy acceptable. It has not been possible in the present study to investigate the role of each potential limiting factor, such as CDOM, SPM, atmospheric correction and the algorithms, on the MODIS chlorophyll-*a* measurements. Instead the overall accuracy of the final MODIS chlorophyll-*a* measurements was assessed by comparing MODIS estimates against field-based chlorophyll-*a* measurements. Thus the errors observed are cumulative errors from all possible sources that cannot be differentiated.

It has been suggested that acceptable accuracy for satellite-based chlorophyll-*a* measurements in the open ocean is within ±35% (McClain 2009). Based upon this goal, the results from this study appear to be reasonable for Spencer Gulf and nearby coastal waters. Measurements from around the SBT aquaculture region near Port Lincoln in the southwest of Spencer Gulf showed that shallow water depth is an important factor to consider, with the relationship between MODIS and field-based measurements clearly improved for water depths of greater than 20 m. Shallow water depth can result in seafloor reflection and overestimation of satellite-based chlorophyll-*a* (Spitzer and Dirks 1987; Estep 1994; Maritorena et al. 1994), but the depth at which it becomes important varies with location and the optics of the water column. Using the equation for apparent optical depth (AOD) from Bailey and Werdell (2006), shown in Chapter 4, we can estimate the depth at which seafloor reflection may become an issue. For the waters near Port Lincoln this depth is on the order of 12 to 22 m depending on the time of year.

Investigation into the possible sources of apparent error between MODIS and field-based measurements has identified that within-pixel spatial variability of chlorophyll-*a* can be considerable, and is likely to be responsible for large discrepancies between the two methods where the field-based measurement is not representative of the surrounding waters. This problem has also been observed in a previous study by Yuan et al. (2005).

Apparent errors can also arise due to temporal variability; although attempts have been made to reduce the influence of this by restricting the time between measurements to 3 hours (Bailey and Werdell 2006). The vertical profile of chlorophyll-*a* in the water column is also likely to be important to the observed accuracy of satellite-based chlorophyll-*a* (Gordon and Clark 1980; Smith 1981; Xiu et al. 2008). Variability in subsurface chlorophyll-*a* may be a reason for the very poor results observed for the Great Australian Bight chlorophyll-*a* data from van Ruth (2009), where samples were collected from 3 m below the surface rather than at the sea surface as for the other datasets.

With the exception of shallow waters, and taking into consideration the apparent errors discussed, MODIS chlorophyll-*a* has compared well against the field-based measurements. This may be due to the lack of terrestrial freshwater input in this coastal region, and thus CDOM and SPM concentrations, although unmeasured, may be lower than in other Case 2 coastal regions. Four different chlorophyll-*a* algorithms were examined to determine the most appropriate for further application. The GSM01 and Carder algorithms showed good results for some of the datasets, but they were not consistent and were unable to be produced for some of the dates required. The Clark algorithm showed good results, but the OC3M algorithm was most accurate and consistent and therefore will be the preferred algorithm for further application. The results of the MODIS chlorophyll-*a* assessment indicate that the MODIS chlorophyll-*a* imagery can be used to understand phytoplankton variability in South Australian waters, as long as care is taken when interpreting the results in shallow areas.

Satellite-based sea surface temperature imagery has been applied more widely than chlorophyll-*a* imagery, and has generally been accepted as an accurate and reliable data source. Despite this there are potential limitations to satellite SST imagery, and thus MODIS SST methods were still compared against field-based SST data to confirm the accuracy in the study area. Satellite SST measurements are affected by atmospheric influences and absorption due to water vapour and other gases is known to influence SST measurements. However, SST algorithms attempt to incorporate the atmospheric influences and reduce these impacts (Zavody et al. 1995; Brown and Minnett 1999). The field-based CTD temperature measurements in this study were collected at depths of between 1 and 3 m below the sea surface, and the satellite SST measurements are a measure of temperature at the immediate surface of the water (Schluessel et al. 1990; Donlon et al. 2002). This difference is most likely responsible for the observed

discrepancies between the methods. However these differences were small and the MODIS SST measurements proved to be very accurate in the study area. MODIS day-time 11 μm SST and night-time 11 μm and 4 μm SST were tested, and statistically the night-time 4 μm method was most accurate. The 4 μm method has advantages over the 11 μm SST due to greater temperature sensitivity and less water vapour absorption. However since the other two methods performed almost as well in this study, these advantages appear to be minimal. The day-time 11 μm SST was selected over the night-time methods for future application. This study has determined that both MODIS chlorophyll-*a* and sea surface temperature measurements are suitable and valid for use in South Australian coastal waters. There are limitations, however, but as long as these are understood then the imagery can be applied to investigate chlorophyll-*a* and sea surface temperature variability in Spencer Gulf and South Australia.

The second objective of this study, after validating MODIS imagery against field-based data, was to apply it to investigate chlorophyll-*a* and sea surface temperature variability in Spencer Gulf and the southern bluefin tuna aquaculture region. Prior to this, techniques designed to investigate variability in remote sensing imagery were reviewed to identify potential methods for the subsequent analysis. The review covered a number of techniques for classification, summarising data, and investigating relationships in the datasets. Several techniques were found that could be applied to MODIS imagery over Spencer Gulf. Methods that were selected for application in Spencer Gulf were cluster analysis, including hierarchical cluster analysis and unsupervised classification, and principal components analysis.

It was observed that the seasonal patterns in MODIS chlorophyll-*a* varied considerably with location. The far north of Spencer Gulf showed much higher concentrations of chlorophyll-*a* than any other location in the study area, but this is likely to be influenced by the water depth, as discussed above. Peak chlorophyll-*a* concentrations in the north of Spencer Gulf occurred between January and May. In the southern gulf the peak occurred from April to July, while outside of the gulf it was between August and October. It is not clear what factors are responsible for the differences observed between these locations, but the hierarchical cluster analysis, unsupervised classification and principal components analysis all indicate that the coast plays an important role in chlorophyll-*a* properties. Perhaps differences in nutrient availability between gulf waters and ocean waters determine the timing of the peaks in chlorophyll-*a* and thus phytoplankton.

The seasonal chlorophyll-*a* pattern near the TFZ was similar to the nearby central Spencer Gulf, with a peak between March and July. The concentrations were greater near the aquaculture region, however, than further offshore in the centre of the gulf. This increase is possibly related to water depth and overestimation of MODIS chlorophyll-*a*, but it is also possible that the TFZ has increased chlorophyll-*a* and phytoplankton as a result of either coastal influences or aquaculture related processes. The daily MODIS chlorophyll-*a* averaged over the TFZ shows a very similar seasonal pattern to that observed nearby from monthly imagery. Maximum chlorophyll-*a* is observed during autumn and winter with minimum chlorophyll-*a* during spring and summer. As mentioned, the annual cycle of chlorophyll-*a* observed in this study is consistent with previous field-based studies (Paxinos 2007; van Ruth et al. 2009).

There is also considerable variability of chlorophyll-*a* in the TFZ. Intra-month temporal variability is observed with greater variability during autumn and winter when the concentration of chlorophyll-*a* is greatest. The spatial variability across the TFZ follows the same pattern, with greater spatial variability when chlorophyll-*a* is highest. These patterns are possibly caused by the movement of small blooms of chlorophyll-*a* though the TFZ during these times. The image of long-term mean chlorophyll-*a* averaged over 6 years shows greater chlorophyll-*a* in the northwest of the TFZ than the southeast. It is likely that this pattern is due to greater flushing of the offshore region by the gulf-wide clockwise circulation and a northwards current through the TFZ (Herzfeld et al. 2009; Tanner and Volkman 2009). The circulation of the region, as suggested by Herzfeld et al. (2009), shows reduced flushing towards the coast and possibly allows for accumulation of nutrients in these areas. This could explain the patterns of chlorophyll-*a* in this study. This may be influenced by water depth and seafloor reflection, which needs to be investigated with field-based surveys, and thus this result should be treated cautiously. However, if this pattern is proven to be correct then this may have implications for the SBT aquaculture industry.

The sea surface temperature was also observed from MODIS imagery of Spencer Gulf and the SBT aquaculture region. The annual range in sea surface temperature for the waters inside Spencer Gulf was greater than outside the gulf, with gulf waters warmer than ocean water in summer but cooler in winter. This has been shown previously by Nunes and Lennon (1986) and Nunes Vas et al. (1990) to be due to the low thermal inertia of Spencer

Gulf. The hierarchical cluster analysis of temporal SST profiles clearly separates stations within the gulf from stations outside the gulf, and the unsupervised classification also confirms that the waters of Spencer Gulf are separate from nearby shelf water based on SST. Across the mouth of Spencer Gulf, the SST front over summer that has been described by Petrusevics (1993) is observed, as is the plume of relatively warm water outside of the gulf from the GAB during winter that was described by Herzfeld (1997). Coastal upwelling is also observable in the monthly SST imagery along the western coast of Eyre Peninsula, the southwest of Kangaroo Island, and the Bonney Coast in the southeast of the state. The location and times of this upwelling agrees with previous studies by Kampf et al. (2004) and McClatchie et al. (2006). Possible evidence of upwelling has also been observed in the seasonal chlorophyll-*a* profiles on the west coast of Eyre Peninsula, with elevated chlorophyll-*a* observed in March. The seasonal SST patterns observed for the tuna farming zone show minimum temperatures on the order of 14.3 ºC in August and maximum temperatures of 21.2 ºC in February. These temperatures differ little from other locations in southern Spencer Gulf, but are quite different from locations outside of the gulf due to the annual range of temperature driven by thermal inertia already discussed. Unlike the chlorophyll-*a* observations around the TFZ, the SST observations were mostly homogenous across the TFZ at any given time. Also there was little short term temporal variability.

7.2 Limitations

In this study MODIS chlorophyll-*a* and SST imagery has been compared to field-based data and shown to perform with acceptable accuracy, with the exception of shallow water regions (and the GAB where the depth of the field-based measurements is believed to be responsible for the poor relationship). As has been discussed, there are a number of apparent errors in the relationship between MODIS and field-based data. Sub-pixel spatial variability in chlorophyll-*a* has been shown to be large and likely to contribute to large differences between the methods. Ideally to eliminate this apparent error source, multiple field-based measurements need to be collected and averaged for each field station, rather than a single point measurement. Future attempts to further investigate accuracy of satellite imagery against field-based measurements in the area should consider averaging multiple measurements across an area to address this issue. Further, the lab methods utilised to calculate chlorophyll-*a* have not been assessed. Instead the field and lab methods have

been assumed to be accurate and the accuracy of the satellite-based measurements was compared to these assumed „ground-truth" measurements. However, it is possible that the field and lab techniques included error sources that have led to inaccurate field measurements. Inaccurate field-based measurements could also contribute to the apparent fine-scale spatial variability in surface chlorophyll-*a*. Furthermore, for the SST measurements no accuracy assessment or calibration was conducted on the CTD instrument, and again only a single point measurement was used. This again may have induced apparent errors into the MODIS SST measurements. The number of samples and the areas covered by the field-based measurements were less than ideal. It would have been preferable to have collected a greater abundance of field-based measurements across a greater range of locations within the study area. For a complete and comprehensive validation of MODIS imagery the radiance measurements of the satellite sensor could have also been assessed against water-leaving radiances measured *in situ*, to assess the sensor performance and atmospheric correction, and the ocean colour algorithms could have been applied to the *in situ* water-leaving radiances to validate the algorithms independently of the satellite sensor and atmospheric correction. However this was not possible with the facilities available. Future research may be able to attempt this comprehensive validation if the need and resources become available.

There were also limitations to the application of MODIS imagery. While the validation section of this project showed that MODIS overestimated chlorophyll-*a* in shallow water, the MODIS imagery used to investigate variability in chlorophyll-*a* was still collected over all regions including the shallow areas. Instead it may have been possible to model from bathymetry data, field-based measurements, and apparent optical depth estimates, regions where seafloor reflection is likely to occur and exclude these areas from subsequent analysis. This was not done and thus care in interpreting data values from the shallower areas needs to be taken.

Seasonal variability of chlorophyll-*a* and SST was assessed over only a 5-year period. This period of time may be long enough to observe general seasonal patterns, but a longer time series is necessary to refine the seasonal patterns further and give less weight to individual years within the climatology. For example in Figure 5.4, station D shows a very high peak in chlorophyll-*a* during July 2003. In the following years the annual peak in chlorophyll-*a* was much lower, and the peak occurred between April and June. However, the July peak of 2003 was large enough to outweigh the peaks of the following 4 years so that the

climatology image over the 5 years shows maximum chlorophyll-*a* in July. Thus to truly understand the seasonal patterns a longer dataset is required, so that anomalous years do not over-influence the climatological averages. Longer time periods could have been assessed for chlorophyll-*a* by utilizing Terra MODIS imagery back to 1999, or even SeaWiFS chlorophyll-*a* from 1997, and AVHRR SST imagery back to 1985. Perhaps future studies could investigate these longer temporal datasets to improve the observed seasonal patterns. Furthermore, long time series imagery could show possible long-term trends. Allen et al. (1994) suggest that time periods of 10 – 15 years could show reliable long-term trends in SST. Previous studies have used multiyear satellite SST imagery to observe increases in global SST (Lawrence et al. 2004; Good et al. 2007).

The investigation of the tuna farming zone used MODIS imagery over a shallow coastal region. The validation part of the study showed shallow water to produce erroneous satellite chlorophyll-*a* estimates. The area of the TFZ subset in Chapter 6 is a similar location to where field-based measurements were collected for the Aquafin CRC Risk and Response dataset. This dataset showed that MODIS chlorophyll-*a* imagery performed reasonably well, but with some overestimation. The TFZ subset avoided the shallowest waters of the region as much as possible whilst still attempting to cover the majority of the Boston Bay and Lincoln Offshore aquaculture zone. MODIS chlorophyll-*a* concentrations in the region will be affected to some degree by shallow water and overestimation, but by avoiding the shallowest areas it is hoped that this will be minimal. In addition, while the daily MODIS imagery provides a more detailed view of variability across the aquaculture region than the monthly composite imagery, it is still very coarse in relation to the individual SBT aquaculture farms. To understand the chlorophyll-*a* changes around individual farms and individual pens requires a sensor with a much higher spatial resolution than the 1 km MODIS imagery. Preliminary attempts to use Landsat TM/ETM+ imagery, with 30 m spatial resolution, were conducted early in this study. However, without a standardised technique to approximate chlorophyll-*a* from Landsat imagery and sufficient field-based measurements to develop a localised chlorophyll-*a* algorithm, it was not possible to apply Landsat to investigate chlorophyll-*a* variability on this farm scale. It is possible to observe changes in water colour characteristics in the visible bands of the Landsat imagery around SBT farms, and previous studies have shown that it is possible to develop local site-specific chlorophyll-*a* algorithms from Landsat imagery (Kim and Linebaugh 1985; Dwivedi and Narain 1987; Tassan 1987; Baban 1993; Lavery et al. 1993; Pattiaratchi et al. 1994; Mayo et al. 1995; Gabric et al. 1998; Han and Jordan 2005).

7.3 Future Research

Despite the limitations observed, this study has shown that MODIS chlorophyll-*a* and SST imagery performs well in South Australian waters. As discussed, there were limitations in the methodology applied in the validation of MODIS imagery. Future studies could improve upon this by: incorporating more extensive field-based datasets from a greater range of marine environments; collecting replicate samples within the area of the MODIS field-of-view to allow for fine-scale variability; investigating subsurface variations; and assessing radiometric measurements to investigate the performance of the satellite sensors, the atmospheric correction procedures, and the algorithms. Validation studies of future sensors, such as the National Polar-orbiting Operational Environmental Satellite System (NPOESS) Visible Infrared Imaging Radiometer Suite (VIIRS) scheduled for launch in 2010 (Lee et al. 2006), will also need to be conducted if the products are to be applied with confidence.

It has been demonstrated that MODIS imagery can be used to understand both the seasonal variability over a large area like Spencer Gulf and more detailed variability over smaller areas such as the southern bluefin tuna aquaculture region. However, due to the coarse spatial resolution of MODIS its applicability to study fine-scale variations is limited. Future studies may benefit from investigating the use of sensors with better spatial resolution to observe relatively small areas such as aquaculture zones. Previous studies have demonstrated that it is possible to develop empirical location-specific chlorophyll-*a* algorithms for Landsat.

Many other studies may be able to benefit from the application of MODIS imagery, such as investigations into the local current systems and coastal upwelling. The local fisheries and aquaculture industries may also find benefits from the imagery. With time series of imagery now extending beyond 10 years it may now also be possible to investigate long-term temporal variability related to climate change. It is hoped that future studies will continue with the application of MODIS and other satellite-based imagery in the region.